EPRI COMMENTS ON

EPA PROPOSED EMISSION STANDARDS/PROPOSED STANDARDS OF PERFORMANCE, ELECTRIC UTILITY STEAM GENERATING UNITS: MERCURY EMISSIONS

National Emission Standards for Hazardous Air Pollutants; and, in the Alternative, Proposed Standards of Performance for New and Existing Stationary Sources: Electric Utility Steam Generating Units; Proposed Rule (Federal Register 69, 20, January 30, 2004)

and

40 CFR Parts 60, 72, and 75 Supplemental Notice for the Proposed National Emission Standards for Hazardous Air Pollutants; and, in the Alternative, Proposed Standards of Performance for New and Existing Stationary Sources: Electric Utility Steam Generating Units; Proposed Rule (Federal Register 69, 51, March 16, 2004)

Docket ID No. OAR–2002–0056

Richard Carlton
rcarlton@epri.com
650-855-2115

Paul Chu
pchu@epri.com
650-855-2812

Leonard Levin
llevin@epri.com
650-855-7929

George Offen
goffen@epri.com
650-855-8942

Janice Yager
jayager@epri.com
650-855-2724

EPRI

3412 Hillview Ave.
Palo Alto, CA 94304-1395

June 16, 2004

EXECUTIVE SUMMARY

EPRI is providing a set of technical comments to the U.S. Environmental Protection Agency to update agency scientists and staff on the status of research into the sources, transport, fate, human exposure, effects, and management practices for environmental mercury. These comments focus on mercury emissions and their fate due to coal-fired U.S. electric utility generating plants. The EPRI comments are intended to both summarize research findings across the mercury research community, and explain in depth some recent findings on mercury behavior addressing particular issues raised in the utility control proposals by the Agency.

The EPRI comments cover a broad range of findings, but key points can be summarized below:

1. Mercury "hot spots", defined as unusually high values of mercury deposition, are not found to have significant contribution from utility mercury emissions. When U.S. geographic locations are defined as "utility-influenced" or "non-utility influenced" based on whether 50% or more of the mercury depositiing there is emitted from utility stacks, the utility-influenced locations together make up only 0.4% of the U.S. land area, and essentially none of these areas are where the highest deposition occurs in the U.S.

2. About 70% of U.S. utility mercury emissions do not deposit within the continental United States, but are dispersed globally. Model results reveal that most mercury depositing in the U.S. (about 75%) originates in other countries or from other continents. Global inventories show nearly half of the anthropogenic emissions to the atmosphere coming from Asia. In 2001 and 2002, EPRI researchers in instrumented aircraft tracked mercury emissions from China into the Pacific Ocean basin moving towards the continental United States, finding nearly 700 tons per year of new mercury being transported in that manner. Measurements above California found two distinct plumes of mercury, tracked by wind data to mainland Asian source regions, crossing into the United States and moving across the country.

3. The changes in mercury deposition that might be brought about due to the proposed EPA utility mercury regulations will range from rather small drops over most of the U.S., to larger reductions in isolated instances primarily in the eastern U.S. Since much of the mercury depositing in the U.S. originates in other countries, U.S.-only management steps provide limited benefit in the form of reduced mercury deposition across most of the country. When the predicted reductions in mercury deposition are used to calculate changes in fish mercury by state, and combined with information on fish consumption and on sport fishing by state, predicted reductions in mercury exposure can be calculated. For the proposed Cap & Trade regulation, these range from a fraction of a percent drop in mercury exposure in western states to more than 6.5% in West Virginia.

4. Recent evidence from ground and aircraft measurements indicates that divalent mercury, when emitted from power plant stacks in emissions plumes, may undergo rapid and efficient chemical reduction to the elemental form. This chemical conversion

does not alter the total amount or rate of mercury emitted from a power plant, but significantly shifts its composition from the divalent to the elemental form. Since the divalent form is about 10^6 (1 million) times as water soluble as the elemental form, such a reaction would quickly reduce the efficiency of wet scavenging, or washout, of mercury. That is the removal mechanism most likely to deposit the soluble divalent form closest to the source and, therefore, at higher concentrations. If continued measurements can demonstrate a stoichiometric relationship between mercury and other plume constituents, allowing this reaction to be broadly applied, this would significantly reduce the attribution of utility plants to nearby mercury deposition.

5. A one-compartment pharmacokinetic model was applied to derive the distribution of scores on the Boston Naming Test for three groups of children: those with no exposure to MeHg; those exposed at the Reference Dose of 0.1 μg/kg/day; and those exposed at four times the Reference Dose. The model was applied to test score results reported in the Faroe Islands study. Results show that mercury exposure of U.S. children *in utero* at the Reference Dose or at four times the Reference Dose would result in imperceptible shifts in the distribution of scores compared to those with no exposure to MeHg.

6. There has been recent discussion that the number of U.S. children born each year "at risk" of neurobehavioral impairment due to mercury dosage to their mothers from fish consumption is 600,000 per year, twice an earlier estimate. The basis for this revised estimate has been attributed to previously unreported ratios of fetal blood mercury:mothers' blood mercury. However, EPA has already incorporated this ratio by including a single uncertainty factor for interindividual variability into the derived Reference Dose;

7. Prior analyses of the potential for individual mercury sources such as a power plant to result in enough mercury in fish in nearby waterways to result in consuming women exceeding the EPA Reference Dose have relied on "point estimates" of mercury exposure. In those cases, high-end (or low probability) combinations of emission rates, stack parameters, environmental variables such as wind and rainfall, and local hydrology have been used to derive high-end results. EPRI instead has undertaken a probabilistic, or Monte Carlo, analysis. In such an analysis, each variable in the exposure equation is represented by a likelihood distribution, and random samples taken from each such distribution to derive a resulting set of probabilities that doses exceed, or under-run, the Reference Dose by various amounts. The EPRI analysis showed that the probability of an individual within 50 km of a coal-burning utility plant in any direction hasonly a 0.6% chance of exceeding the Reference Dose, and that drops by a factor of 15, to 0.04%, for any of the CAIR, MACT, or C&T regulatory approaches.

BACKGROUND

On January 30, 2004, the U.S. Environmental Protection Agency (EPA) published a notice of proposed rulemaking (40 CFR Parts 60 and 63: "Proposed National Emission Standards for Hazardous Air Pollutants; and, in the Alternative, Proposed Standards of Performance for New and Existing Stationary Sources: Electric Utility Steam Generating Units; Proposed Rule") to reduce emissions of mercury from coal-fired electric utility steam generating units, and of nickel from oil-fired electric utility steam generating units. In the proposed rule, EPA sets forth two alternative approaches to regulating mercury emissions from coal-fired electric utility steam generating units, as well as setting emission standards for nickel emissions from oil-fired electric utility steam generating units. Further details proposed by EPA on that aspect of the proposed rule, in addition to discussion of stack monitoring requirements, were published by EPA on March 16, 2004.

In this set of comments, EPRI addresses several fundamental scientific and technical questions raised by the proposed rulemaking and its alternative approaches. The discussion is presented in three sections. Section A introduces key technical issues and summarizes EPRI research findings on those issues. Section B presents extended technical discussions of several of those issues at a level of analysis useful for understanding the detailed approaches and results. Section C consists of a list of published reports, peer-reviewed literature, abstracts and papers from technical conferences, and other original source material serving as foundations for the analyses presented in earlier discussions. These materials will be submitted separately to the EPA docket.

EPRI's comments are an attempt to provide an integrated technical assessment of our understanding of mercury that may be useful in national decisionmaking. These comments discuss mercury emissions on a global and national scale (both anthropogenic and natural sources), relate those emissions to deposition patterns using various modeling and analysis techniques, and then estimate how changes in emissions and deposition patterns following from EPA's proposed rules would impact exposure to the US population, in particular to women of child bearing age. The comments also discuss other important issues related to mercury, such as the status of mercury emissions monitoring and control technologies and the overall scientific basis of EPA's reference dose, which is the driver for regulating mercury emissions to protect public health. We also comment on the issue of "hotspots" that has become a concern, especially for the proposed Cap & Trade option. EPRI also discusses other issues related to model runs, including the ability of the models themselves to replicate realistically the behavior of mercury in the environment.

EPRI's extensive research program on environmental mercury has been conducted over the past 15 to18 years, beginning with development of the first versions of the EPRI Mercury Cycling Model in investigations conducted jointly with agencies of the State of Wisconsin. These comments are intended to reflect the most recent findings of not only that program, but the many other research programs on mercury underway nationally and globally.

OUTLINE OF THIS DOCUMENT

This document is intended as a focused set of discussions on recent research findings regarding mercury in the environment, its sources globally and within the United States, and its cycling through the atmosphere and into aquatic systems. The discussions are organized around key issues in Section A:

1. the mercury "hot spot" issue;
2. the global balance of mercury,
3. the origins of mercury depositing within the United States, based on model results;
4. direct observation of mercury emissions from Asia moving into the United States;
5. how exposure to mercury might change with utility controls in place;
6. evidence for mercury reactions in power plant plumes;
7. how mercury regional-scale models may overestimate deposition rates for the substance;
8. the cycling of mercury through terrestrial and aquatic systems;
9. some issues regarding mercury health effects;
10. a clarification of the exposure level of U.S. children to methylmercury;
11. the manner in which power plant stacks might be sampled for compliance testing;
12. differences in estimates of how quickly U.S. utilities under Cap & Trade would reach full compliance with the regulations;
13. a maximum likelihood approach to local-scale exposure from power plant mercury emissions;
14. the status of mercury control technologies; and
15. a new assessment of the relative costs vs. effectiveness of utility mercury control measures.

Following these brief research summaries, Section B provides three detailed technical appendixes, explaining respectively the methodology and findings for looking at locations with relatively high deposition values; the modeling and assumptions that went into the costing model used and its conclusions about regulatory scenarios, and the methodology and a sample state calculation for assessing drops in human exposure to methylmercury via fish consumption under the two proposed scenarios. Finally, Section C is a listing of reports, publications, and documents providing technical foundations for the work described here. These documents have been submitted separately to EPA in electronic format, but are also available in printed form.

A. SUMMARY DISCUSSION OF TECHNICAL FINDINGS REGARDING MERCURY

A.1. MERCURY DEPOSITION "HOT SPOTS"

There is no evidence of utility-caused deposition "hot spots" under either EPA regulatory proposal.

There has been public discussion about the possibility that the proposed EPA MACT and Cap & Trade rules will not fully alleviate the existence of presumed mercury "hot spots." A number of definitions of mercury "hot spots" have been used recently. EPRI defines a mercury "hot spot" as a geographic location with total deposition of divalent mercury at levels that will result in mercury levels in consumable fish in underlying surface water drainages representing a potential for consuming women of childbearing age in the same state to exhibit mercury levels in blood exceeding the EPA Reference Dose equivalent. Concerns have also been expressed that the rules, especially Cap & Trade, could exacerbate or create new hot spots. EPRI has performed an extensive modeling exercise with state-of-the-art tools and data to explore projected deposition patterns under both regulatory proposals. EPRI's analysis shows that:

(a) The highest levels of mercury deposition anywhere in the continental United States are brought about primarily by non-utility sources (even after accounting for MACT rules on those non-utility sources).
(b) The Cap & Trade proposal would produce larger and more widespread reductions in mercury deposition compared to current emissions than would the MACT proposal, particularly in regions with the highest deposition currently.

No one has yet provided measurement data that identify 'hot spot" situations for mercury under current emissions conditions. In fact, it is unclear what the definition of a "hot spot" actually is.[1] EPRI has addressed this issue by simulating deposition patterns with a combination of models to predict emissions of mercury under several regulatory scenarios. The models estimate emissions and then simulate deposition based on our current understanding of atmospheric chemistry and transport in the atmosphere. EPRI has modeled current and scenario deposition patterns where the only changes introduced are those representing proposed utility emissions regulations (e.g., MACT or Cap & Trade). Consequently, all other sources modeled, such as power plants in Asia, chloralkali plants, and U.S. waste incinerators, are held unchanged from their most recent mercury emissions patterns (except that historical emissions of municipal and medical incinerators have been reduced to reflect MACT standards that have been promulgated since the emissions inventory was

[1] Indeed, the formal definition of a "hot spot" expressed by EPA is one that could only be resolved using modeled estimates of deposition. EPA, in the rule preamble, defines a mercury "hot spot" as a mercury deposition point dominated by utility plant contributions whose removal would result in fish tissue levels dropping from above to below the Fish Tissue Criterion of 0.3 ppm. The agency goes on to provide a practical definition, namely, whether implementation of a MACT rule or a Cap & Trade rule would result in a greater or lesser occurrence of "hot spots." We have not attempted to address this definition as it requires models and information not currently available regarding how modeled deposition translates into localized fish tissue concentrations.

created.) This modeling does not predict outcomes at fixed dates in the future, because all the non-utility emissions may also change in the intervening years; however, it does provide useful information about differences in deposition patterns that would result from specific individual alternative policy scenarios, such as the proposed utility mercury rules.

Figure A.1-1 shows EPRI's modeled deposition (a) before implementation of any utility mercury reduction measures, compared to (b) after implementation of the proposed MACT and (c) after implementation of the proposed Cap & Trade policy. In preparing these simulations, it is assumed that no emissions reduction policy changes occur other than those on utility mercury emissions.[2] Figure A.1-1 demonstrates that the MACT and Cap & Trade policies produce a reduction mercury deposition on the order of 5 to 7% nationally, on average. Neither proposal would substantially alter the presence of high deposition values occurring as "peaks" in the Mid-Atlantic and southern New England states. This is because the deposition in those areas is dominated by non-utility local sources.

Although the differences between Figure A.1-1(b) and A.1-1(c) appear modest, one can discern that the Cap & Trade proposal is projected to extend the reductions in deposition that would be achieved by MACT alone, by further reducing the levels of deposition that appear in the Base Case. There are no areas of current (Base Case) deposition that become exacerbated under either the Cap & Trade or the MACT scenarios. In particular, there are no new areas of significantly high deposition under the Cap & Trade case, thus belying concerns raised by some investigators[3].

Figure A.1-1 thus indicates that the Cap & Trade proposal should not be expected to produce new areas of high values of deposition, nor to increase deposition in areas that models show as having high values under current emission conditions. Moreover, the analysis indicates that the Cap & Trade proposal should be viewed as generally better than the MACT proposal at reducing both deposition in defined areas as well as deposition levels overall. This statement is substantiated by Figure A.1-2, which maps the *differences* in projected deposition between the MACT and the Cap & Trade scenarios in 2020.[4]

Figure A.1-2(a) shows the areas where the Cap & Trade total Hg deposition flux is at least 1 $\mu g/m^2$-y lower than deposition under the MACT. It can be seen that much of the eastern US would experience lower deposition as a result of the proposed Cap & Trade rule, compared to the MACT proposal. Changes in the Mid-Atlantic States are not as pronounced as in other areas, since the main causes of peak deposition there are primarily non-utility mercury sources, including municipal waste and medical incinerators.

---

[2]Panel (a) of Figure A.2-1, the 2004 Base Case, assumes Clean Air Act Amendments of 1990 Title IV compliance, and NOx SIP Call compliance, only. The proposed Clean Air Interstate Rule (CAIR) [formerly the Interstate Air Quality Rule (IAQR)] is applied in the modeling for Panels (b) and (c). These panels reflect 2020 deposition projections for their respective scenarios for mercury emissions compliance that ensues following full implementation of the CAIR and any mercury control cobenefits entailed by that rule alone.

[3] One model anomaly arises from the modeling of new generating capacity likely to be introduced between 2004 and 2020. Since the exact location of new power plants is unknown at this time, new capacity is modeled by adding it proportionately to existing power plants and their stacks. Thus, some current power plants will appear to have greater than 100% capacity factor for out years, due not to their growth, but to their surrogate role in carrying the future new capacity for a given region.

[4] Negative values in Figure A1-2 imply that deposition is lower under the Cap & Trade than the MACT. Positive values imply that deposition is higher under the Cap & Trade than under the MACT.

Figure A.1-2(b) maps all the areas where deposition flux under the Cap & Trade proposal is at least 1 μg/m^2-y *higher* than under the MACT. Although there are some grid cells that are projected to have higher deposition under the Cap & Trade proposal vs. under MACT, they are isolated outcomes scattered throughout the eastern U.S. These cells account for less than 0.06% of total land area in the continental U.S. This analysis indicates that, even where Cap & Trade may result in slightly higher deposition levels than MACT (but still lower than in the Base Case), there will not be a tendency to exacerbate existing areas of highest deposition. Those areas of existing high deposition that show no significant reduction of deposition under the Cap & Trade policy are areas that are dominated by non-utility sources of mercury, such as municipal and medical waste incinerators, *even after accounting for the MACT rules that have been promulgated for those non-utility sources.*

Overall, the absolute differences between MACT and Cap & Trade deposition are fairly small. The scattered areas where deposition is projected to be lower under the MACT rule than under the Cap & Trade rule differ by only a few percent. In fact, only two isolated grid cells (one each in Pennsylvania and Colorado) are predicted to have deposition under Cap & Trade that is more than 10% higher than under the MACT rule. However, these areas would experience less than 3 μg/m^2-y higher deposition, against current peak deposition rates exceeding 100 μg/m^2-y.

Another method of assessing the potential for "hotspots," particularly those due primarily to utility emissions, is to define "utility-dominant" deposition locations *a priori* and then simulate the effect of the proposed regulations at these locations.. These locations are then "tagged" as utility-dominated for further analysis, and their relative standing in rank-ordered deposition locations is tracked. For this analysis, EPRI defined locations under the 2004 Base Case scenario that had 50% or greater deposition from utility sources as being "utility-dominant." The TEAM regional deposition model was first run for the 2004 Base Case, and deposition values for each location archived. TEAM was then run with all U.S. coal-fired utility emissions of mercury set to zero, and new deposition values with zero utility mercury input compared to those for the 2004 Base Case.

All locations where deposition dropped by 50% or more were tagged as "utility-dominant." Those locations were then tracked separately as TEAM was run for the 2020 MACT and 2020 Cap & Trade scenarios. In this way, the changes in "utility-dominant" locations for 2004 were assessed for both regulatory scenarios. Results of this analysis are shown in Figure A.1-3. The total surface area in 2004 covered by "utility-dominant" was 0.4% of the U.S., so that deposition into 99.6% of U.S. surface area was dominated by other, non-utility mercury sources. After either MACT or C&T were instituted, the 0.4% fraction dropped to less than 1/10th of that value. Thus, a very small fraction (less than one half percent) of U.S. land area has mercury deposition dominated by utility emissions; this fraction decreases further under both C&T and MACT.

More detailed discussions of the deposition and emissions projections supporting these findings can be found in Appendixes B.1 and B.2.

Figure A.1-1. Simulated mercury total deposition fluxes (µg/m^2-y) in the (a) 2004 Base Case, (b) 2020 MACT, and (c) 2020 Cap & Trade scenarios.

(a)

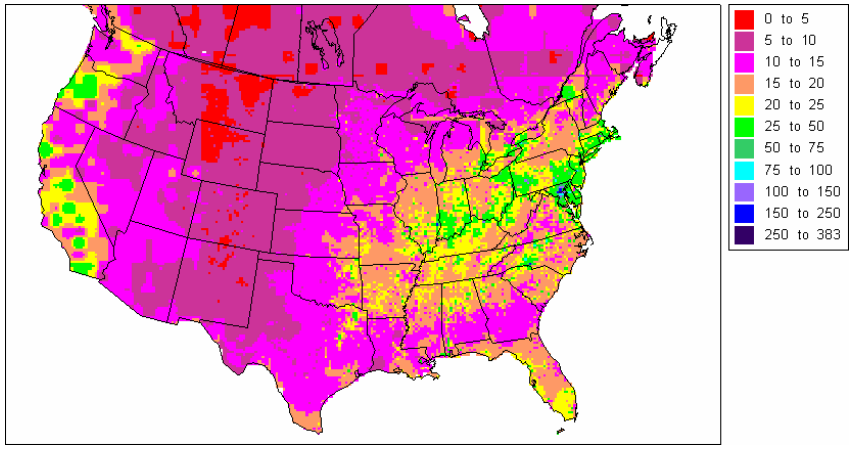

(b)

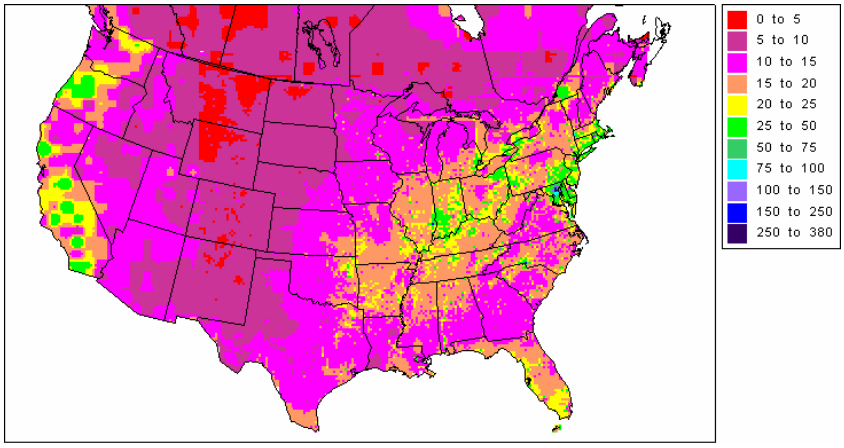

(c)

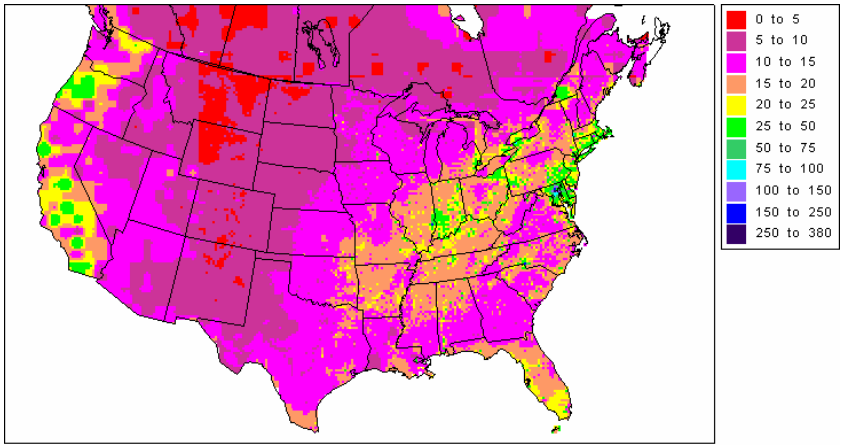

Figure A.1-2. Differences in simulated Hg total deposition fluxes (μg/m^2-y) between the 2020 C&T and 2020 MACT scenarios [(C&T)–(MACT)]. Areas where C&T deposition is lower than that of MACT are shown in the upper panel (a) and areas where C&T deposition is higher than of MACT are shown in the lower panel (b).

(a) Areas where C&T deposition is lower than that of MACT

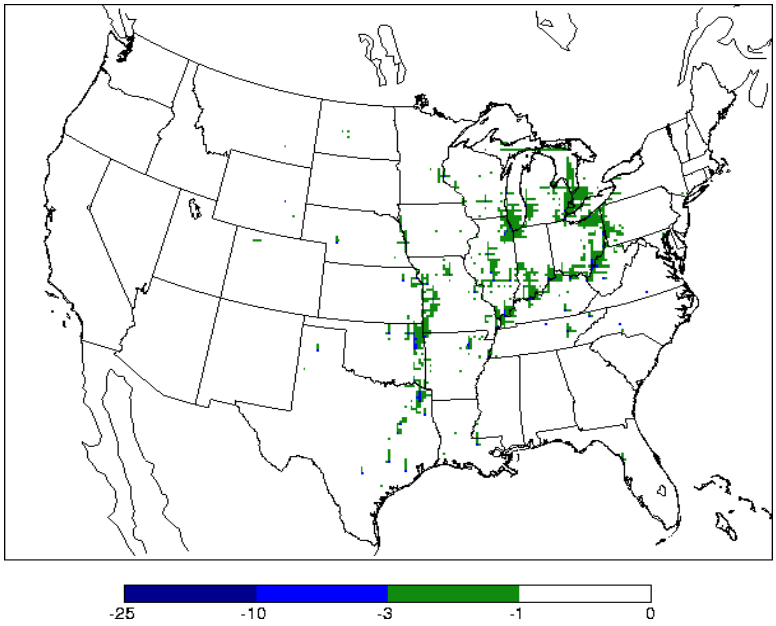

(b) Areas where C&T deposition is higher than that of MACT

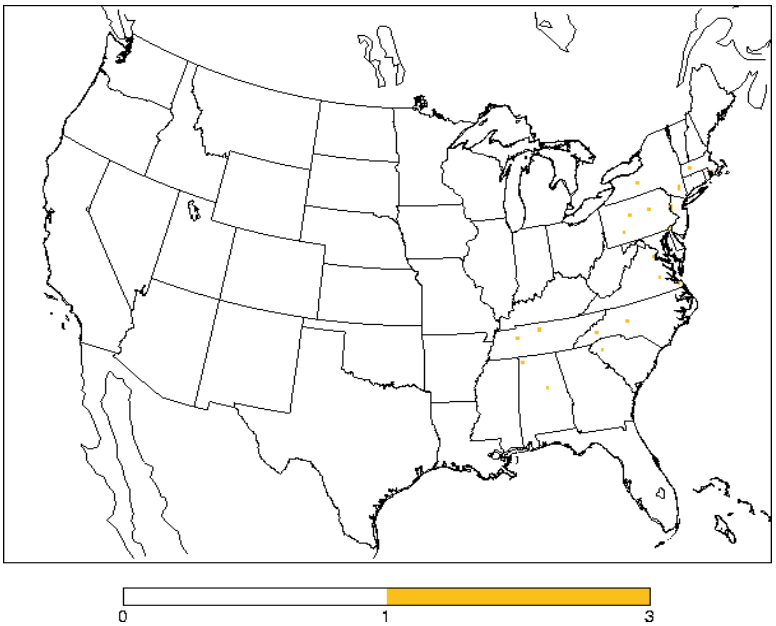

Figure A.1-3. Deposition rates for "utility-dominant" (green) deposition locations vs. "nonutility-dominant" deposition locations (blue) based on a 50% utility-emitted mercury contribution to total mercury deposition for the 2004 Base Case.

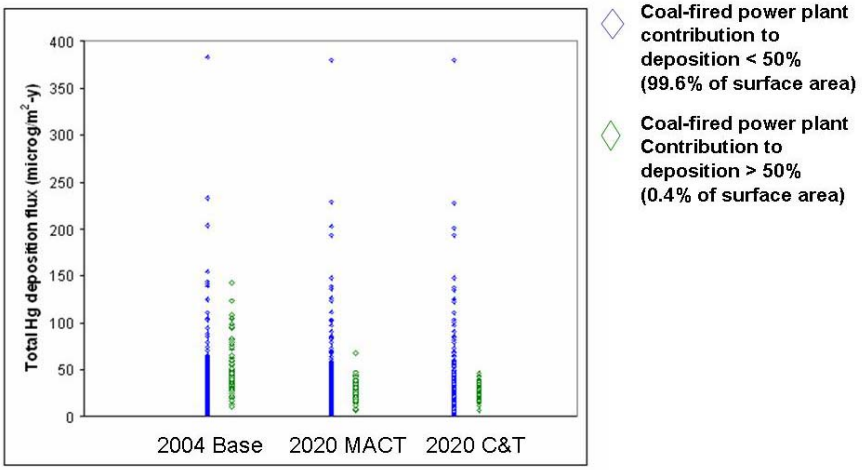

A.2. CONTRIBUTION OF U.S. SOURCES TO GLOBAL EMISSIONS

Emissions from U.S. power plants are estimated to contribute less than 2% to global anthropogenic mercury emissions and 1% to total emissions from all sources.

Mercury is a global pollutant whose worldwide origins must be considered in assessing relationships between sources and downwind receptor points. Global anthropogenic emissions of mercury are estimated to be 2143 Mg/year for 1998 (Seigneur et al., 2004). Asian emissions contribute about half of that total. North American (US, Canada and Mexico) emissions from all anthropogenic sources contribute about 10% to global anthropogenic emissions.

U.S. coal-fired power plant mercury emissions are estimated to contribute less than 2% of global anthropogenic mercury emissions and about 1% of all global emissions when natural sources are included (Seigneur et al., 2004). Mercury emissions from coal-fired power plants in the United States are estimated to be 42.8 Mg/year in Base Case year 2004. Those mercury emissions are expected to decrease under the two mercury control scenarios proposed by EPA (MACT and Cap & Trade) as well as the separately proposed Clean Air Interstate Rule (CAIR, formerly Interstate Air Quality Rule, or IAQR). EPRI's modeling analyses predicts that U.S. coal-fired power plants' contribution to global anthropogenic emissions by 2020 would be about 1.4, 1.3 and 0.6% for the CAIR, MACT, and Cap & Trade options, respectively. These percentages assume that global emissions do not change appreciably over this period. Given the plans for new coal-fired power plants worldwide, we can expect such emissions will continue to increase with time outside the United States (Slemr, 2003; Pacyna, 2003). In that likelihood, U.S. emissions will represent an even lower fraction of global and regional emissions.

A.3. ORIGINS OF MERCURY DEPOSITING IN THE UNITED STATES: MODEL RESULTS

Modeling results show that, for much of the continental United States, mercury deposition is dominated by mercury emissions outside the country, particularly from Asia, and that only a small fraction of U.S. land area is subject to a majority of its deposition of mercury originating with U.S. domestic sources. This limits the ability of U.S. mercury source controls to reduce U.S. mercury deposition.

Work by a number of investigators, including Seigneur et al. (2004), has attempted to clarify the location of atmospheric emission sources contributing to mercury deposition within the United States. Using global inventories by Pacyna et al. (2003) and others, it is possible to simulate mercury emissions globally on gridded domains, and then transport this mercury via global circulation and atmospheric chemistry to the boundaries of finer-scale sub-domains covering the continental U.S. As indicated in the next section of these comments, the transport of mercury across the globe has been measured by aircraft, thus supporting the modeling described herein.

The work by Seigneur et al. used a global Chemical Transport Model of 8° longitude by 10° latitude, providing boundary conditions to the EPRI TEAM (Trace Element Analysis Model) mercury chemistry and transport model covering central North America (southern tier of Canada to northern Mexico, including all of the continental U.S.) at 100 km resolution, to calculate U.S. and non-U.S. contributions to deposition in the U.S. Later calculations have been done for a nested grid within the primary continental TEAM grid, resolved to 20 km grid squares, for the eastern 2/3 of the United States.

The performance of the models was evaluated against data available from the U.S. national Mercury Deposition Network (MDN); MDN data consist of weekly average values of mercury wet deposition and mercury concentrations in precipitation at stations in a national network. For the coarse grid model simulations, run with 1998/1999 global and U.S. national mercury inventory data (1999 for U.S. power plants and incinerators, 1998 for all other sources) and synthetic 1998 meteorological data, station data for MDN from 1998 were used. Three global emission scenarios were used that differed in their distribution of background emissions among direct natural emissions and re-emissions of natural and anthropogenic mercury. North American anthropogenic sources were calculated to contribute from 25 to 32% to the total mercury deposition over the continental United States (depending on the scenario of background emissions employed).

More recent findings have recalculated U.S. and non-U.S. source contributions to U.S. mercury deposition at a 20-km grid scale. These results reinforce the earlier findings, that for most of the U.S., mercury deposition is dominated by distant sources uncontrollable by domestic action to lower mercury emissions. At selected receptors within the U.S., the contribution of U.S. anthropogenic emissions ranges from 5 to 50%; with the higher values of relative contributions generally lying in the region from Pennsylvania eastward through southern New England, to Massachusetts. Asian anthropogenic emissions are calculated to contribute from 16 to 31% of deposition at points within the United States, while natural

emissions contributed from 18 to 35%. Figure A.3-1 shows, at the 20 km resolution, percent contributions of non-U.S. anthropogenic sources to U.S. total (wet+dry) deposition of ionic plus particulate mercury. (These are the two forms of mercury most readily transformed into the organic methylmercury form that may accumulate in fish later consumed by humans.) Mass balance calculations indicate that about 75% of the total mass of mercury depositing to the U.S. each year originates outside the United States (the model results already account for U.S. emissions transported globally one or more times and then depositing in the U.S.).

Figure A.3-1. Percent contributions of sources other than U.S. anthropogenic mercury sources to U.S. mercury deposition, 20-km grid for central and eastern U.S., 100-km grid for western U.S.

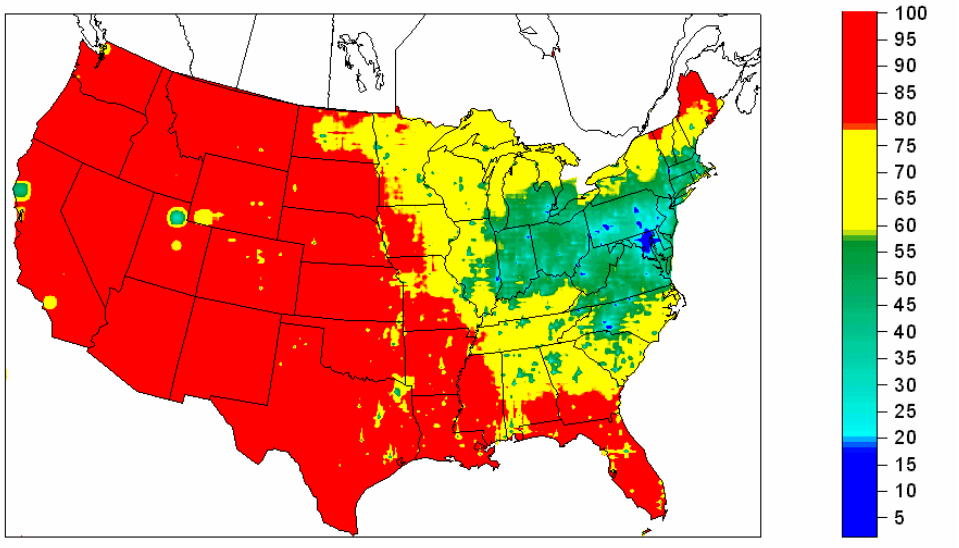

A.4. ORIGINS OF MERCURY DEPOSITING IN THE UNITED STATES: OBSERVATIONAL EVIDENCE

Following model results indicating large inputs from other continents, particularly Asia, to U.S. mercury deposition, EPRI undertook aircraft measurements of mercury emissions from China into the Pacific Basin, and tracked those emissions across the Pacific Ocean and into the United States. Using wind data, the mercury entering the U.S. was found to originate in both southeastern China and in Central Asia.

During EPRI experiments off East Asia in 2001, and off the U.S. west coast in 2002, researchers with the National Center for Atmospheric Research, the University of Iowa, and others used aircraft of NCAR, NOAA, and other agencies to measure mercury fluxes, forms, and profiles in the two regions. In 2001, units of the ACE-Asia experiment flew transects off the southeast coast of China to sense and track mercury emissions from the industrial complex surrounding the city of Shanghai, China. Preliminary estimates by Friedli et al. (2004) for the net mercury export from China are 6 to 16 tons per year of crustal mercury during the North China dust storms, about 165 t/y of gas-phase mercury from biomass combustion, and roughly 660 t/y from industrial sources, mostly from coal combustion.

Radke et al. (2004) flew a C-130 aircraft in both transects and profiles over the eastern Pacific in spring 2002. Back-trajectory calculations showed that two distinct mercury plumes detected at 5700 m and 7300 m msl could be traced respectively to the southeast China industrial complex, and to biomass burning in Central Asia or beyond. Forward trajectories of the two mercury intrusions moved them over the southeastern United States, then northeastward over the western Atlantic.

Radke et al. concluded that mercury intrusions, as a result of Asian mercury emissions maintained their well-distinguished form for several thousand kilometers, and were steered by boundary layer to upper air currents across the Pacific and into the United States. The presence of semi-permanent high pressure systems over the northern north Pacific implies steering currents that will frequently and consistently move the large Asian mercury emissions plume into U.S. territory.

A.5. CHANGES IN MERCURY EXPOSURE DUE TO DECLINES IN MERCURY EMISSIONS FROM UTILITY CONTROL SCENARIOS

The mercury emissions reductions proposed by EPA would result in slightly lower exposure to mercury by U.S. women of childbearing age. These improvements to public health would vary by location across the United States.

The reduced emissions of mercury from electric utility coal-fired power plants that would occur under EPA's MACT or Cap and Trade proposals would result in reduced mercury deposition across the U.S., and presumably to lower concentrations of methylmercury in fish in U.S. lakes and rivers. To a much lesser extent, reductions in U.S. emissions will result in reduced deposition on the oceans and to lower concentrations of methylmercury in marine fish. Calculations were carried out to assess how much change in mercury exposure would result following implementation of the various proposed rules.

In order to carry out these assessments, a number of assumptions had to be made to accommodate the understanding of mercury dynamics in water bodies and aquatic ecosystems, and to fit the estimated changes in deposition rates into a framework that includes the data on the geographic distribution of fish mercury concentrations. These assumptions are explained in more detail in Appendix B.

Briefly, it was assumed that mercury concentrations in fish respond instantaneously to changes in deposition, which in turn respond at once to changes in emissions. It is likely that fish response takes several years or longer to fully equilibrate with changes in mercury deposition, while deposition likely responds relatively quickly to changes in emissions. Both remain to be validated by full data sets.

Appendix B-3 provides a full description of the methodology used, while Figure A.5-1 shows the results of the assessment. In general, the analyses show that in comparison to 1999 levels, the average exposure will decrease by about 1.46% across the US under the Cap & Trade scenario. Under the MACT or CAIR scenarios, the average exposure would be reduced by about 0.9%. In some states, the reduction in exposure could be as much as 6.5%. These results are based on models and assumptions that tend to overestimate the effects of reductions in deposition on exposure, so they should be considered conservatively high. Comparison of relative changes in exposure under the two 2020 scenarios, relative to 1999, illustrates that, with respect to the deposition case under CAIR, Cap & Trade is in every case more protective that MACT, that is, for every state for which data are available, there is a greater decrease in exposure under C&T than under MACT.

Figure A.5-1. Calculated average change in methylmercury intake by state under proposed EPA MACT (upper panel) and Cap & Trade (lower panel) rules for utility mercury emissions; 2020 scenarios compared with 1999 exposures.

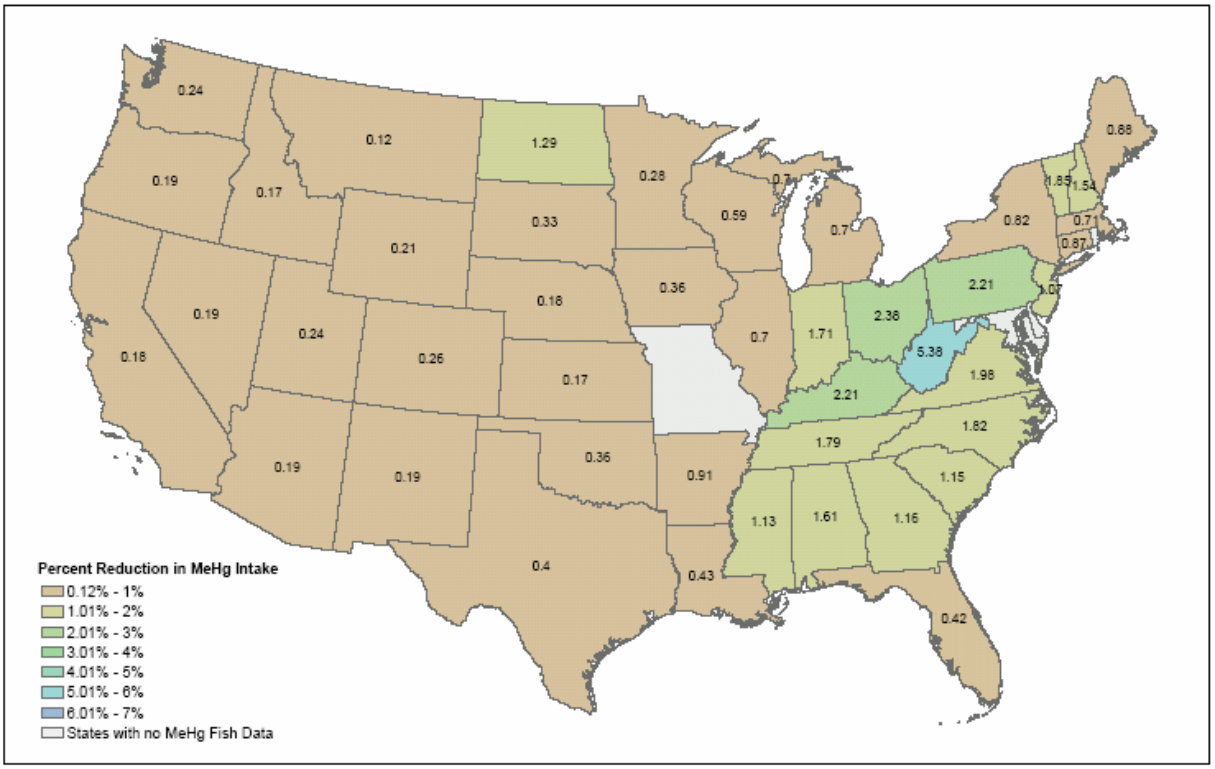

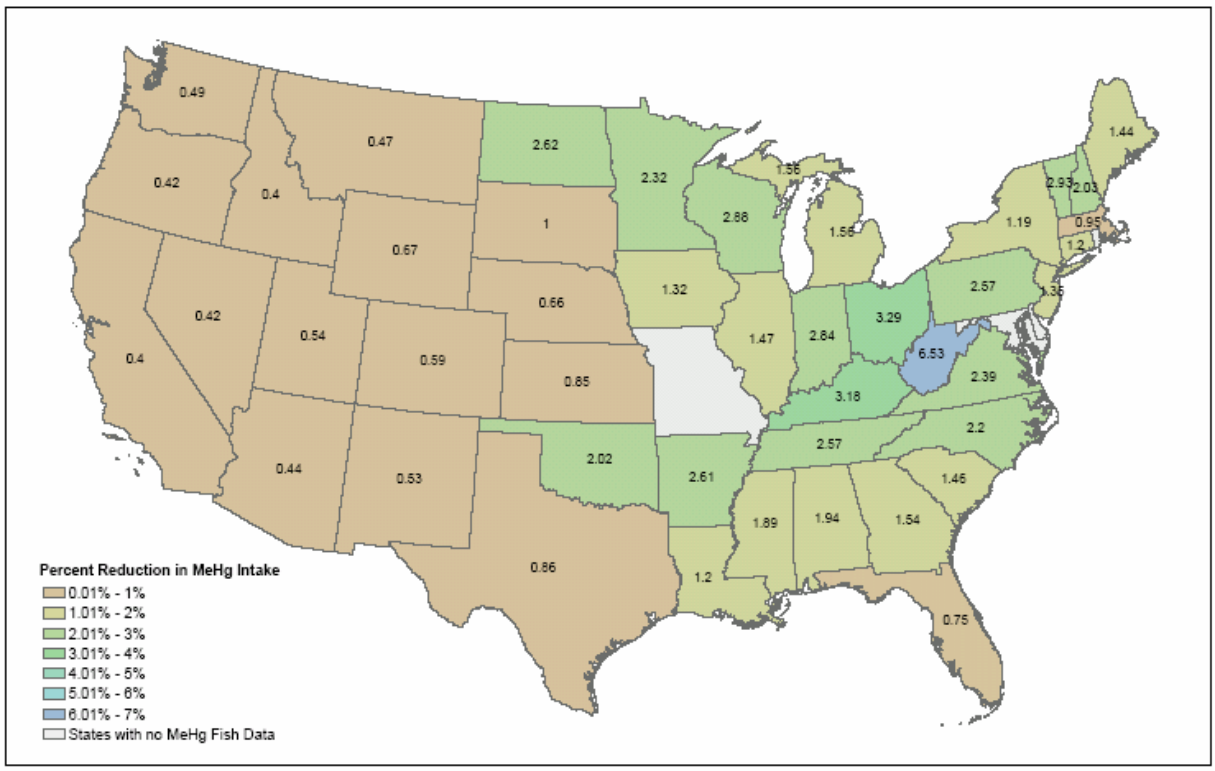

A.6. MERCURY CHEMISTRY IN POWER PLANT PLUMES

There is increasing evidence from laboratory, pilot-scale, and full-scale measurements that the divalent form of mercury may convert to the far less soluble elemental form within power plant plumes. This apparently rapid and complete conversion would reduce local-scale deposition from power plants significantly, if it is found to hold for a wide range of such sources.

Models of atmospheric mercury processes assume that the form of mercury occurring within power plant stacks is the same as that which enters the free atmosphere, with no chemical alteration occurring in the emissions plume. Prestbo and others have demonstrated the likelihood of significant mercury chemical reactions occurring in power plant plumes (Prestbo et al., 1999; MDNR-PPRP, 2000; EERC, 2001).

The evidence for such reduction comes both from measurements in plume dispersion simulation chambers operated at both pilot combustors and operating power plants, and from field observations at a mercury deposition measurement station downwind from a coal-fired power plant. The mechanism, rate, and conditions required for such reactions are still highly uncertain; but a program of field measurements in power plant plumes has begun to clarify the issue.

Emissions of mercury from elevated combustion stacks may occur in one or more of three chemical forms, or "species": elemental mercury [Hg(0)]; divalent, or ionic, mercury [Hg(II)], which is generally found (at room temperature) combined with other substances into mercury salts; and particulate-phase mercury [Hg(p)], which is chemically mostly Hg(II) but barely reactive due to combination with solid-phase material in the atmosphere. The primary forms of interest are Hg(0) and Hg(II), since particulate-phase mercury occurs in proportions of less than 5% in utility emissions.

Since Hg(II) is readily soluble in water and aqueous media (some six orders of magnitude more soluble than is Hg(0)), near-source deposition via solution into precipitation will be greater for sources emitting mostly the divalent form. Hg(0) typically is deposited over much wider areas, at lower concentrations than deposition closer to the sources. Its atmospheric lifetime is a few months, until oxidation and deposition occur.

Measurements have been carried out using chambers to simulate plume conditions at both power plants and waste combustors. The chamber studies found that, at coal-fired power plants, there was evidence of a very rapid reduction of the Hg(II) to Hg(0), of the order of a 30 to 50% conversion within a few minutes. These findings provide important new information on the true speciation of mercury from power plant stacks.

To verify these preliminary results, EPRI undertook a field program at several power plants using a combination of aircraft measurements, surface observations, in-plant measurements, and coal sampling. EPRI equipped an aircraft for repeated mercury measurements within the power plant plume at a range of downwind distances from the source. In steady wind conditions, these intersections with the plume represent fixed time-of-transit and relatively steady-state combinations of reaction products. The aircraft sampling and analysis equipment consisted of a Tekran 2537A/1130 Mercury Vapor and Speciation unit, with ancillary fast

sensors for CO, NOx, and SO2 used to trigger zero air input and discriminate between in-plume and ambient air samples.

To date, two power plants have been measured under this program: Plant Bowen, Georgia Power, Cartersville, Georgia; and the Pleasant Prairie Power Plant (P4), We Energies, Pleasant Prairie, Wisconsin. Results of the field measurement experiments were similar at each plant.

Plant Bowen: Prior to the fall 2002 field measurement experiment at Plant Bowen, matched observations of power plant mercury emissions and ground-level mercury measurements at a surface station at Yorkville some 25 km to the south southwest were correlated to gauge possible plume reactions following stack emissions. Edgerton (2004) analyzed air mass trajectory data using the NOAA HYSPLIT 4 Lagrangian trajectory model to visualize atmospheric transport during plume impingement events from Plant Bowen on the Yorkville station.

Coal data and continuous emission monitor (CEM) data for regional coal-fired power plants were obtained from Southern Company for specific days when a plume event was observed. These data were used to calculate a variety of emission ratios for elemental and divalent mercury at the sources, which were then compared with observed ratios at the sites. Repeated site measurements during a plume incursion at Yorkville were then compared with expected ratios in the plume expressed as the ratio at the source 25 km distant. Figure A.16-1 shows the outcome of this comparison for a single day's plume event. The proportion of Hg(II) at Yorkville was significantly lower than the expected ratio, while that of Hg(0) was significantly elevated. The ratio of Sox to Hg(tot) was used as a conservative plume tracer during these events, using the elevated Sox levels due to the stack emissions as the plume indicator.

Pleasant Prairie Power Plant (P4): P4 is a 1210 MW subbituminous coal-fired plant with two boiler units exiting from a single 450-foot exhaust stack. Predictions from the EPA ICR coal, mercury, and chlorine database indicated that both units were expected to emit about 85% elemental mercury, 14% oxidized, and less than 2% particulate-phase. Field research at the Pleasant Prairie Power Plant was carried out in August-September 2003. Sampling flights consisted of repeated plume transects at four sampling points between the stack location and 10 nautical miles downwind.

In-stack sampling was carried out simultaneously with aircraft operations for comparison of the ratios of divalent and elemental mercury to total mercury in the plume with those in the stack. In addition, a static plume dilution chamber used in earlier tests was run at the site for method validation purposes.

The data from Pleasant Prairie (summarized in Table A.6-1) show that, from the stack to the closest sampling distance, there was a significant increase in the elemental mercury concentration and a corresponding decrease in the divalent mercury concentration.

EPRI modeling sensitivity studies have been carried out using a range of values for the conversion rate of divalent to elemental mercury in plumes. The minimum and maximum measured values for these rates have been 14% and 67% reduction per hour of the divalent to the elemental form of mercury in plumes. These model plume reduction scenarios have shown significantly lower deposition from power plant mercury emissions in regions east of the Ohio River valley than was evident in the 2004 Base Case scenario (with no plume reactions

included). Model performance for the northeastern United States improved significantly when compared to data, yet good correspondence continued between data and model results throughout the balance of the country. These initial demonstrations of the significance of a potential reduction reaction may imply that utility power plant mercury emissions contribute less to downwind wet deposition than has been assumed previously.

Fig. A.16-1. Observed (Obs) and expected (Exp) emission ratios for Hg species, plume event of July 20, 2001. Units are pg/m^3 per ppb of SO_2.

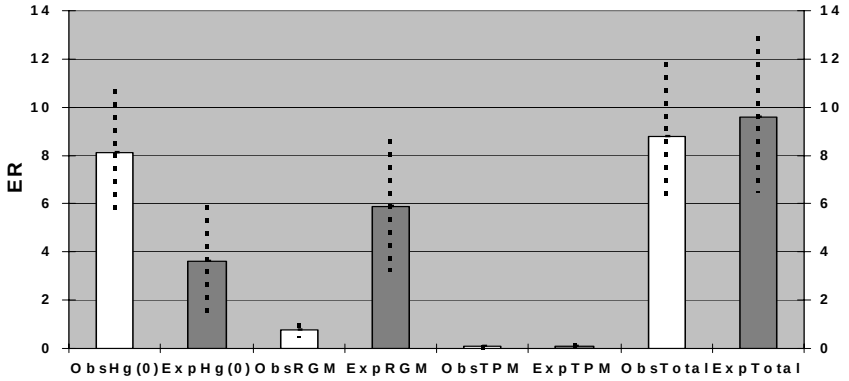

Table A.6-1. Mercury speciation proportions at Pleasant Prairie stack and in aircraft plume transects, August-September 2003.

Flight:	1	2	3	4	5	Average across flights
STACK MEASUREMENTS						
% Hg(0)	67	56	69	69	69	66
% Hg(II)	33	44	31	31	31	34
PLUME MEASUREMENTS						
0-Mile Sample Point						
% Hg(0)	85	79	75	82	82	81
% Hg(II)	14	21	25	17	17	19
5-Mile Sample Point						
% Hg(0)	90	83	93	89	89	90
% Hg(II)	9	17	7	10	11	9
10-Mile Sample Point						
% Hg(0)	91	85		87	88	91
% Hg(II)	9	14		13	12	9

A.7. ESTIMATES OF MERCURY DEPOSITION BY ATMOSPHERIC MODELS

The Eulerian regional models have been shown to systematically overestimate both wet and dry deposition when compared with estimated values from Gaussian plume models, typically used for local-scale (<50 km from source) simulations.

Both U.S. EPA and EPRI have been employing Eulerian regional models for simulating both deposition patterns of mercury under current emissions, and how those deposition patterns might change under proposed utility mercury regulation. There is strong evidence that those models tend to overestimate near-source ground-level concentrations and deposition of mercury when compared to equivalent calculations using plume simulation local-scale models. This overestimate may range from moderate (multiplicative factor of 1.5) to large (factor exceeding 3). The overestimates are due to the fact that regional models unrealistically deposit the mercury to ground level closer to the source than do single-source plume models. In addition, regional models do not include likely mercury reduction reactions in plumes that tend to reduce nearby mercury deposition. While comparisons imply that the regional models perform reasonably well for wet deposition, indications are that these models overestimate dry deposition. Further details are provided in Sections B and C.

There are several consequences due to these issues of model precision. First, it helps explain why models tend to show higher deposition than is measured by mercury monitoring stations in some regions of the United States. Second, these overpredictions of deposition will tend to overestimate (or make more conservative) the assessments of how much mercury is entering various waterbodies, accumulating in fish and eventually resulting in a potential exposure to humans. Thus, the information shown later on exposure, assuming the assumptions on mercury cycling in the environment are reasonable, can be considered as high-end estimates.

A.8. MERCURY CYCLING IN TERRESTRIAL AND AQUATIC ENVIRONMENTS

The state-of-the-science is too imprecise to predict either the timing or the magnitude of fish mercury concentration changes due to changes in atmospheric deposition.

Relative to other metals, the biogeochemical cycling of mercury is complex (Figure A.8-1). Two major factors are: (1) under certain circumstances mercury can form organic complexes (e.g., methylmercury, dimethylmercury, etc.), and (2) mercury has a significant atmospheric component in its cycle. Formed in anoxic zones in aquatic systems, methylmercury is the major organic form; in freshwater systems only about 1-2% of total mercury occurs in the organic form. Methylmercury bioconcentrates in aquatic organisms after it is initially taken up by algae and then transferred via predation up the food chain. The bioaccumulation factor (BAF) for methylmercury from water column to top-level pisciverous fish can be well over one million. However, BAFs vary widely among systems and there is poor correlation between the concentration of methylmercury in water and total mercury in fish, indicating that site-specific conditions affect mercury behavior. Elemental mercury is volatile and has been

observed to evade to the atmosphere from both water bodies and faunal and ground surfaces in terrestrial environments. Much remains to be learned about fluxes of gaseous mercury in ecosystems. The complexity of mercury's behavior in the environment is such that many questions cannot yet be answered including:

- If power plant mercury emission rates are reduced, what will be the response of fish mercury?
- How long will it take before seeing a response in fish?

These questions and many others are being investigated in a whole-ecosystem mercury loading experiment, Mercury Experiment to Assess Atmospheric Loading in Canada and the United States (METAALICUS), being conducted at the Experimental Lakes area in Canada. The team of investigators from the U.S. and Canada is investigating essentially each flow path shown in Figures A.8-1 and A.8-2

Figure A.8-1. Schematic of mercury cycling processes in a typical lake.

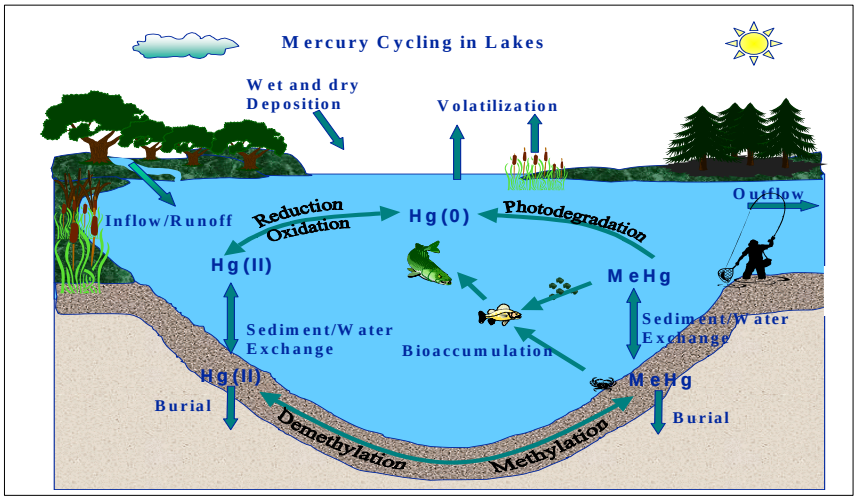

In the METAALICUS study, mercury is being added to the ecosystem in the form of stable (non-radioactive, non-decaying) mercury isotopes in amounts to simulate total mercury deposition of ca. 22 µg/m^2-y, about 5 times the area's current background rate. Three mercury isotopes are used, ^{202}Hg for the lake surface, ^{200}Hg for surrounding catchment and ^{198}Hg for a small adjacent wetland. The team of scientists investigating vegetation and soils is examining the processes shown in Figure A.8-2.

Figure A.8-2. Terrestrial mercury fluxes and processes investigated in METAALICUS.

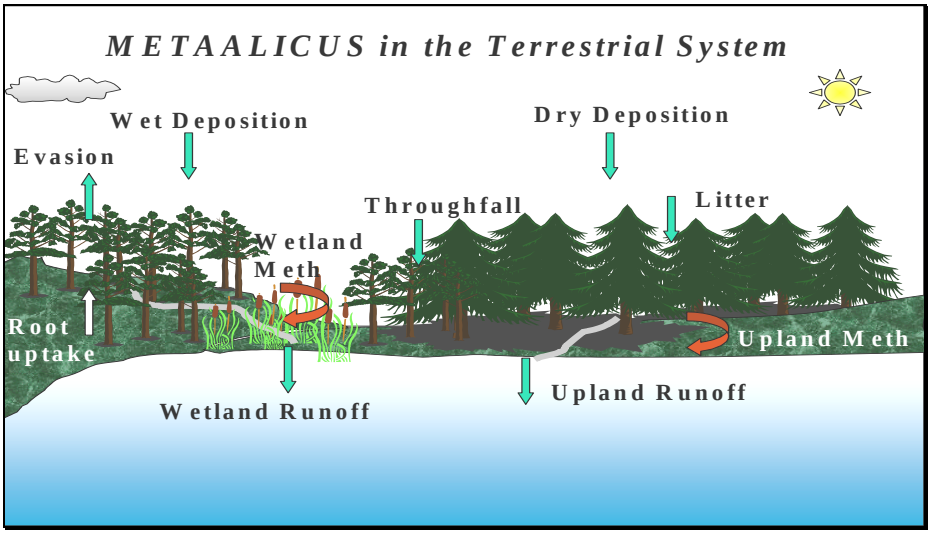

The isotopes were applied yearly in the period 2001-2003, with another application planned in 2004. Different isotopes were used each year in each compartment (water body, wetlands, and uplands) of the lake watershed. Because of the time required to process samples, results from 2003 are not yet fully available. The first two years showed that mercury added directly to the lake surface began to be converted to methylmercury quickly and was observed in fish in the same season. Furthermore, significant amounts (20-30%) of isotope added directly to the lake were re-emitted through time to the atmosphere (Lindberg, unpublished data). After two years, approximately one quarter of the mercury in young perch was due to mercury added directly to the lake surface (Blanchfield, unpublished data). Newly added mercury appeared to be more available to bacteria to convert to methylmercury than mercury that was in the system for longer periods (Gilmour et al., 2003). In contrast, the movement of mercury in soils of the terrestrial system did not appear to respond as quickly to changes in atmospheric deposition (Hintelmann et al. 2002). Very little of the mercury applied to the upland and wetland had emerged after the first 2 years of additions. These results together suggest that lakes receiving the bulk of their mercury directly from deposition to the lake surface (e.g. some seepage lakes) would see fish mercury concentrations respond more rapidly to changes in atmospheric deposition than lakes receiving most of their mercury from terrestrial runoff. Regardless of the initial findings from the METAALICUS study, the two fundamental questions about magnitude and timing of the response of fish mercury concentrations cannot yet be answered. The study will continue for several years after the artificial additions cease at end of 2004. The results of a return to the background loading rate will then be examined.

The knowledge gained from METAALICUS is being used to improve EPRI's Dynamic Mercury Cycling Model (D-MCM). In turn, modeling results are used to improve the experimental approaches. This iterative, process-based approach allows the researchers not only to document what is happening, but also to understand *why*. This is necessary to permit METAALICUS study results to be used to make predictions for other systems.

EPRI's D-MCM has been used to model numerous lake systems to predict the timing and magnitude of fish responses to decreased mercury loadings. Sensitivity analysis has revealed

that small changes in assumptions about depth of the active sediment layer and the exchangeability of inorganic mercury between sediment and water result in large changes in fish responses. In modeling runs simulating fish mercury in four regionally separated U.S. lakes, when the active sediment layer was assumed to be 3 cm thick and inorganic mercury on particles was assumed to be freely exchangeable with the water, fish mercury concentrations were predicted to require from 40 to 160 years following load reductions to reach 90% of new steady state concentrations. However, when the active layer was reduced from 3 to 1 cm and the exchangeability of mercury between sediment and water was reduced by 90%, the predicted time for fish mercury concentrations to reach 90% of steady state came down to 23 years (EPRI 2003). These sediment parameters are a focus of current research in the METAALICUS project.

It will be some time before model simulations can provide accurate predictions of the timing and magnitude of fish mercury changes following loadings reductions. Even more challenging is the need to predict just how much loadings should be reduced to see fish mercury concentrations reach desired levels.

A.9. MERCURY HEALTH EFFECTS

The risk of adverse neurodevelopmental effect for children exposed to MeHg in utero at or above 0.1 µg/kg-day, the EPA Reference Dose (RfD) for methylmercury, is not detectable above background occurrences. Thus, the entire basis for establishing the potential risks of mercury exposure is thrown into question.

Characterizing children exposed above the U.S. EPA Reference Dose (RfD) as "at risk" carries the implicit assumption that the RfD represents a bright line delineating safe and harmful exposures. To state that exposures above the RfD places children "at risk", without qualifying terms to explain or quantify that risk, is misleading.

In establishing the RfD, results from several neurodevelopmental tests administered to 7 year olds in the Faroe Islands were applied by USEPA to qualitatively corroborate results from the primary test used to establish neurodevelopmental adverse effect, the Boston Naming Test (BNT) (Grandjean et al., 1997). The numerical value of the MeHg RfD is based directly on results from the BNT as administered in the Faroes study.

The BNT was originally developed as an aid in identifying adult (usually elderly) individuals with aphasia (Goodglass & Kaplan, 1983a, 1983b; Kaplan et al., 1983). Aphasia can be recognized as a defect in expression by speech or of comprehending spoken or written language and is often related to dementia, stroke, or other brain trauma. The average expected score in normal children ("norm") for the BNT (apparently without cues, or direction toward a response by the test administrator) was originally determined by Goodglass and Kaplan, the developers of the BNT, on 5 children whose mean age was 7.5 years. The mean score for these 5 children was 37.0 with a standard deviation (SD) of 4.15 and a range of 34-45 (Goodglass & Kaplan, 1983b, p. 8).

Subsequently, 241 normal US children, aged 6-12 years were scored on the BNT (Halperin et al., 1989). Among these, forty 7-year olds were tested who scored a mean of 38.83 (SD 6.0) without cues. With phonemic cueing, the average score for these 40 children improved to 40.73 (SD 4.3). The authors concluded that, in children, the BNT score relates more to acquired word knowledge than to word retrieval or fluency, and that verbal memory appears to be independent of these linguistic functions.

For comparison, Figure A.9-1 shows BNT scores for 7-year-old children exposed to methylmercury *in utero* in the Faroes (NRC, 2000); this plot indicates that at the lowest exposure value experienced (mercury in cord blood of 1 μg/L), the BNT scores appeared to be between 25 and 27 (no unexposed control group was tested in this study). This difference in average baseline score between Faroese children and normal US children is striking; it suggests that factors other than or in addition to exposure – such as word knowledge and test administration procedures – may have influenced test score outcomes.

Figure A.9-1. Boston Naming Test Score vs. cord blood mercury concentration for the Faroe Island cohort. Dose-response curves fitted to cord-blood mercury data for linear, square root and log transformation models are shown. (NRC, 2000, p. 296).

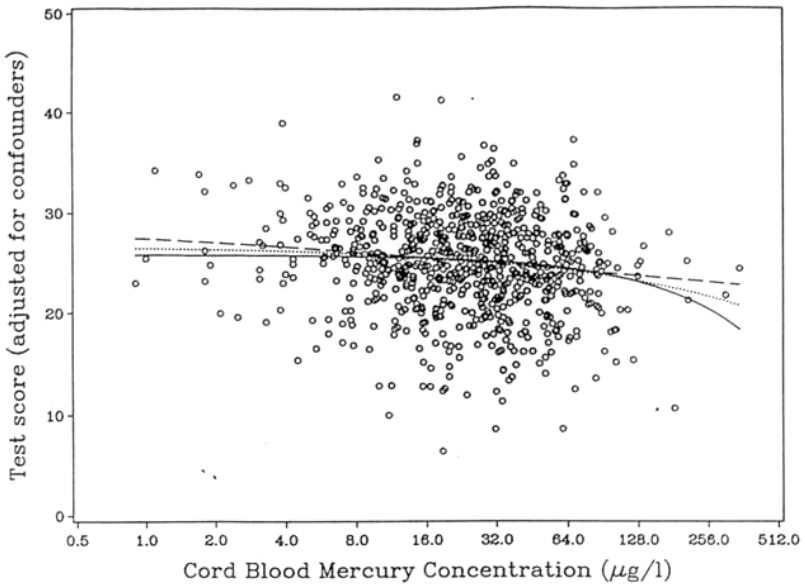

Neurodevelopmental tests, in general, have not been found to be useful in diagnosing specific school learning problems (Berninger & Colwell, 1985). In terms of educational findings, the BNT appears to be significantly related to reading comprehension, again illustrating that BNT scores are likely to be related to word knowledge rather than verbal memory or word retrieval.

More recently, it has been shown that three different seemingly correct interpretations by professional psychologists of the scoring methods published by Kaplan et al. (1983) for the BNT resulted in large, clinically significant differences in the total score (Lopez et al., 2003).

This brief review of the BNT illustrates that large uncertainties exist in the administration, scoring, and clinical interpretation of the test, particularly in children. Failure of the BNT to

successfully meet the basic criteria associated with a valid test that would accurately reflect an adverse health effect requires further examination.

The dose-response model relied upon by the 1999-2000 National Research Council panel for recommending the methylmercury RfD was examined (NRC, 2000). This model predicts that expected scores of all exposed children (not just those whose mothers were exposed above the RfD) on the BNT administered at seven years of age in the Faroes are shifted downward by an amount proportional to the concentration of methylmercury in the children's cord blood. Figure A.9-2 below shows the distribution of test scores predicted by this model in children of mothers unexposed to methylmercury, compared to children whose mothers were exposed at the RfD. The difference in these distributions, which is barely discernable in Figure A.9-2(a), corresponds to a change in the mean score on a standardized test of 0.25%. Assuming that the BNT mean score without cues for US 7 year olds is 38.83 (Halperin et al., 1989), the expected mean score for the approximately 300,000 children exposed per year at the RfD is 38.73 – a decrement of 0.1 point that is clearly not detectable, and not meaningful given the standard deviation of 4 to 6 on BNT scores.

Further, in the U.S. NHANES data set (USDHHS 2002), the 99.8th percentile level of blood mercury levels among U.S. women of childbearing age (2nd highest value among 1588 measurements from such women) was 22 μg/L, corresponding to a mercury intake of 3.8 times the RfD. It is thus estimated that 8000 children (or 0.02% out of a total of 3,900,000 born) are born in the U.S. every year to mothers exposed above this level, which corresponds to exposures among women in the Faroe Islands who were high consumers (3 or more dinners per week) of pilot whale with a high content of methylmercury (Grandjean et al. 1992). These 8,000 children represent only 2.7% of the 300,000 estimated as being born yearly to mothers exposed above the RfD. Figure A.9-2(b) shows the increment of expected change in the test score distribution resulting from this exposure level, which corresponds to a change in the mean score on a standardized test of 1.6%. Again, assuming the average score on the BNT for U.S. seven year olds is 38.83, the expected average score for children exposed at 3.8 times the RfD would be 38.21. Clearly this difference is also not detectable given the high variance on tests of this nature and, in particular, on the Boston Naming Test—the test results in the Faroes study upon which the numerical value of the RfD is based.

Fig. A.9-2. Predicted distribution of performance in children not exposed to methylmercury and in children whose mothers were exposed at the RfD (Panel a) or at 3.8 times the RfD (Panel b), using the NRC model.

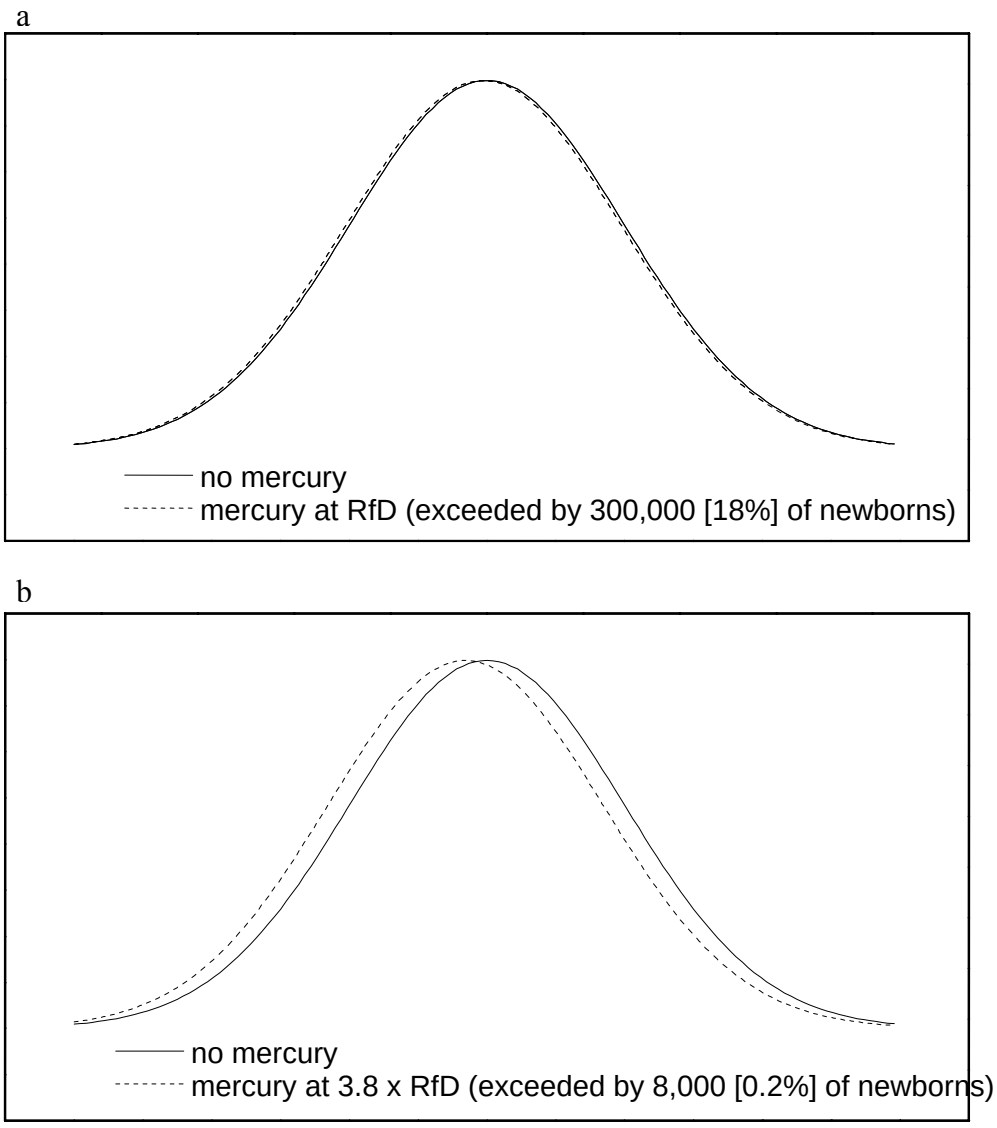

These calculations involve extrapolation beyond the range of the data, however, these estimates are no more uncertain than estimates of cancer risk from low exposures, for which data are generally unavailable as well. The NRC model used in developing Figure A.9-2 assumes that there is no lowest threshold for effect and that the risk varies linearly with exposure. As such, risks illustrated by this figure are more likely to be overestimates than underestimates.

The purpose of the foregoing informative analysis is not to minimize or dismiss the potential health risk from exposure to methylmercury; an actual decrease in neuropsychological health

should be treated in a serious manner if it is posed. However, it is important to have a clear understanding of the nature and severity of potential risks from exposure to methylmercury as they occur in the U.S., particularly at and above the RfD. The estimates shown here indicate that there is essentially no discernable adverse neurobehavioral effect for *in utero* exposure at the RfD or at 3.8 times the RfD. This conclusion renders use of the term "children at risk" essentially meaningless in this context.

A.10. MERCURY EXPOSURE OF U.S. CHILDREN

The estimate that more than 600,000 US children have an exposure to methylmercury at or above the EPA Reference Dose (RfD) of 0.1 µg/kg-d is not supportable. It is based on the 1.7:1 ratio of cord blood to maternal blood mercury that has already been accounted for by EPA in the derivation of the RfD uncertainty factor.

Mahaffey et al. (2004) discuss the ratio of fetal blood mercury to maternal blood mercury. The article states:

> "Applying the overall population estimate for adult women of 7.8% having BTHg ≥ 5.8 µg/L (Schober et al. 2003) to the number of newborns in 2000 (Ventura et al. 2003) suggests that > 300,000 newborns per year may have had increased risk of adverse neurodevelopmental effects as a result of in utero MeHg exposure if a 1:1 ratio of cord blood Hg to maternal blood Hg is assumed. More recent evaluation (Stern and Smith 2003) of the ratio between cord to maternal blood Hg concentrations indicates that cord blood is, on average, 70% higher in Hg concentration than is maternal blood. Assuming the ratio of 1.7:1.0 and calculating the average BTHg associated with the benchmark dose lower limit and RfD (using the same UF of 10) suggests that a BTHg ≥ 3.5 µg/L may be associated with increased risk to the developing fetal nervous system."

A reasonable inference to draw from these statements, and those made in a public presentation, is that information developed since the derivation of the methylmercury RfD in 2001 now indicates that the RfD may be insufficiently protective, leading to an estimate of at least 630,000 children at risk (Mahaffey, 2004b). However, in the IRIS description of how the methylmercury RfD was derived (at <http://www.epa.gov/iris/subst/0073.htm>), the blood ratio is discussed:

> Typically, a strong correlation exists between maternal-blood mercury concentrations and fetal-blood mercury concentrations, as shown by cord-blood. A review of the literature identified 21 studies that reported cord-blood mercury and maternal blood mercury data (Amin-Zaki et al., 1974; Baglan et al., 1974; Dennis and Fehr, 1975; Pitkin et al., 1976; Kuhnert et al., 1981; Nishima et al., 1977; Lauwerys et al., 1978; Fujita and Takabatake, 1977; Kuntz et al., 1982; Tsuchiya et al., 1984; Truska et al., 1989; Sikorski et al., 1989; Hansen et al., 1990; Soong et al.,1991; Soria et al., 1992; Ong et al., 1993; Akagi et al., 1997; Yang et al., 1997; Ramirez et al., 2000; Bjerregaard and Hansen, 2000; Vahter et al., 2000). Overall, data from these studies indicate that cord-blood mercury is higher than maternal blood mercury. The composite ratio from the studies reporting methylmercury concentrations indicates that the cord-blood: maternal blood ratio is around 1.7. These values are ratios of means and do not reflect the full range of variability in the individual mother-fetal pairs. Vahter et al. (2000) reported the 5th and 95th percentiles of cord:maternal Hg to be 0.88 and 3.1. Individual data were available from Fujita and Takabatake (1997); ratios calculated from these data ranged from 0.78 to 4.36.
>
> EPA has chosen not to make a numerical adjustment between cord-blood and maternal-blood mercury. At this time the relationship between cord-blood and maternal-blood mercury is considered subject to variability and uncertainty, and is to be included in the determination of the uncertainty factor (UF)."

As this excerpt from U.S. EPA IRIS database indicates, EPA recognized at the time the RfD was being derived that the ratio of cord blood mercury to maternal blood mercury was of the order of 1.7:1, and chose to include this factor in the uncertainty factor. Stern and Smith (2003) as cited in Mahaffey et al. (2004a) is consistent with EPA's analysis in IRIS. The assertion that new information has been developed (Mahaffey, 2004b) that would alter the RfD does not appear to reflect the reality that the cord blood to maternal blood mercury ratio has already been accounted for in the derivation of the RfD. Explicit inclusion of the 1.7:1 ratio as a modifying factor in a new calculation of the Reference Dose would be double-counting, essentially weighting the factor at twice its true value, and introducing a numerically conservative factor that is unwarranted by the data.

A.11. STACK SAMPLING FOR COMPLIANCE TESTING

The sorbent trap method (proposed Method 324) is applicable to all sources and does not require special QA/QC requirements. Detailed instructions on the use of this method would insure that all interested testing firms and analytical laboratories use the same procedures.

The monitoring provisions of the supplemental proposed rule include a number of limitations on the use of sorbent traps and specify extensive QA/QC requirements. Field results have shown that this method is equally applicable to units of all size and emission level. The trap method has produced equivalent results to the accepted reference method (Ontario Hydro Method) in all tests conducted to date. Instrument drift is not an issue with a sorbent trap method, so standard intervals for relative accuracy audits are adequate. Further, by the nature of this method, the routine QA provided during sampling and analysis (blanks, spikes, and leak checks) actually exceeds that required for continuous analyzers. Regarding sampling rate, the stepped approach to flow proportional sampling is more difficult to achieve then continuous proportional sampling. Moreover, EPRI tests have shown that proportional sampling provides <2% improvement in accuracy relative to constant flow sampling and introduces more likelihood of sampling error or equipment failure. While dual or paired sampling reduces the chance of missing data, the trade-off between the use of dual/paired sampling and the risk of experiencing missing data seems appropriately to be a user decision. If paired sampling is used, standard practice is to report the average when the relative percent difference (RPD) is less then 30%. If the RPD value exceeds 30%, both values are typically deleted.

A.12. ATTAINMENT OF EMISSIONS CAPS

Modeled predictions of when emissions would ultimately reach the 15 ton/yr Phase II cap in the proposed Cap & Trade rule are sensitive to model assumptions concerning co-benefits, control effectiveness, and other poorly determined variables. EPA assumptions produce a longer phase-in period than the set of assumptions used by EPRI, considered more realistic based on research results.

EPRI simulations indicate Hg emissions would reach 15 tons in 2020, due to a lower estimate of mercury banking occurring in Phase I Cap & Trade compared to results from the EPA

modeling. EPRI estimates that mercury emissions in 2018 would be 23.9 tons, but fall to the Phase I target of 15 tons within two years (i.e., by 2020). The relatively smaller bank of allowances accumulated in Phase I Cap & Trade would be completely depleted during the years 2018 and 2019.

As for any national-scale modeling of economic processes, assumptions will likely differ from eventual reality. However, EPRI selected its assumption to represent what we believe to be reasonable national and regional patterns and "best estimates".

The differences in emissions banking behavior between EPRI simulations and EPA's results are due to three factors (evidence supporting each of the following points is provided in Appendix C):

1. EPA assumes larger Hg reductions from key SO_2 and NOx controls ("co-benefits") than is the current technical consensus.
2. EPA's cost and effectiveness assumptions for removal of Hg using activated carbon injection are more pessimistic than those incorporated in the EPRI model.
3. Other EPA assumptions appear to cause the model to rely more on FGD retrofits over coal switching for units to achieve SO_2 targets than EPRI assumes.

The net effect of these three differences is substantially greater banking during Phase I in EPA's simulations than in EPRI's. EPA's model will generate lower marginal costs ($/lb Hg removed) to exactly meet a Phase I cap of 34 tons, yet it will generate higher marginal costs to exactly meet a Phase II cap of 15 tons. Therefore, in the absence of banking, allowance prices simulated by EPA's model would increase at a more rapid rate than they would increase in the EPRI simulations. The least-cost response to a banking provision is to decrease emissions below the cap in the early phase in such a way that the marginal cost is higher at the start, and lower at the end. Because the EPA model faces a higher rate of increase in marginal costs prior to banking, it generates a larger amount of banking in the early years, and hence a later date when the last cap is physically achieved. EPRI's simulations employ assumptions which EPRI researchers view as more realistic and thus result in the 15 ton cap being met by 2020.

A.13. PROBABILISTIC ASSESSMENT OF MERCURY EXPOSURE FROM INDIVIDUAL POWER PLANTS [

A probabilistic analysis of mercury exposure near power plants shows extremely low likelihood of exposures exceeding the EPA Reference Dose under 2004 conditions, and an order of magnitude drop in these probabilities under either MACT or Cap & Trade.

The potential health effects of mercury emissions from individual power plants can be examined using a probabilistic approach that takes into account the uncertainties and variability associated with the fate and transport of mercury in the environment. The analysis would then assess the likelihood of exposure at levels above the Federal Reference Dose for all U.S. residents living within local scale (that is, within 30 miles or 50 km) of a coal-fired power plant.

EPRI conducted this analysis of the impacts of individual plant exposure following the methodology of Lohman et al. (2000). The processes simulated include the emission of mercury from an individual power plant, its atmospheric transport, transformation and deposition to a watershed, its fate and transport within the watershed and the corresponding lake, its bioaccumulation in the aquatic food chain, and exposure of sensitive individuals via fish consumption.

The probabilistic analysis includes both variability (i.e., aleatory uncertainties) and uncertainty (i.e., epistemic uncertainties) in the analysis input variables.

Variability is accounted for in several components of the model: power plant mercury emissions (across the U.S. population of coal-fired power plants); atmospheric dispersion characteristics (stack characteristics, local terrain, and meteorology, including precipitation); the location of receiving waters with respect to the power plant emissions; fate and transport of mercury in the watershed; mercury cycling in the target lake; bioaccumulation of mercury in fish; fish consumption; and body weight of women of childbearing age. Table A.13-1 lists the probability distributions used to represent variability.

Uncertainty is accounted for in other model components: the Hg(II) (divalent mercury) emission rate, dry deposition velocity of Hg(II), lake pH, lake temperature, concentrations of dissolved organic carbon and chloride in the lake, particle sinking velocity in the lake water column and sediment burial rate. Table A.13-2 lists the probability distributions used to represent uncertainties.

The mercury power plant emission distributions were constructed from emission files used in the modeling of national utility mercury emissions (Charles River Associates, 2004). Those represented four different emission scenarios: 2004 Base Case, 2020 CAIR, 2020 MACT and 2020 Cap & Trade (C&T) scenarios. The analysis was conducted on a power plant basis (rather than on a stack basis). Because Hg(0) is not deposited locally, we only considered Hg(II) emissions [Hg(p) emissions were treated as Hg(II) for the purpose of this analysis].

The dry and wet deposition fluxes of mercury were based on those obtained in four recent case studies. Those case studies included three actual power plants in different eastern U.S. environmental settings; one of those power plants was analyzed under two operational settings, before and after installation of a wet scrubber respectively.

The deposition fluxes obtained in those case studies were modeled over 40 sectors, spaced at 10 km radii to a distance of 50 km from the plant, and spanning a 45 degree angle. It was assumed that a lake could be located in any of those sectors. The deposition fluxes were normalized to a unit emission rate of Hg(II). Therefore, distributions of 160 dry and wet fluxes (40 sectors x 4 case studies) were constructed for wet and dry deposition. These distributions account for the variability in stack characteristics, meteorology (including precipitation), and local terrain.

The watershed, lake and bioaccumulation components of the analysis were identical to those used by Lohman et al. (2000). The human exposure component of the study was selected to be identical to that used by Seigneur et al. (1997).

The analyses were conducted using the model developed by AER for previous probabilistic exposure studies (Seigneur et al, 1997; Lohman et al., 2000). The probabilistic calculations were performed with the Crystal Ball© software. A one-dimensional approach was used, thereby combining variability and uncertainties into a single analysis (Lohman et al., 2000).

The results of these emission scenarios are summarized in Table A.13-3 and depicted for the 2004 base scenario in Figure A.13-1.

The EPA reference dose of 10^{-4} mg/kg-day is exceeded by 0.6% of residents living within 50 km of any power plant for the 2004 Base Case, and by 0.04% of such residents for each of the three 2020 scenarios for CAIR, MACT and C&T. Thus, the fraction of the local population that may be exposed to doses exceeding the EPA Reference Dose decreases under both the C&T and MACT scenarios. Because this analysis included scenarios that may not actually exist (e.g., lakes were located anywhere around a power plant with equal probability), it is likely to provide an upper limit on population exposure.

Table A.13-1. Probability distributions used to represent variability.

Variable	Distribution function	Characteristics	Source
Hg(II) emission rate	Actual distribution	NA	CRA, 2004
Dry deposition flux	Actual distribution	NA	AER, 2004
Wet deposition flux	Actual distribution	NA	AER, 2004
Watershed fate and transport	Lognormal truncated	Mean=2.42, sigma=0.38	Lohman et al., 2000
Lake cycling	Lognormal truncated	Mean=45.4 y/m, sigma=26.3 y/m	Lohman et al., 2000
Bioaccumulation factor	Lognormal truncated	Mean=390,000 l/kg sigma=218,000 l/kg	Lohman et al., 2000
Fish ingestion rate	0 up to 65th %tile, exponential truncated above 65th percentile	Mean=3.7 g/day, maximum value=200 g/day	Seigneur et al., 1997
Body weight	Lognormal	Mean=66 kg, sigma=13 kg	Seigneur et al., 1997

Table A.13-2. Probability distributions used to represent uncertainties.

Variable	Distribution function	Characteristics	Source
Hg(II) emission rate	Normal	Sigma=5%	This work
Dry deposition velocity	Lognormal	Sigma=0.25 cm/s	Lohman et al., 2000
Precipitation	Normal	Sigma=5%	This work
Lake pH	Normal	Mean=7.7, sigma=0.3	Lohman et al., 2000
Chloride concentration	Normal	Mean=8.5 mg/l, sigma=1.04 mg/l	Lohman et al., 2000
DOC concentration	Normal	Mean=3 mg/l sigma=0.67 mg/l	Lohman et al., 2000
Lake temperature	Normal	Mean=21.9 C sigma=1.5 C	Lohman et al., 2000
Particle settling rate	Normal	Mean=0.75 m/day, sigma=0.204	Lohman et al., 2000
Burial rate of sediments	Normal	Mean=1.83 mm/y, sigma=0.5 mm/y	Lohman et al., 2000

Table A.13-3. Human Dose (mg/kg-day) from the four emission scenarios

Statistic	**2004 Base**	**2020 CAIR**	**2020 MACT**	**2020 C&T**
Mean	3.5×10^{-6}	5.64×10^{-7}	5.27×10^{-7}	4.79×10^{-7}
90%	4.83×10^{-6}	3.27×10^{-7}	3.13×10^{-7}	1.62×10^{-7}
95%	1.39×10^{-5}	1.34×10^{-6}	1.22×10^{-6}	6.93×10^{-7}
97.5%	3.00×10^{-5}	3.93×10^{-6}	3.41×10^{-6}	1.94×10^{-6}
% at which Dose = 1×10^{-4} mg/kg-day	99.4	99.95	99.96	99.96

Figure A.13-1. The cumulative frequency distribution of human mercury dose in the 2004 Base Case scenario

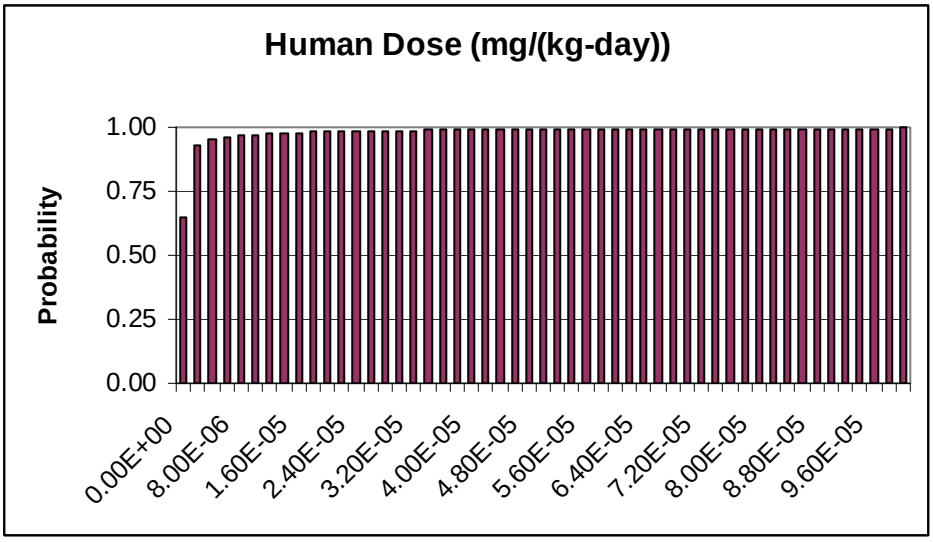

A.14. STATUS OF MERCURY CONTROL TECHNOLOGIES

Mercury control technologies are not yet commercially available, although significant research is underway by the private and public sectors. Before commercial availability is achieved, technologies must be tested over sufficiently long periods, assessed with regard to their applicability to the range of coals and emission control technologies in place, and examined with regard to costs and potential impacts on plant performance.

EPA has based its proposed MACT limits on the mercury emission levels measured at existing coal-fired power plants. In these plants, mercury is captured by the air pollution control devices (APCDs) used to capture particulate (fly ash) and/or SO_2. No power plants currently employ controls specifically for mercury. Over the course of the past 15 years, EPRI has performed extensive research to understand the character of mercury emissions and how to reduce them. Despite the efforts of these parties, no mercury-specific control technologies have been tested sufficiently to determine the sustainable mercury emission levels they can provide, their applicability to the range of coals and air pollution controls (for particulate, NOx, and SO2) used by the power industry, their potential impacts on boiler performance or the environment, and their costs.

This work has been conducted in collaboration with the power generation industry electricity generators and their suppliers, the U.S. Department of Energy, and the U.S. EPA. The industry's contribution to this work through EPRI has ranged from $1-2M/yr in the late 1980's and early 1990's to nearly $7M/yr over the past few years; industry, DOE, and others have spent equivalent or greater amounts during this period. The result has been a significant improvement in the understanding of mercury chemistry, but with substantial gaps still remaining, and the conception, development and short-term proof-of-concept testing of numerous potential mercury controls at scales up to and including full-scale. Longer-term tests of the most promising technologies are currently underway in a public/private collaboration with major funding from DOE; the first round of tests are planned for 2004-2006, and DOE is soliciting proposals for a second round of tests (on technologies not yet ready for field testing when the first round was solicited a year ago) that could start in 2005. EPRI agrees with EPA that, despite the efforts of these parties, none of these technologies are currently adequately tested and/or used in commercial applications to determine the sustainable mercury emission levels they can provide, their applicability to the range of coals and APCDs used by the power industry, their potential impacts on boiler performance or the environment, and their costs. This statement applies equally to mercury controls for existing and new units.

The following discussion responds to EPA's request for comments on the status of sorbent injection, the use of selective catalytic reduction (SCR) to enhance mercury capture by particulate and SO_2 controls, and other technologies in the development pipeline.

Sorbent Injection. Figure A.14-1 summarizes the results obtained to date on sorbent injection ahead of an electrostatic precipitator (ESP) by EPRI or from projects with EPRI involvement (including DOE-funded projects).[5] These are all short-term tests (hours to a few days) on power plants with large ESPs. They show a strong dependence of performance

[5] Further details are contained in *Analysis of Key Parameters Impacting Mercury Control on Coal-Fired Boilers,* Sjostron, S., et al., Air Quality IV, Arlington, VA, September 2003

(mercury emission reduction at a given sorbent injection rate) with fuel. However, in most cases, we have data for just one site for any given fuel, so we do not know if each line is unique or representative of that class of fuel. This is a critical knowledge gap, because it prevents suppliers and users from being able to extrapolate performance at these sites to any other "similar" site. Therefore, users cannot procure a sorbent injection system with confidence of its mercury removal performance; hence the technology should not yet be considered as commercially available.

Fig. A.14-1. Mercury removal by activated carbon injection ahead of an ESP

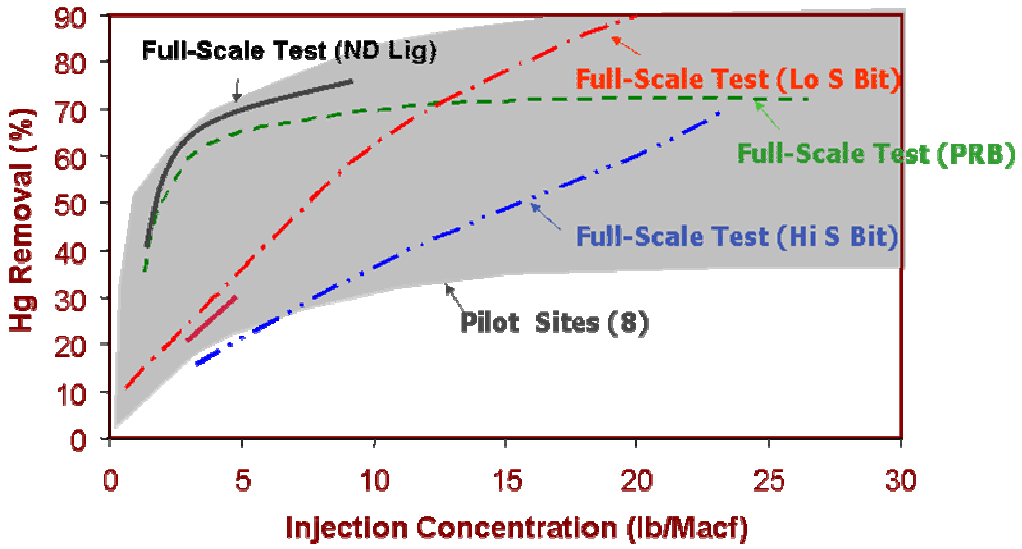

Data from the site burning North Dakota (ND) lignite (Figure A.14-1) suggest that the mercury removal performance is the same as with Powder River Basin (PRB) coal (at the Pleasant Prairie station). Also, small slipstream pilot tests at two other plants burning PRB showed performance curves similar to those obtained at Pleasant Prairie.[6] However, recent data (not yet publicly released) from a site with two boilers burning a low-sulfur eastern bituminous coal and equipped with a small ESP showed much lower mercury removals with sorbent injection than measured at the LSEB site (large ESP) in Figure A.14-1. One unit could not achieve greater than 40% mercury capture with sorbent injection (beyond the capture by the existing ESP and SO_2 scrubber), while the other unit, which uses SO_3 flue gas conditioning to improve ESP performance, was limited to 30% incremental mercury capture with sorbent injection. Further, the ESPs at this site experienced severe arcing under certain circumstances with sorbent injection.

It should be noted that the mercury removal performance is not the same for all bituminous coals – the one site burning high-sulfur eastern bituminous (HSEB) experienced much lower mercury removals by sorbent injection than the site burning a low-sulfur eastern bituminous (LSEB). Thus, sorbent performance, as understood today, is not necessarily equally effective on all units in a given subcategory proposed by EPA.

[6] While slipstream tests are a useful indicator of potential performance – i.e., they suggest where full-scale testing is merited – they should not be considered a replacement for full-scale results.

Because these tests have been short duration and only the recent tests cited above have been on a small ESP, several operability questions remain – applicability to small ESPs (will other sites experience the same constraints noted above), impact on ESP operation in general (it has been postulated that the impact of the fine carbon particles on ESP performance could take several weeks to be noticed in a large ESP), potential for corrosion (activated carbon can oxidize SO_2 to SO_3, which can then react with water to form sulfuric acid leading to the potential for corrosion wherever the acid-laden carbon deposits on a surface), and release/vaporization of chemicals used to enhance the performance of the activated carbon (e.g., bromine, iodine, etc.). The DOE/industry collaboration to conduct numerous full-scale, longer-term field tests over the next four to five years is designed to address many of these unknowns.

EPRI's TOXECON™ process (sorbent injection between the primary particulate control and a polishing baghouse added behind the primary device) has also seen only limited testing. Following the apparent success of the short-term tests at Alabama Power's Plant Gaston, the plant, DOE, EPRI and other power producers agreed to conduct longer-term tests (up to nine months, given the long time required to see performance impacts – especially increased pressure drop – on baghouses) on this configuration. Those tests are showing that conditions at the plant can change over the period of a year (approximate time between the end of the initial tests and the start of the longer tests) in a way that impacts TOXECON™ performance. The longer-term program is nearing completion and has investigated a number of process changes, such as variable injection rates, different bag materials, changes to boiler operation to produce a more consistent fly ash, etc. At the same time, EPRI has conducted both 20 acfm and 1MW equivalent slipstream tests of TOXECON™ on the flue gas from two different plants burning PRB. The preliminary results at these two sites were similar but with slightly lower mercury removals at low injection rates than at Gaston. The first "commercial" installation is currently being procured by We Energies for their Presque Isle station under a DOE Clean Coal Power Initiative – a program that cost shares risk with the private sector for demonstration of new technologies. Therefore, it reasonable to state that this technology is still in the development stage and not yet commercially available.

The EPA proposal notes that suppliers and researchers are developing and testing chemically impregnated and other sorbents intended to improve mercury capture by conventional PM and SO_2 controls. The EPA proposal correctly states that "this technology is not currently available on a commercial basis and has not been installed, except on a demonstration basis, … " EPRI has conducted proof-of-concept tests at a ND lignite-fired and a PRB-fired site on (a) halogen-treated sorbents and (b) conventional activated carbon with halogens injected into the boiler. These two sets of tests showed promise (Figure A.14-2 for a comparison between the chemically treated carbons and conventional ACI) and merit further evaluation to determine if this performance can be sustained and what impacts the halogens might have. We found that up to half of the iodine in an iodide-impregnated sorbent leaves the sorbent through volatilization, but we do not know what the impact of this iodine is on the power plant or the environment. Others are trying bromine-impregnated sorbents (DOE project with Sorbent Technologies), which have also shown promise in a few proof-of-concept tests at full-scale, or non-carbon sorbents (e.g., Amended Silicates™) that would not impact ash sales. Again, these are all short-term experiments at available sites and focus primarily on mercury removal. Therefore, even more so than conventional activated carbon discussed above, these novel sorbents, while promising enough to merit further testing (e.g., the DOE/industry full-scale,

longer-term field tests currently underway), cannot be considered as commercially available – known to be widely applicable with sustainable performance, impacts, and costs well defined.

Fig. A.14-2. Comparison of mercury removal by activated carbon injection ahead of an ESP with conventional and iodated sorbents

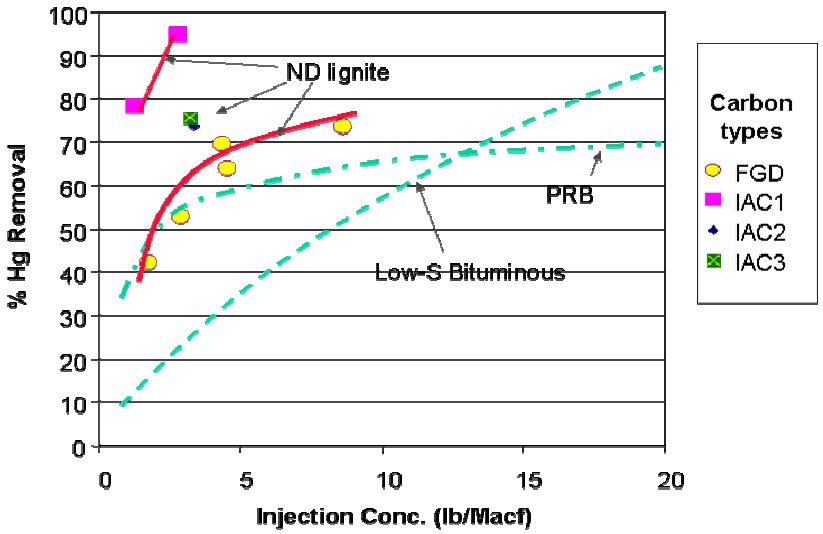

Selective Catalytic Reduction (SCR). In certain flue gases, SCR catalysts appear to promote the oxidation of elemental (or metallic) mercury to the soluble (ionic) form for subsequent capture in a wet SO_2 control (typically a flue gas desulfurization unit, or FGD). As shown in Figure A.14-3, the SCR increased the soluble fraction of mercury entering the FGD to a level above 80% at six sites firing a bituminous coal as well as at one with a blend of 40% bituminous/60% PRB[7]. The soluble mercury fraction in the flue gas varied between 80% and 90+%, but the reasons for this variation are not yet understood. We also do not have enough data to assess the oxidation activity of SCR catalysts when exposed to flue gas from plants firing different blend ratios of PRB and bituminous. Laboratory and field pilot-scale slipstream results are being planned for 2004-2005 to seek explanations for these variations in oxidation activity of the SCR.

[7] In this discussion of the impacts of SCR on mercury capture, "bituminous" will always mean eastern bituminous, as no tests were conducted at plants firing a western bituminous coal with an SCR.. Note, also, in Figure A.14-3 that the sites labeled S2-1, S2-2, etc. refer to sites that were tested in successive years – i.e., during the 1st, 2nd, and (in the case of S2) third ozone season. Thus the maximum operating time on any SCR catalyst tested is about 10,000 hr compared to catalyst guarantee lifetimes for NOx of 16,000 to 24,000 hrs

Fig. A.14-3. Mercury oxidation following particulate controls for different coals

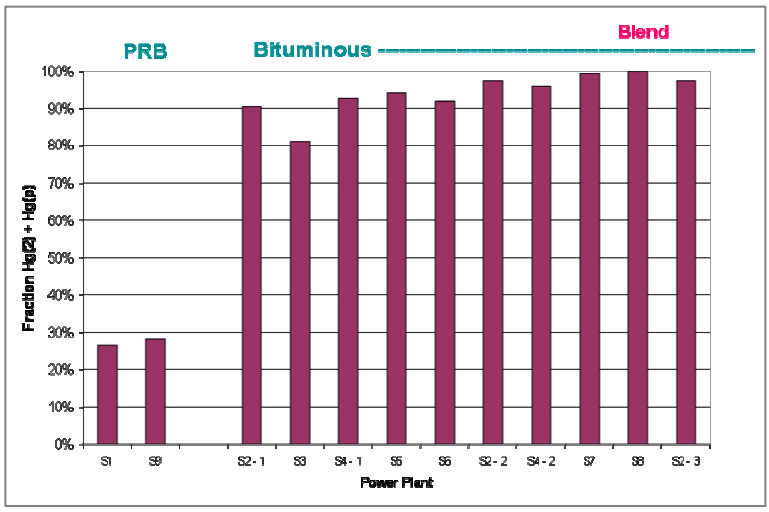

Only three of these sites had an SO_2 control, and they captured 85%-90+% of the total mercury during the test period. Of these three plants, two were equipped with an FGD that used magnesium-enhanced lime and one was equipped with a combined SO_2 and particulate scrubber. In 2004, we will conduct tests (several in collaboration with DOE) at additional sites, including 3-4 equipped with limestone forced oxidation scrubbers, the most prevalent design in use or being procured today. As also shown in Figure A.14-3, the two sites that burn PRB showed very little, if any, oxidation due to the SCR, and PRB-fueled plants need the oxidation boost more than plants firing bituminous coal because they inherently produce a low percentage of soluble mercury in the flue gas. We continue to investigate why SCR catalysts do not oxidize more mercury with PRB-generated flue gas and whether simple solutions exist to overcome this limitation.

Other issues are the effect of catalyst type, age, and other flue gas properties on oxidation activity. Pilot slipstream tests on five catalysts at the AEP Rockport station (87% PRB/13% bituminous) showed differences in oxidation activity among the catalysts and, most notably, in the effects of age - some of the catalysts lost up to 50% of their ability to oxidize the elemental mercury after only 2000 hrs, while others did not. The concern over catalyst age is less significant for bituminous coals, where tests at two power plants over three ozone seasons indicate no apparent drop-off in mercury oxidation. In summary, the potential co-benefits of SCR along with SO_2 control is more likely for bituminous coal power plants than for PRB coals. Because of these uncertainties, EPRI agrees with EPA's assessment that SCR has not yet been demonstrated as a reliable, widely applicable technology for consistently promoting the reduction of mercury emissions at plants also equipped with an SO_2 control.

EPRI has not seen a significant, repeatable impact of an SCR on mercury capture by a downstream ESP.

Other Oxidation Processes. EPRI and DOE are developing and field testing low-temperature catalysts that could be installed in the back end of an ESP or behind a baghouse to oxidize elemental mercury at sites equipped with an SO_2 control that fire coals that do not produce high soluble mercury fractions. This technology is still very much in the early development

stage, just nearing completion of a year-long pilot slipstream test on the first of four fuels to be investigated.

EPRI, DOE, and several other firms are trying the injection of chemicals, typically halogens, into the boiler of power plants that do not inherently produce high percentages of soluble mercury in an attempt to provide conditions similar to those in eastern bituminous fired boilers, which typically produce flue gases with over 60% oxidized mercury. Due to concerns about the representativeness of pilot combustors in simulating the mercury oxidation process, especially in the presence of excess oxidants, these developers are going directly to the field for their studies, and those tests can only be conducted at full-scale. The first such tests that were publicly disclosed were conducted in early 2003 (by EPRI) and stimulated the interest in this approach by several other firms. Thus, this process is very much in the early development stage.

Novel processes. Almost by definition, these are emerging technologies and, therefore, not developed and tested enough to be offered commercially with guarantees and confidence in their sustainable performance and general applicability. For example, EPRI is testing its fixed structure with adsorbent surface, called MerCAP™, in a slipstream pilot under a DOE-sponsored project, as well as at other sites in smaller scale. As an indicator of the history of new technologies, early tests suggested this approach would be widely applicable. In later testes, we discovered that, in its current configuration, it is limited to low-SO_2 flue gas, such as following an FGD or spray dryer, where it has the promise of being a cost-effective control with no impact on the power plant or ash sales.

Integrated Environmental Controls. A 50 MW demonstration unit of the Powerspan ECO® process is currently in start-up, and EnviroScrub has announced that it is also planning a 50 MW demo of its Pahlman technology following an apparently successful test at a few MW scale of the pollutant capture portion of the process (i.e., not yet integrated with the sorbent regeneration process). In a small industrial boiler test of its 3-stage Ashworth Combustor™, ClearStack Combustion has found enough mercury in the slag from its 1st stage gasifier to imply very high mercury removals. ClearStack is planning an 80 MW demo in 2005-7. No other emerging integrated environmental controls are known to be this far advanced. Therefore, EPRI believes that these technologies, while promising, fall in the category of, according to EPA's criteria, "not currently available on a commercial basis and has not been installed, except on a demonstration basis, on any electric utility unit on the U.S. to date."

A.15. COSTS vs. EFFECTIVENESS OF UTILITY MERCURY CONTROL APPROACHES

A Cap & Trade program has been demonstrated to be more cost-effective than a MACT program in achieving the same level of overall emissions.

In May 2003, EPRI released a Technical Report ("A Framework for Assessing the Cost-Effectiveness of Electric Power Sector Mercury Control Policies," EPRI Report 1005224, May 2003) that estimated the relative costs of alternative utility mercury control policies and compared these to their relative effectiveness in reducing the average Hg blood levels in

women of childbearing age in the U.S.[8] The analysis compared the Hg Cap & Trade provisions of the Clear Skies Act (CSA) of 2003 to a generic MACT standard of 2.2 lb/10^{12} Btu for all generating units. These two policies are reasonably similar to the two alternative Hg rules proposed by EPA.

The cost-effectiveness analysis found that the CSA Cap & Trade alternative would cost less than an illustrative MACT rule on a present-value basis by about a factor of 3, yet it would produce slightly larger deposition changes and MeHg exposure reductions by 2020. In either case, however, the effectiveness of the policies in reducing deposition of mercury in the U.S. appeared small. The average estimated deposition change (relative to a reference case that reflected co-benefits from the CSA's caps for SO_2 and NOx) was a reduction of only 1.2% for the MACT and 1.5% for the Cap & Trade policy. The average change in MeHg blood concentrations in women of childbearing age due to the Hg provisions themselves was only 0.41% for the MACT and 0.47% for the CSA policy. Less than 0.1% of women would be brought below the EPA Reference Dose as a result of either of these reduction possibilities.

EPRI has analyzed EPA's December 2003 rule proposals using the same analysis framework (but with greater detail and updated modeling assumptions) and finds a similar comparison. The proposed MACT rule is estimated to cost *five times as much as* the proposed Cap & Trade rule on a present value basis. The Cap & Trade rule is estimated to cost $2 billion (in 1999 dollars) for mercury controls alone (that is, not including the costs associated with mercury control associated with CAIR co-benefits), and the MACT rule is estimated to cost $10 billion (1999 dollars) more than the CAIR alone.] In 2020, estimated total deposition is 2% less under the Cap & Trade rule than it would be under the CAIR alone in that year. Interestingly, by 2020, total deposition is no different with or without the MACT because the co-benefits from SO_2 and NOx controls under the CAIR alone produce comparable divalent Hg(II) reductions by 2020 to those achieved with the MACT.[9] Thus, the relative cost-effectiveness of the proposed Cap & Trade rule compared to the proposed MACT rule appears to be even greater than was estimated for the two alternatives studied in the May 2003 EPRI publication.

In summary, the primary apparent difference between the proposed MACT rule and the Cap & Trade rule is that MACT provides earlier reductions than the proposed Cap & Trade policy. However, this earlier implementation leads to a small percentage change in deposition (and hence in exposure) but at an additional $8 billion (present value) in costs. More information is provided in Appendix B.2 below.

[8] A copy of the report, "A Framework for Assessing the Cost-Effectiveness of Electric Power Sector Mercury Control Policies", (EPRI Technical Report #1005224), May 2003, is submitted as an attachment in Section D of these comments.

[9] By 2020, the MACT has slightly lower total Hg emissions than the CAIR alone, but all of the difference is Hg^0 emissions, which have minimal effect on deposition.

References, Section A

AER, 2004. TRUE Case Studies, Reports to EPRI, Palo Alto, CA.

CRA, 2004. Power plant mercury emission files, Charles River Associates, Inc., Washington, DC.

Edgerton, ES, 2004, "Comments on Mercury Speciation in Coal-Fired Power Plant Plumes," Atmospheric Research & Analysis, Inc., Cary, NC 27513, June 8, 2004

EPRI 2003. Factors affecting the predicted response of fish mercury concentration to changes in mercury loading, EPRI, Palo Alto, CA. Technical Report # 1005521.

Friedli, HR, LF Radke, R Prescott, P Li, J-H Woo, GR Carmichael, 2004; Mercury in the atmosphere around Japan/Korea/China as observed during the 2001 ACE-Asia field campaign: measurements, distributions, sources and implications; *J. Geophys. Res*., in press.

Gilmour, C.C, J.P. Hurley, H. Hintelmann, C.L. Babiarz, A. Heyes, R. Harris, M. Turner, D. Bodaly, and J.W.M. Rudd. "Methylation of Hg deposited to aquatic landscapes: A preliminary budget for MeHg formed from Hg stable isotope additions to METAALICUS Lake 658." Am. Soc. Limnol. Oceanogr. Aquatic Sciences Meeting, Salt Lake City, UT, Feb 2003.

Goodglass H, E Kaplan (1983a) *The Assessment of Aphasia and Related Disorders*, Lea and Febiger, Philadelphia.

Goodglass H, E Kaplan (1983b) Boston Naming Test Scoring Booklet in: The Assessment of Aphasia and Related Disorders, Lea and Febiger, Philadelphia.

Grandjean P, P Weihe, PJ Jorgensen et al. (1992) Impact of maternal seafood diet on fetal exposure to mercury, selenium, and lead. *Arch Environ Health* **47**: 185-95.

Grandjean P, P Weihe, RF White, R Debes, S Araki, K Yokoyama, K Murata, N Sorensen, R Dahl, PJ Jorgensen (1997) Cognitive deficit in 7-year-old children with prenatal exposure to methylmercury. *Neurotox Teratol* **19**: 417-428.

Halperin JM, JM Healey, E Zeitchik, W Ludman, L Weinstein (1989) Developmental aspects of linguistic and nmestic abilities in normal children. *J. Clin. Exper. Neuropsych.* **11(4)**: 518-528.

Hintelmann, H, R Harris, A Heyes, JP Hurley, CA Kelly, DP Krabbenhoft, S Lindberg, JWM Rudd, KJ Scott, and V St. Louis, 2002. Reactivity and Mobility of New and Old Mercury Deposition in a Boreal Forest Ecosystem during the First Year of the METAALICUS Study. *Environ. Sci. Technol*., **36**:5034-5040.

Kaplan E, Goodglass H, Weintraub S (1983) Boston Naming Test. Lea & Febiger, Philadelphia.

Lohman, K, P Pai, C Seigneur, D Mitchell, K Heim, K Wandland and L Levin, 2000. A

probabilistic analysis of regional mercury impacts on wildlife, *Hum. Ecol. Risk Assess.*, **6**: 103-130.

Lopez MN, Arias GP, Huner MA, Charter RA, Scott RR (2003) Boston Naming Test: Problems with administration and scoring. Psychological Reports 92: 468-472.

Mahaffey KR, RP Clickner, CC Bodurow (2004a) Blood organic mercury and dietary mercury intake: National Health and Nutrition Examination Survey, 1999 and 2000. *Environ Health Perspect* **112,** 562-570.

Mahaffey KR (2004b) "Methylmercury: Epidemiology Update" Presented at the National Forum on Contaminants in Fish, San Diego, California, January 27, 2004.

NCHS 2002 National Health and Nutrition Examination Survey. Hyattsville, MD: National Center for Health Statistics. Available: http://wwwcdc.gov/nchs/nhanes.htm

NRC (National Research Council) Committee on the Toxicological Effects of Methylmercury, 2000. Washington, DC National Academies Press

Pacyna, JM, EG. Pacyna, F Steenhuisen, S Wilson, 2003; *Atmosph. Env.,* **37**: 109-117

Radke, LF, HR Friedli, BG Heikes, 2004; Atmospheric Mercury Over the NE Pacific During ITCT2K2: Gradients, Residence Time, Stratosphere-Troposphere Exchange and Long-Range Transport; *J. Geophys. Res.,* in press.

Seigneur C, K Vijayaraghavan, K Lohman, P Karamchandani, C Scott, 2004; *Environ. Sci. Technol*., **38**:555-569

Seigneur, C, P Pai, M Gerath, D Mitchell, G Hamby, G Gong, C Whipple and L Levin, 1997. Probabilistic assessment of regional mercury exposure, *Water Air Soil Pollut*., **97**, 159-168.

Vijayaraghavan, K., C. Seigneur, K. Lohman, P. Karamchandani,L. Levin, J. Jansen, 2003. Simulation of mercury deposition over the eastern United States with a fine spatial resolution. Air Quality-IV: Mercury, Trace Elements, and Particulate Matter, September 22-24, 2003, Arlington, Virginia.

SECTION B. TECHNICAL APPENDIXES

The following material provides full technical discussion of models, methods, assumptions, and data analyses used in the assessments carried out by EPRI for this study of the operational and environmental consequences of the proposed rulemaking steps by EPA. In addition, EPRI is submitting electronically and physically (Section C. PUBLICATIONS AND REPORTS) a series of peer-reviewed scientific journal articles, EPRI technical reports, contractor reports, meeting abstracts, and other material dealing with environmental mercury sources, emissions, controls, fate and transport, and human exposure and health effects. These reports are selected for their relevance to agency decisionmaking and full technical information on current understanding of mercury.

APPENDIX B.1

ANALYSIS OF LOCATIONS WITH HIGHER MERCURY DEPOSITION VALUES

B.1.1. TECHNICAL APPROACH

Introduction

As part of the analysis of environmental consequences of proposed EPA regulation of utility mercury emissions, EPRI developed a methodology to investigate the occurrence, locations, and source sensitivity of locations with mercury deposition near the high end of the modeled distribution. This section of the study sought out which locations in the model domain across the continental U.S. showed highest deposition rates annually, among all the locations modeled. The discussion that follows explains the methodology used to establish the presence, distribution, and location of these high-end points on the deposition distribution. The location references are with regard to the model grid cells used, each encompassing a 20 km by 20 km rectangular area.

Emissions

The North American anthropogenic mercury emission inventory used in this modeling study has been described earlier (Pai et al., 2000, Seigneur et al., 2001, 2004a). The North American anthropogenic mercury emission inventory in the continental domain is summarized by source category in Table B.1-1. The category for waste incineration includes municipal and medical waste incinerators. The values in parentheses represent updated 1999 Hg emissions after MACT implementation on these incinerators. Hg emissions from commercial incinerators are included in the "other sources" category in Table B.1-1. This category also includes sources such as electric arc furnaces, electric lamp breakage, cement manufacturing, oil burning, wood burning, iron-ore roasting, landfills and others. Mercury emissions from electric arc furnaces are from the 1996 EPA National Emission Inventory (NEI) and are believed to be underestimated (CCC, 2004).

The background emissions of Hg(0) include natural emissions from active volcanoes and from the mercuriferous crustal formations of western North America, as well as re-emissions of deposited mercury. We assume that 50% of deposited mercury is re-emitted (Seigneur et al., 2004a).

Table B.1-2 presents the estimated global anthropogenic mercury emissions inventory (Seigneur *et al.*, 2004a) for comparison. A comparison of Tables B.1-1 and B.1-2 shows that U.S. power plant emissions constitute less than 2% of total global anthropogenic Hg emissions. The long atmospheric residence time of Hg (Schroeder and Munthe, 1998) and the small fraction of U.S power plant emissions in the global pool of Hg illustrates the significance of the contribution to U.S. deposition of Hg emissions from continents other than North America. This is discussed in greater detail later in this section.

Table B.1-1. Anthropogenic Hg emissions (Mg/yr) in the North American modeling domain

Source Category	United States	Southern Canada	Northern Mexico	Total
Power plants	41.5	1.3	9.9	52.7
Waste incineration	28.8 (8.2[a])	(b)	(b)	28.8 (8.2[a])
Mobile sources	24.8	(b)	(b)	24.8
Non-utility coal burning	12.8	(b)	(b)	12.8
Chlor-alkali facilities	6.7	0.05	(b)	6.8
Mining	6.4	0.3	(b)	6.7
Other sources	30.9	13.0	23.6	67.5
Total	151.9 (131.3[a])	14.7	33.5	200.1 (179.5[a])

(a) Values in parentheses are 1999 Hg emissions after MACT implementation on incinerators
(b) Included in "other sources"

Table B-1.2. Global Anthropogenic Hg Emissions (Mg/yr)

Continent	Total Hg
North America	209
South & Central America	176
Europe	326
Asia	1138
Africa	246
Oceania	48
Total	2143

MODELING SCENARIOS

The modeling system used here consists of two chemistry transport models (CTM): a global CTM (Shia *et al*., 1999) and a continental/regional CTM (TEAM: Seigneur et al., 2004; Vijayaraghavan et al., 2003). The following modeling scenarios were conducted using TEAM with spatially and temporally varying boundary conditions provided by the global CTM.

Base Emission Scenario for 2004

The Base Case emission scenario uses the emission inventory of the 1998/99 Base Case with two exceptions:

- Incinerator emissions reflect some MACT implementation
- Coal-fired power plant emissions were estimated for 2004 electricity demand

Mercury emissions from coal-fired power plants are estimated to be 42.8 Mg/y in 2004 (see Table B.1-3).

Table B.1-3. Nationwide mercury emissions[a] (Mg/yr) from coal-fired power plants

Scenario	2004	2020
Base	42.8	--
CAIR	--	29.7
MACT	--	27.8
C&T	--	13.6

(a) Only emission scenarios that were performed here are attributed a mercury annual emission rate; others are denoted by (--). Emissions in Mg/yr can be converted to short tons per year by multiplying by 1.10.

CAIR Scenario for 2020

Deposition under the 2020 CAIR scenario was calculated as a relative deposition difference from the 2004 Base Case. The dry, wet and total Hg deposition fluxes were calculated as [(CAIR – Base) / Base], i.e., a negative percentage represents a decrease in Hg deposition from the 2004 base scenario.

The largest decreases in total Hg deposition tend to occur in the eastern United States with isolated areas of decreases exceeding 10% occurring also in areas such as northeastern Texas, North Dakota and the Midwest. Increases are limited to isolated grid cells (in Montana, Texas, Illinois, Tennessee, Florida and New Hampshire); they are typically in areas of low to moderate Hg deposition and are less than 18%.

MACT Scenario for 2020

Similarly, relative differences were calculated between deposition under the MACT scenario for 2020 and that under the 2004 base scenario. Decreases in total mercury deposition in excess of 10% occur mainly in the eastern United States. Some areas show decreases in excess of 30%. Isolated grid cells show increases (of at most 11%) associated with increased electricity demand in Montana, Colorado, Texas, Florida, Illinois and New Hampshire. The actual increase in Hg deposition in these grid cells is less than 1 $\mu g/m^2$-y. Thus the 2020 MACT scenario does not create any hot spots of mercury deposition in the United States.

Overall, the MACT scenario is similar to the CAIR scenario but with slightly greater decreases. Also, the MACT scenario has fewer areas where mercury deposition increases from the Base Case.

C&T Scenario for 2020

Relative differences (in %) between the C&T scenario for 2020 and the 2004 base scenario were calculated in terms of ((C&T – Base) / Base), i.e., a negative percentage represents a decrease in Hg deposition from the 2004 base scenario.

Decreases in total mercury deposition in excess of 10% occur mainly in the eastern United States. Some areas show decreases in excess of 30%. Isolated grid cells show increases (of at most 4%) associated with increased electricity demand in Colorado, Texas and New Hampshire.

Figure B.1-1 shows a comparison of the C&T and MACT scenarios for Hg total deposition. Overall, the C&T scenario leads to greater decreases in mercury deposition than the MACT scenario. There are also fewer grid cells that show increases in mercury deposition. Those increases are limited to isolated grid cells, they are small (less than 3 $\mu g/m^2$-y) and they occur in areas that have low mercury deposition.

It is important to understand how current mercury deposition patterns in the U.S. are impacted by deposition changes brought about by emissions changes due to regulation. Figure B.1-2 presents a distribution of total Hg deposition for the 2004 base scenario and the 2020 emission scenarios. This distribution is based on different ranges of Hg total deposition in the 2004 base scenario: from 0 to 10, 10 to 15, 15 to 20, 20 to 30, 30 to 50 and above 50 □g/m2-y. What is revealed by Figure B.1-2 is that, most of the mercury depositing across the continental United States is made up of large areas of moderate deposition (the central 3 groups of columns on the graph), with lesser mass deposited at the highest and lowest ends of the distribution. The EPA management steps proposed make the largest difference in net mass transfer at values of moderate deposition. This is because the steps are imposed without regard to speciated composition of mercury emissions, nor of source-receptor relationships between areas of deposition at the higher end of the spectrum and the sources contributing to that deposition. As noted elsewhere, the primary contributors to these areas of higher deposition are not utility plants, but other source types.

All emission scenarios show about the same decrease for the grid cells that have very high Hg deposition (> 50 $\mu g/m^2$-y) in the 2004 scenario. This result suggests that the remaining Hg deposition in those grid cells is likely due in great part to sources other than power plants. Little change is obtained in the grid cells with very low Hg total deposition (< 10 $\mu g/m^2$-y), which suggests that these areas are not significantly affected by power plant emissions. In the other deposition ranges, it appears that the 2020 C&T scenario is the most effective for reducing Hg total deposition. Differences among the other two 2020 scenarios (CAIR and MACT) are small.

Figure B.1-1. Differences in simulated Hg total deposition fluxes (µg/m^2-y) between the 2020 C&T and MACT scenarios ((C&T – MACT)/MACT).

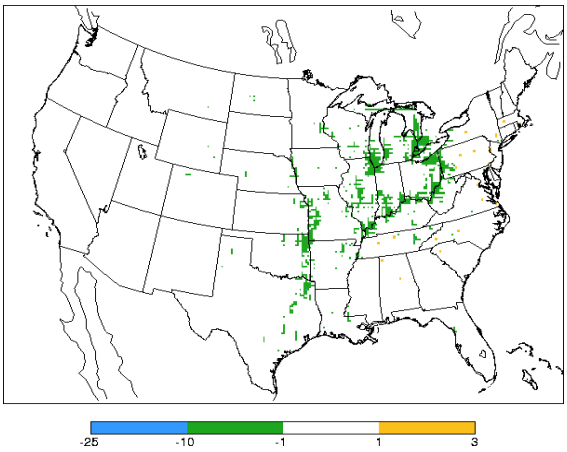

Figure B.1-2. Distribution of total Hg deposition by annual Hg deposition rate at 20-km grid resolution, based on different ranges of deposition rate in the 2004 Base Case scenario.

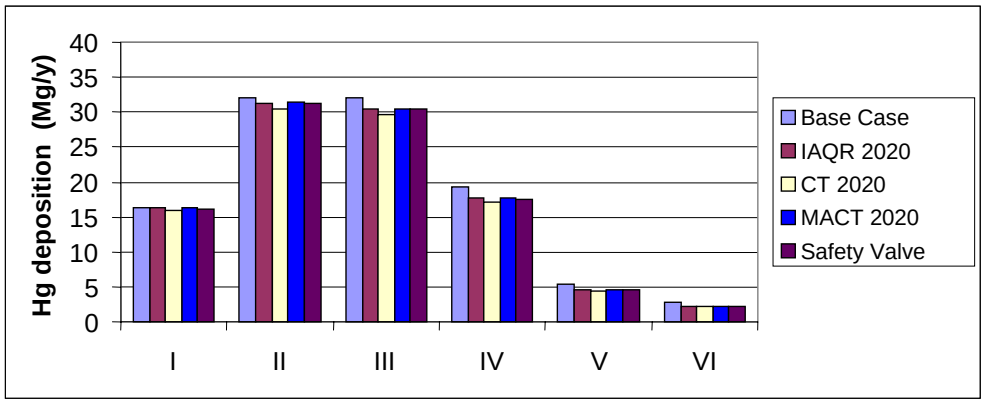

Group	From (µg/m^2-y)	To (µg/m^2-y)
I	0	10
II	10	15
III	15	20
IV	20	30
V	30	50
VI	50	

MERCURY DEPOSITION IN SELECTED AREAS

Note Concerning Bias in Deposition Calculations Using Regional Grid Models

As noted above in this document, analyses of both wet and dry deposition calculated using regional-scale Eulerian grid models, such as the TEAM component of the MSS here, lead to systemic high bias in the calculated values when compared with values derived from local-scale plume models. In the case of five power plants used for checking these overestimates, the value of the overestimate is roughly a factor of two. This overestimate is due to several factors, but primarily the manner in which regional grid-cell models mix emissions constituents down to ground level immediately after emission and close to the source, and with the constraints put on vertical mixing by those grid models.

Global Contributions at Selected Receptors

The global contributions of natural emissions and anthropogenic emissions by continent were estimated at selected receptors following the methodology of Seigneur et al. (2004a). All receptors except the Colorado location were sited within the model's 20-km fine resolution grid. Colorado lies within the broader 100 km grid.

The 18 receptors are:

1. Brule River, WI (MDN site WI08)
2. Devil's Lake, WI (MDN site WI31)
3. Sleeping Bear Dunes National Lakeshore, MI
4. Lake Erie, PA (MDN site PA30)
5. Huntington Wildlife Refuge, NY (MDN site NY 20)
6. Greenville Station, ME (MDN site ME09)
7. New Castle, NH (MDN site NH05)
8. Pines Lake, NJ
9. Great Smoky Mountains National Park
10. Longview, TX (MDN site TX21)
11. Upper Lavaca Bay, TX
12. Louisiana/Mississippi southern border
13. Mobile Bay, AL
14. Ichawahoa-chaway Lake, GA
15. Apalachicola Bay, FL
16. Lake Barco, FL
17. Everglades National Park, FL (MDN site FL11)
18. Gulf of Mexico.

Table B.1-5 presents the global contributions to Hg total deposition at these receptors. Overall, the global contributions are similar to those reported by Seigneur et al. (2004a) using the coarse 100 km resolution. The highest North American contributions are lower in the fine grid simulation than in the coarse grid simulation. The highest North American contributions are lower typically in the fine grid simulation than in the coarse grid simulation. For example, the North American contributions to the receptors in New Jersey and New Hampshire decreased from 80 to 53% and from 61 to 43%, respectively. All receptors but two showed decreases in North American contributions when using the fine 20-km resolution. The two sites that show an increase had contributions of 24 and 32%.

Contributions from Asia dominate anthropogenic contributions from other continents with values ranging from 16% at the New Jersey receptor to 31% at the upper Lavaca Bay, Texas receptor. Natural emissions are estimated to contribute from 18% at the New Jersey receptor to 35% at the upper Lavaca Bay, Texas, receptor. Contributions from U.S. anthropogenic sources range from 5% at Apalachicola Bay, FL to 50% at Pines Lake in New Jersey.

Table B.1-5. Relative global contributions (%) of anthropogenic continental emissions and natural emissions to total mercury deposition at selected receptors in the fine grid domain.

Receptor[a]	NA[b]		SA[d]	Europe	Asia	Oceania	Africa	Natural
	U.S.[c]	Other NA						
1 (WI)	24%	2%	5%	8%	25%	1%	5%	29%
2 (WI)	29%	3%	5%	7%	23%	1%	5%	27%
3 (MI)	26%	2%	5%	8%	24%	2%	5%	29%
4 (PA)	47%	4%	4%	5%	16%	1%	4%	19%
5 (NY)	24%	5%	5%	7%	24%	2%	5%	28%
6 (ME)	16%	10%	5%	8%	25%	2%	5%	29%
7 (NH)	40%	4%	4%	6%	19%	1%	4%	22%
8 (NJ)	50%	3%	3%	5%	16%	1%	3%	18%
9 (TN)	28%	3%	5%	7%	24%	1%	5%	27%
10 (TX)	30%	3%	5%	7%	23%	1%	4%	26%
11 (TX)	5%	4%	7%	10%	31%	1%	6%	35%
12 (LA)	11%	4%	6%	9%	30%	1%	6%	33%
13 (AL)	14%	5%	6%	9%	28%	1%	5%	32%
14 (GA)	16%	4%	5%	9%	28%	1%	5%	32%
15 (FL)	6%	5%	6%	10%	31%	1%	6%	35%
16 (FL)	16%	3%	5%	9%	28%	1%	6%	32%
17 (FL)	8%	6%	6%	9%	30%	1%	6%	34%
18 (GM)	4%	5%	6%	10%	32%	1%	6%	36%

(a) See text for receptor list, corresponding state in parentheses (GM is the Gulf of Mexico).
(b) North America
(c) U.S. anthropogenic
(d) South and Central America

Total Mercury Deposition over the United States

Table B.1-6 presents the simulated total Hg deposition over the contiguous United States. The results from the coarse grid domain were used for the western states and the results from the fine grid domain were used for the central and eastern states. Hg deposition shown here and elsewhere in this section includes deposition of reactive gaseous mercury and that of particulate-bound mercury. The largest decrease (7%) with respect to the 2004 base scenario is calculated for the 2020 C&T scenario.

Table B.1-7 presents the simulated total Hg deposition over the central and eastern United States for the various scenarios simulated here. The total Hg deposition is calculated to be 109.8 Mg/y in 2004 (note that about 70% of Hg deposited to the continental United States originates from outside North America (Seigneur et al., 2004a)). The CAIR and MACT scenarios lead to decreases in total Hg deposition over the central and eastern United States with respect to the 2004 base scenario of 6.7% in 2020. The C&T scenario leads to the largest decrease of all the scenarios considered here by 2020 (9.3%). Decreases in Hg deposition are greater than those obtained over the entire contiguous United States for all emission scenarios because there are more coal-fired power plants in the central and eastern United States than in the western United States.

Total Mercury Deposition over the Great Lakes

Table B.1-8 presents the total Hg deposition over the North American Great Lakes (Lakes Erie, Huron, Michigan, Ontario and Superior) for the various scenarios simulated here. With respect to the 2004 base scenario, the CAIR scenario leads to a 5.4% decrease in Hg deposition. The MACT scenario leads to a 5.1% decrease by 2020. The C&T scenario leads to a 10.5% decrease by 2020.

Table B.1-6. Total Hg deposition over the contiguous United States for the 2004 base and 2020 emission scenarios.

Scenario	Hg deposition (Mg/yr)	Decrease in Hg deposition[a]
Base 2004	151.0	--
CAIR 2020	143.4	5.0%
MACT 2020	143.4	5.0%
C&T 2020	140.5	7.0%

(a) Decrease with respect to the 2004 base scenario

Table B.1-7. Total Hg deposition over the central and eastern United States for the 2004 base and 2020 emission scenarios.

Scenario	Hg deposition (Mg/yr)	Decrease in Hg deposition[a]
Base 2004	110.8	--
CAIR 2020	103.3	6.8%
MACT 2020	103.3	6.7%
C&T 2020	100.5	9.3%

(a) Decrease with respect to the 2004 base scenario

Table B.1-8. Total Hg deposition over the North American Great Lakes for the 2004 base and 2020 emission scenarios.

Scenario	Hg deposition (Mg/yr)	Decrease in Hg deposition[a]
Base 2004	1.85	--
CAIR 2020	1.75	5.4%
MACT 2020	1.75	5.1%
C&T 2020	1.65	10.5%

(a) Decrease with respect to the 2004 base scenario

ANALYSIS OF AREAS OF HIGH MERCURY DEPOSITION

The areas that have the highest modeled values of Hg deposition in the 2004 Base Case were analyzed to evaluate whether power plant emissions contribute in any significant manner to deposition in those areas. First, the three grid cells with the highest mercury deposition in each state of the fine-grid domain were identified to determine the impact of controls on deposition in each of those states. Among those analyzed here are the eleven grid cells that have Hg total deposition in excess of 100 $\mu g/m^2$-y. Analysis of sources contributing to the deposition in the grid cells with the highest Hg deposition indicates that they are affected primarily by local emissions from medical waste incinerators. Four of the eleven grid cells listed here are apparently affected by regional emissions from power plants in Pennsylvania and West Virginia (as discussed above, those power plant contributions may be overestimated). Note that these contributions to Hg deposition in the cells decrease from the 2004 base scenario to the 2020 emission scenarios. For example, under the 2020 CAIR scenario the Pennsylvania grid cells drop below 40 $\mu g/m^2$-y and the West Virginia grid cell is at 60 $\mu g/m^2$-y. Under the 2020 C&T scenario, these Pennsylvania grid cells decrease further and the West Virginia grid cell is at 43 $\mu g/m^2$-y. The grid cells with Hg deposition in excess of 100 $\mu g/m^2$-y in 2020 are impacted primarily by sources other than coal-fired power plants because their Hg deposition rates change little in response to the utility mercury emissions control scenarios simulated here. Thus deposition in those cells is primarily made up of mercury emitted by non-utility sources throughout.

B.1.2. DEPOSITION ESTIMATES IN REGIONAL GRID-SCALE vs. LOCAL PLUME-SCALE DISPERSION MODELS

Three-dimensional (3-D) grid-based models are used to calculate the atmospheric deposition of mercury (Hg) on global, continental and regional scales (e.g., Bergan et al., 1999; Petersen et al., 2001; Bullock and Brehme, 2002; Seigneur et al., 2004; Dastoor and Larocque, 2004). Such models are appropriate to calculate mercury deposition at regional and larger scales but the 3-D grid structure is likely to lead to overestimates of mercury deposition at local scales, i.e., at scales commensurate with that of the grid resolution. The reason for such overestimates is that those models do not resolve transport, dispersion and deposition processes at scales finer than the grid size. As a result, the emissions from major point sources such as power plants are instantaneously mixed within the grid cell volume into which they are released (following calculated plume rise). Such mixing can lead to overestimates of both dry deposition and wet deposition of mercury.

To address this issue, mercury deposition fluxes calculated by a 3-D grid-based model, TEAM (Pai et al., 1997; Seigneur et al., 2004) were compared with those from a plume model, TRUE (Constantinou and Seigneur, 1993), which provides a fine spatial resolution of the transport, dispersion and deposition of mercury emitted from point sources.

MODEL SIMULATIONS

Grid-based Model Simulations

The grid-based simulations were conducted with TEAM using 1998 meteorology and 1998/1999 emissions data. The boundary conditions were provided by a global model as described by Seigneur et al. (2004). TEAM was applied over North America using a 100 km resolution and in a nested domain covering the central and eastern United States using a 20 km resolution (Vijayaraghavan et al., 2003). Note that the polar stereographic projection of TEAM leads to a grid resolution that is not exactly 20 km, depending on latitude difference from the latitude of domain origin (spacing is less than 20 km in the region considered here). Following Seigneur et al. (2003), the mercury deposition fluxes include Hg(II) and Hg(p) but do not include Hg(0). Hg(0) tends to be readily re-emitted to the atmosphere and is typically not an input to watershed and lake models.

Next, simulations were conducted without mercury emissions from five individual power plants. The difference between the base simulation and each sensitivity simulation represents the dry, wet and total deposition fluxes of mercury from an individual power plant.

Plume Model Simulations

Plume simulations were conducted for the five power plants using the atmospheric model of TRUE. This model is based on the Industrial Source Complex Long Term model (ISC-LT, Version 2). It includes the same chemical kinetic mechanism for mercury as TEAM. It also includes dry deposition and wet deposition of Hg(II) and Hg(p) using species-specific deposition characteristics (i.e., deposition velocities for dry deposition and scavenging coefficients for wet deposition). Meteorological variables are input as annual frequencies and the model calculates annual deposition fluxes at an array of receptor points distributed around the power plants. The same emissions of mercury species (i.e., Hg(0), Hg(II) and Hg(p)) were

used for TRUE as for TEAM. These were based on EPRI analysis of the EPA utility mercury ICR stack flue gas data set; no changes in speciation were incorporated to account for potential in-plume redox reactions of mercury following stack emissions.

The dry, wet and total deposition fluxes are calculated over 80 sectors that are defined by radial distances (every 5 km from the source up to 50 km downwind) and angular directions (every 45º from north). The mercury deposition fluxes in those sectors were combined to calculate the corresponding mercury deposition fluxes in the TEAM grid cells. This step required (1) the conversion of results from the TRUE map projection system (latitude-longitude) to the TEAM map projection system (polar stereographic) and (2) the calculation of the deposition fluxes from TRUE over TEAM grid cell areas that are 16.7 km x 16.7 km (278 km^2). The matching of TRUE output by sector with the TEAM grid cells introduces a small uncertainty for sectors that overlap two grid cells. In those cases, the deposition is distributed over the two grid cells based on the average deposition for that sector. This is an approximation because near the stack, there is a gradient for dry and wet deposition that may affect this distribution. However, this is only an issue for sectors that (1) are overlapping two cells and (2) overlap in a downwind direction (i.e., one grid cell is closer to the source than the other). Overall, this approximation has only a small effect on the TRUE deposition results.

The mercury deposition characteristics of TRUE were adapted to be consistent with those of TEAM for each power plant as follows. Dry deposition velocities are calculated hourly in TEAM for all mercury species according to land use and meteorological conditions. We calculated the annual deposition velocity for each mercury species (i.e., Hg(II) and Hg(p)) in the grid cells where the power plants were located. These deposition velocities were then used as annual dry deposition velocities in TRUE. In TRUE, the plume material is not depleted by dry deposition, thereby providing an overestimate of dry deposition at longer distances. However, the amount of plume material that is removed by dry deposition within 50 km (i.e., the area of interest) is small, ranging from 1 to 6% (see Section 5) and the associated overestimation is, therefore, acceptable for the purpose of this study.

Wet deposition scavenging coefficients are calculated hourly in TEAM for all mercury species according to precipitation intensity. On the other hand, TRUE uses an annual average precipitation intensity based on annual precipitation amount and precipitation frequency. The annual precipitation amounts were identical in TEAM and TRUE but the precipitation intensities differed (uniform in TRUE and variable in TEAM). Because the scavenging coefficients of Hg(II) and Hg(p) are strong functions of precipitation intensity, it was necessary to adapt the TRUE precipitation frequency for consistency with TEAM. Since the mercury amount removed by rain is based on a vertically-integrated value, it is not influenced by the vertical structure of the models and, averaged over a large enough area, should not be a function of the horizontal structure of the models. Therefore, TRUE precipitation intensity and frequency were adjusted so that (1) the annual precipitation amount remained constant and (2) wet deposition in TEAM and TRUE matched within the study area (where the study area is defined as the area within 50 km from the source). The TRUE wet deposition algorithm depletes plume material as a function of distance from the stack. However, plume material that is downwind as the rain event starts is not deposited by precipitation because the wet deposition calculation originates at the stack. In TEAM, plume material that has been transported to downwind grid cells will be deposited as the rain event occurs. Therefore, TRUE will tend to underestimate wet deposition farther from the stack compared to TEAM.

COMPARISON OF TEAM AND TRUE MERCURY DEPOSITION RATES IN THE TEAM GRID SYSTEM

Overview

We compare the mercury deposition rates calculated with TEAM and TRUE in the grid cell where the power plant is located (hereafter referred to as the central grid cell) and over a gridded area extending up to 50 km. For the purpose of this comparison, we included all grid cells that were located within 50 km of the source for at least 90% of their surface area. For grid cells that were partially located within a radius of 50 km from the plant, the mercury deposition rate within that grid cell in TEAM was scaled down to represent the grid cell area located within 50 km from the plant.

There are two major differences in the treatment of power plant mercury emissions between the grid model, TEAM, and the plume model, TRUE.

First, in TEAM the emissions of the power plant are diluted instantaneously after plume rise in a grid cell located above the central grid cell where the power plant is located. This dilution occurs regardless of where the power plant is located within the central grid cell (i.e., whether it is at the center of the cell or near one of its boundaries). TRUE treats the plume rise, dispersion, transport and deposition of the power plant emissions explicitly with respect to the exact location of the power plant. If a power plant is located near the boundary of two grid cells, the power plant-emitted material will be distributed (according to the frequency of wind directions) by TRUE between those two grid cells. Therefore, different results will be obtained with TRUE if the power plant is located at the center of the grid cell or near one of the cell boundaries.

Second, the grid structure of TEAM favors dilution of the emissions from the power plant. In TEAM, the plume is first distributed over one or more grid cells in the vertical direction based on the plume centerline (after plume rise) and the initial plume depth. Next, the plume material released in a grid cell aloft is distributed vertically via vertical diffusion and, in some cases, vertical advection. On the other hand, the plume model, TRUE, tends to keep the plume material aloft except under very unstable atmospheric conditions that lead to fumigation and rapid mixing to the ground. Thus, vertical dilution in the grid model leads to greater ground-level concentrations near the source in TEAM than in TRUE. The difference between the grid model and the plume model is expected to be greater for cases of intermediate effective stack height. For plumes that are released at very high elevations, vertical dilution in the grid model may bring only a negligible amount of plume material into the surface layer. For plumes that are released near the ground, both the grid model and the plume model will show plume material at ground level. Therefore, cases of plumes released at moderate elevations should show greater discrepancies, with the grid model predicting some plume material in the surface layer and the plume model predicting plume material mostly aloft.

As shown below, the highest dry deposition with TEAM always occurs in the central grid cell because vertical mixing of emissions aloft leads to the highest ground-level concentrations in the central grid cell. On the other hand, the highest dry deposition with TRUE never occurs in that central grid cell. The plume remains aloft long enough that the highest ground-level concentrations do not occur near the stack but farther downwind. In these simulations, the maximum ground-level concentrations occur within 7 and 10 km from the stacks for four of

the five power plants. For one power plant, they occur within 2.5 and 6 km from the stacks. However, the sector ranging from 10 to 15 km in the prevailing downwind direction typically presents the highest dry deposition rate because the plume ground-level concentrations are lower upwind of the point of maximum ground-level concentrations than downwind of that point.

For wet deposition, the highest deposition occurs in the central grid cell with both TEAM and TRUE because wet deposition removes mercury along a vertically integrated column and vertically-integrated concentrations are highest in the grid cell where the power plant is located for both models. Because wet deposition is more important than dry deposition in those case studies, the central grid cell is the grid cell with the highest mercury deposition for both TEAM and TRUE.

Table B.1-9 presents the comparison of mercury deposition rates calculated with TEAM and TRUE. In the central grid cell, the ratio of the TEAM to the TRUE deposition rates ranges from 1.1 to 2.6 for wet deposition, from 8 to 34 for dry deposition and from 1.6 to 3.4 for total deposition. We discuss below the results obtained for each individual power plant.

Table B.1-9. Comparison of TEAM grid model and TRUE plume model mercury deposition rates (g/y) for the five power plants.

Power plant	Grid cells[a]	Wet deposition			Dry deposition			Total deposition		
		TEAM	TRUE	Ratio	TEAM	TRUE	Ratio	TEAM	TRUE	Ratio
A	Central	3004	1520	**2.0**	2219	65	**34**	5222	1585	**3.3**
	50 km radius	7170	7030	1.0	3760	1168	3.2	10929	8198	1.3
B	Central	1822	706	**2.6**	809	62	**13**	2631	769	**3.4**
	50 km radius	3846	3821	1.0	1413	624	2.3	5259	4445	1.2
C	Central	811	596	**1.4**	578	22	**27**	1389	618	**2.2**
	50 km radius	1877	1869	1.0	1107	428	2.6	2984	2297	1.3
D	Central	493	225	**2.2**	196	26	**7.6**	689	251	**2.7**
	50 km radius	1028	1019	1.0	584	358	1.6	1612	1377	1.2
E	Central	270	238	**1.1**	126	8	**16**	396	246	**1.6**
	50 km radius	679	673	1.0	273	140	2.0	952	813	1.2

(a) The central grid cell is the grid cell where the power plant is located; the 50 km radius grid cells are those grid cells for which at least 90% of the grid cell area is within 50 km of the power plant.

COMPARISON OF TEAM AND TRUE MERCURY DEPOSITION RATES IN THE PROXIMITY OF THE POWER PLANTS

The comparison of TEAM and TRUE simulation results presented in Section 3 showed that TEAM overestimated mercury total deposition compared to TRUE by a factor of 1.6 to 2.4 for five power plants. These overpredictions are due to (1) the treatment of transport and deposition processes in TEAM (e.g., enhanced vertical dispersion of plume material) and (2) the fact that the exact location of power plants is not relevant in TEAM because emissions are diluted into the entire grid cell. The second factor is particularly important when the power plant is located near a grid cell boundary. TRUE will then disperse the plume over two TEAM grid cells. However, making a correction to TEAM outputs based on those results could lead to underestimates of actual power plant contributions to local deposition because, in cases where the plant is near a cell boundary, part of the correction corresponds to dispersing the power plant emissions over a couple of grid cells. Therefore, it is also of interest to only account for the grid treatment of the power plant emissions. To that end, we evaluated the TEAM/TRUE ratios for equivalent areas (278 km^2 which is the area of the central grid cell).

The results are presented in Table B.1-10 for the five power plants. The TRUE mercury deposition results were calculated over an area centered at the power plant and equal to that of the TEAM grid cell (i.e., a radius of 9.4 km from the power plant). Since the plant location within the grid cell is no longer taken into account in this comparison, the TEAM/TRUE ratios are lower. For wet deposition, the TEAM/TRUE ratios now range from 1.1 to 1.4 (compared to a range of 1.1 to 2.6 previously). For dry deposition, the TEAM/TRUE ratios now range from 8 to 24 (compared to a range of 8 to 34 previously). For total deposition, the TEAM/TRUE ratios range from 1.5 to 2.1 .

As mentioned earlier, TRUE underestimates wet deposition at longer distances because it does not account for the presence of some plume material downwind as the rain event starts. This formulation of wet deposition in TRUE may explain some of the greater wet deposition rates calculated by TEAM compared to TRUE. As a lower-bound scenario, we can assume that no overestimation should be attributed to TEAM for wet deposition (see Table B.1-11); then the ratios of TEAM and TRUE total deposition rates range from 1.3 to 1.7. These ratios should be seen as lower bounds since no overestimation was attributed to TEAM for wet deposition.

Table B.1-10. Comparison of TEAM and TRUE mercury deposition rates (g/y) over a 278 km2 area around each of the five power plants.

Power plant	Wet deposition			Dry deposition			Total deposition		
	TEAM	TRUE	Ratio	TEAM	TRUE	Ratio	TEAM	TRUE	Ratio
A	3004	2368	**1.3**	2219	93	**24**	5222	2461	**2.1**
B	1822	1375	**1.3**	809	56	**14**	2631	1431	**1.8**
C	811	657	**1.2**	578	41	**14**	1389	698	**2.0**
D	493	355	**1.4**	196	26	**8**	689	380	**1.8**
E	270	248	**1.1**	126	10	**13**	396	258	**1.5**

Table B.1-11. Comparison of TEAM and TRUE mercury deposition rates (g/y) over a 278 km2 area around each of the five power plants, only accounting for differences in dry deposition (i.e., lower bound for TEAM/TRUE ratios).

Power plant	Wet deposition			Dry deposition			Total deposition		
	TEAM	TRUE[b]	Ratio	TEAM	TRUE	Ratio	TEAM	TRUE	Ratio
A	3004	3004	**1.0**	2219	93	**24**	5222	3097	**1.7**
B	1822	1822	1.0	809	56	14	2631	1878	1.4
C	811	811	**1.0**	578	41	**14**	1389	852	**1.6**
D	493	493	**1.0**	196	26	**7.5**	689	519	**1.3**
E	270	270	**1.0**	126	10	**13**	396	280	**1.4**

.

(a) The TRUE wet deposition rate was assumed to be equal to the TEAM wet deposition rate for this comparison.

MERCURY DEPOSITION IN THE PROXIMITY OF POWER PLANTS: FRACTION OF EMISSIONS AND CONTRIBUTION TO TOTAL DEPOSITION

Fraction of Power Plant Emissions Deposited Locally

We present in Table B.1-12 the fraction of the power plant emissions of total Hg that is deposited locally. First, we present the fraction deposited within an area of about 278 km^2 around the power plant, i.e., in the grid cell where the power plant is located for TEAM and within a radius of 9.4 km from the power plant for TRUE. For TEAM, the deposited fraction ranges from 1.6% to 2.4%. For TRUE, the deposited fraction is lower and ranges from 0.8% to 1.3%.

Second, we also present the fraction deposited within 50 km from the power plant. For TEAM, the deposited fraction ranges from 3.5% to 5.1%. For TRUE, the deposited fraction ranges from 2.7% to 3.8%.

Thus, these results suggest that about 1% of the power plant emissions of total Hg is deposited within a radius of about 10 km from the plant (based on the TRUE simulation results). Furthermore, more than about 95% of the emissions of total Hg from those power plants is transported and deposited beyond 50 km from the plants.

Fraction of Total Mercury Deposition Due to the Power Plant Emissions

Table B.1-13 presents the contributions of the power plant emissions to total mercury deposition in the TEAM grid cells where the power plants are located.

The TEAM simulations lead to contributions of the power plant emissions that range from 9% to 53%. These contributions are overestimates for the reasons discussed earlier. If we calculate the power plant contributions with the plume model, TRUE, with the exact locations of the power plant within the grid cells of interest, the contributions of the power plant emissions range from 5% to 16%. If we consider an area of 278 km^2 around each power plant (i.e., the area of the center of the grid cells of interest), then, the contributions of the power plant emissions calculated by TRUE range from 6% to 25%.

Table B.1-14 presents the contributions of the power plant emissions to total mercury deposition within 50 km of the power plants. Those contributions range from 1 to 10%.

Table B.1-12. Fractions of the power plant emissions of total Hg simulated by TEAM and TRUE to deposit within a 278 km^2 area around the power plant and within a 50 km radius (about 8000 km^2) from the power plant.

Power plant	Grid cells[a]	Wet deposition		Dry deposition		Total deposition	
		TEAM	TRUE[b]	TEAM	TRUE[b]	TEAM	TRUE[b]
A	Central	1.4%	1.1%	1.0%	0.04%	2.4%	1.2%
	50 km radius	3.4%	3.3%	1.8%	0.5%	5.1%	3.8%
B	Central	1.5%	1.3%	0.6%	0.04%	2.1%	1.3%
	50 km radius	3.1%	3.1%	1.1%	0.5%	4.2%	3.6%
C	Central	1.0%	0.8%	0.7%	0.05%	1.6%	0.8%
	50 km radius	2.2%	2.2%	1.3%	0.5%	3.5%	2.7%
D	Central	1.2%	0.9%	0.5%	0.1%	1.7%	0.9%
	50 km radius	2.6%	2.5%	1.5%	0.9%	4.0%	3.4%
E	Central	1.2%	0.6%	0.6%	0.04%	1.8%	1.1%
	50 km radius	3.0%	3.0%	1.2%	0.6%	4.2%	3.6%

[a] The central grid cell is the TEAM grid cell where the power plant is located; the grid cell is about 20 km by 20 km.
[b] An area centered at the power plant and with a 11.3 km radius (i.e., with the same area as the center grid cell) was used here for the central grid cell comparison.

Table B.1-13. Calculated contributions of power plant emissions to total mercury deposition in the grid cells where the power plants are located.

Power plant	Total Hg deposition (g/yr)	Power plant contribution TEAM	Power plant contribution TRUE central grid cell[a]	Power plant contribution TRUE 11.3 km radius[b]
A	9941	53%	16%	25%
B	8075	33%	10%	18%
C	8075	17%	8%	9%
D	4642	15%	5%	8%
E	4393	9%	6%	6%

[a] The contribution is calculated based on the exact location of the power plant in the central grid cell
[b]The contribution is calculated for an area around the power plant that is equivalent to the central grid cell area (278 km^2)

Table B.1-14. Calculated contributions of power plant emissions to total mercury deposition within 50 km (8000 km^2) of the power plants.

Power plant	Power plant contribution TEAM	Power plant contribution TRUE
A	10%	8%
B	6%	5%
C	3%	2%
D	1%	1%
E	1%	1%

References, Section B.1

Bergan, T., L. Gallardo and H. Rohde, 1999. Mercury in the global troposphere: A three-dimensional model study, *Atmos. Environ., 33*, 1575-1585.

Bullock, O.R. and K.A. Brehme, 2002. Atmospheric mercury simulation using the CMAQ model: formulation, description and analysis of wet deposition results, *Atmos. Environ., 36,* 2135-2146.

CCC, 2004. Clean Car Campaign, Toxics in vehicles – Mercury - implications for recycling and disposal, www.cleancarcampaign.org/pdfs/eafdata.pdf.

Constantinou, E. and C. Seigneur, 1993. A mathematical model for multimedia health risk assessment, *Environ. Software, 8*, 231-246.

Dastoor, A.P. and Y. Larocque, 2004. Global circulation of atmospheric mercury: a modelling study, *Atmos. Environ., 38*, 147-161.

NADP/MDN, 2004. National Atmospheric Deposition Program (NRSP-3)/Mercury Deposition Network, NADP Program Office, Illinois State Water Survey, 2204 Griffith Drive, Champaign, IL.

Pai, P., P. Karamchandani and C. Seigneur, 1997. Simulation of the regional atmospheric transport and fate of mercury using a comprehensive Eulerian model, *Atmos. Environ., 31*, 2717-2732.

Pai, P., D. Niemi and B. Powers, 2000. A North American inventory of anthropogenic mercury emissions, *Fuel Process. Technol., 65-66*, 101-115.

Petersen, G., R. Bloxam, S. Wong, J. Munthe, O. Kruger, S.R. Schmolke and A.V. Kumar, 2001. A comprehensive Eulerian modelling framework for airborne mercury species: model developoment and applications in Europe, *Atmos. Environ., 35*, 3063-3074.

Schroeder, W.H. and J. Munthe, 1998. Atmospheric mercury – An overview, *Atmos. Environ., 32*, 809-822.

Seigneur, C., P. Karamchandani, K. Lohman, K. Vijayaraghavan and R.-L. Shia, 2001. Multiscale modeling of the atmospheric fate and transport of mercury, *J. Geophys. Res., 106*, 27795-27809.

Seigneur, C., K. Lohman, K. Vijayaraghavan and R.-L. Shia, 2003. Contributions of global and regional sources to mercury deposition in New York State, *Environ. Pollut., 123*, 365-373.

Seigneur, C., K. Vijayaraghavan, K. Lohman, P. Karamchandani and C. Scott, 2004. Global source attribution for mercury deposition in the United States, *Environ. Sci. & Technol., 38*(2), 555-569.

Shia, R.L., C. Seigneur, P. Pai, M. Ko, N.D. Sze, 1999. Global simulation of atmospheric mercury concentrations and deposition fluxes. *J. Geophys. Res., 104*, 23747-23760.

Vijayaraghavan, K., C. Seigneur, K. Lohman and P. Karamchandani, L. Levin and J.J. Jansen, 2003. Simulation of mercury deposition over the eastern United States with a fine spatial resolution. Air Quality-IV: Mercury, Trace Elements, and Particulate Matter, September 22-24, 2003, Arlington, Virginia.

APPENDIX B.2

PROJECTED MERCURY EMISSIONS AND COSTS OF EPA'S PROPOSED RULES FOR CONTROLLING UTILITY SECTOR MERCURY EMISSIONS

Anne E. Smith
Scott J. Bloomberg
John L. Rego

Charles River Associates
Washington, DC

John H. Wile

E&MC Group
Stony Brook, NY

June 10, 2004

I. PURPOSE OF THIS PAPER

This paper documents the methods, data, and output of the analysis Charles River Associates (CRA) used to produce projections of speciated mercury (Hg) emissions under the two alternative policy proposals that EPA published in the *Federal Register* on January 30, 2004 for controlling utility Hg emissions. The emissions projections were developed using the Electric Power Market Model (EPMM), which is a tool for simulating future operational decisions and costs of the U.S. and Canadian electric power sector under various demand, price, technology, and policy conditions. The emissions projections documented in this paper were used as inputs to the Trace Element Analysis Model (TEAM), which is a global atmospheric mercury cycling model that was developed for EPRI by Atmospheric and Environmental Research, Inc. (AER). The combined outputs of the EPMM and TEAM modeling efforts provide insights about the likely differences between the two proposed Hg rules in terms of how they can be expected to affect spatial patterns of mercury deposition.

This paper contains the following sections:

II. OVERVIEW OF THE ANALYSIS

The Electric Power Market Model (EPMM) is a linear programming model with intertemporal optimization or "foresight". EPMM simulates a competitive market for electric power and determines the mix of system operational choices that minimizes the present value of incremental costs in meeting electric demands in the 33 interconnected U.S. and Canadian electric markets, while also meeting other system requirements, including emissions caps or emissions rate limits. Incremental costs include (1) fixed and variable operating costs (including fuel costs and emissions allowance costs) for all units and (2) the capital costs for investments in new units and retrofits at existing facilities. This least-cost outcome is the outcome that would be expected to occur in competitive wholesale power markets. In the process of estimating and minimizing incremental costs, EPMM produces projections of control technology retrofits and emissions by unit. EPMM outputs also comprise regional competitive energy prices (by year, season and load period), regional capacity prices by year, and equilibrium allowance prices for each capped emission species by year.

EPMM was originally developed by Dr. John Wile of E&MC Group for use in analyzing utility emissions policies related to sulfur dioxide (SO_2) and nitrogen oxides (NO_x). In 2001, CRA and E&MC Group initiated a collaboration to enhance EPMM to be able to address multi-pollutant policies for the electric industry, including Hg and CO_2. Enhancements to EPMM that are especially relevant to the current analysis effort included adding logic and data to project mercury emissions from electricity generation, and to simulate a range of mercury control policies, including the unit-specific controls of a maximum achievable control technology (MACT) policy as well as Cap & Trade policies. Special effort has been given to developing and incorporating into the model a sound representation of:

- Hg content of available types of coals,
- Co-control of Hg by existing types of control equipment on power units,
- Costs and effectiveness of emerging technologies designed specifically to remove Hg from stack gases, and
- Relative shares of key chemical species in the portion of the Hg that is emitted from the stack, accounting for the specific set of controls and coal that a generating unit has in place.

Additionally, the model logic was enhanced to be able to simulate unit-by-unit emissions rate limits more precisely than the typical linear programming model. For each Hg control technology retrofit investment, EPMM identifies the operational level that will just satisfy each unit's unique emissions reduction need. This logic enhancement allows EPMM to avoid the excess control and excess costs that other similar models, such as EPA's IPM model, project when simulating unit-specific control requirements. Model logic was also added that would allow consideration of future technological improvement in the still-immature Hg control methods.

EPMM has been run using input data from standard government sources that are publicly available. For example, it relies on the U.S. Energy Information Administration (EIA) and Federal Energy Regulatory Commission (FERC) for data on the universe of U.S. generating units, and for prices of primary fuels used in generation. It uses North American Electricity

Reliability Council (NERC) data for forecasted demand by region, and transmission capabilities among regions.

EPA is the primary source for data on emissions rates and for control technology cost and effectiveness. The one exception is for Hg control and emissions data. Hg control technology is developing at a rapid rate, and this analysis has used information provided by EPRI and affiliated researchers for assumptions on costs and effectiveness of activated carbon injection (ACI). Assumptions regarding Hg co-benefits from existing control equipment and for Hg speciation rules were developed primarily from EPA's 1999 Information Collection Request (ICR) data. Industry researchers and EPA, however, have differing opinions on how to extrapolate ICR data to unit configurations that were not represented, or which were poorly represented in the ICR sample. Co-benefits assumptions used in this analysis reflect judgments of EPRI and other industry researchers on Hg control. This paper documents all of the above assumptions.

This paper also reports how EPMM produced unit-specific emissions projections for the key species of Hg emissions, ionic mercury (Hg^{2+}) and elemental mercury (Hg^{0}), that AER used to generate estimates of national Hg deposition patterns under the two EPA Hg policy proposals. The outputs of the EPMM modeling effort described here were the core scenario-specific inputs to a fate and transport modeling effort. Figure I-1 illustrates the flow of information in this overall analysis process. The dotted line in Figure I-1 encircles the specific elements of the overall analysis process that are documented in this paper.

Figure I-1. Diagram of Information Flows in EPRI Analysis of Hg Deposition Impacts of Alternative Policy Proposals

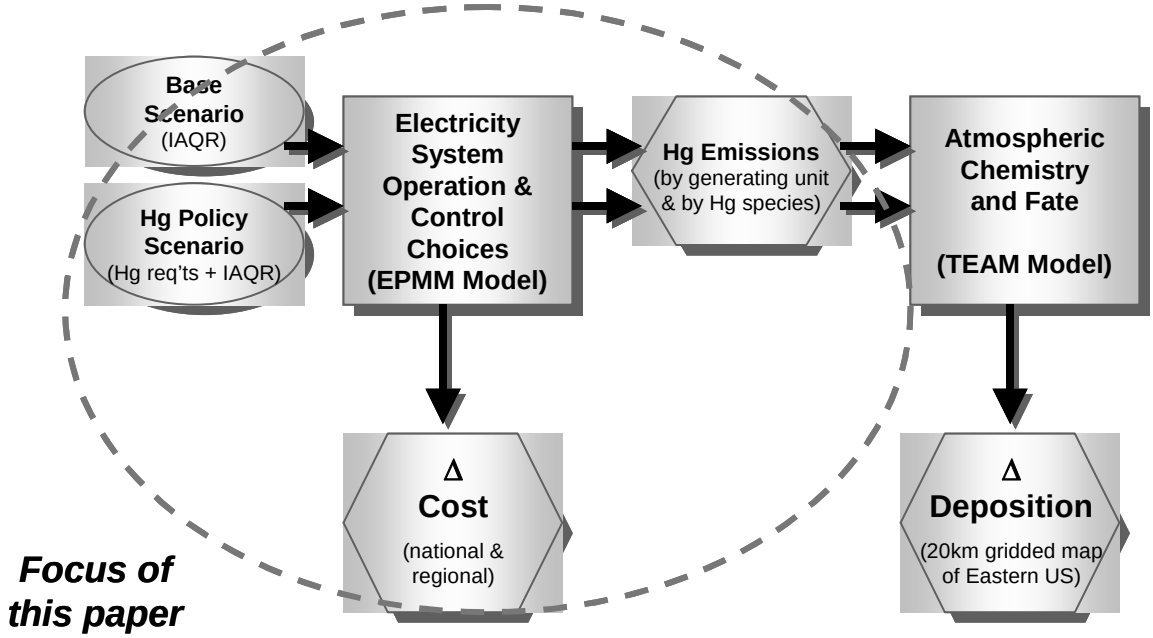

The analysis focused on a comparison of the EPA Hg Cap & Trade proposal to its proposed MACT scenario. Both of those scenarios were modeled individually. However, because decisions on SO_2 and NO_x controls can play an important role in determining Hg emissions, and the species of Hg emitted, the analysis also had to make specific assumptions about what SO_2 and NO_x policies would also be in effect. Given EPA's stated preferences in the proposals, emissions limits like those in the proposed Interstate Air Quality Rule (CAIR) were assumed to be implemented simultaneously with the Hg proposals. Thus, each of the following scenarios was simulated with EPMM:

1. **Base Case** – includes existing national (Title IV, NO_x SIP Call) and state regulations.
2. **CAIR Only** – includes provisions of the proposed CAIR, as well as existing national and state regulations.
3. **CAIR + Hg Cap & Trade** – includes provisions of the proposed CAIR and the proposed Cap & Trade provisions of the Hg Rule, as well as existing national and state regulations.
4. **CAIR + Hg MACT** - includes provision of the proposed CAIR and the alternative MACT provisions of the Hg Rule, as well as existing national and state regulations.

III. DESCRIPTION OF THE MODEL USED

OVERVIEW OF THE ELECTRIC POWER MARKET MODEL

EPMM employs detailed unit-level information on the more than 10,000 generating units in the United States and Canada and simulates the implications of policy options on operational and generation construction decisions. There are 33 regions in EPMM based on NERC sub-regions.[10] The United States is divided into 28 regions (Figure III-1). There are also 5 regions reflecting Canadian markets, which are interconnected with the U.S. These geographical boundaries reflect regions in which electricity generation units are generally dispatched as a system, or power pool. Power can flow between these regions, but such flows are constrained by the available capacity of transmission lines that connect them. Thus, most determinants of power system investment and operation decisions tend to relate to demand and generating units specific to each region.

Environmental regulations, (whether unit-specific, regional, or national) also affect system decisions within each region. Both emissions rate limits and emissions caps (which effectively place an operational cost on each unit's emissions) can affect the mix and timing of new capacity additions as well as retrofits at existing facilities, fuel choice by all units, and dispatch of all units. EPMM captures all of these impacts in the process of optimizing unit responses to environmental policies. EPMM projects these decisions by accounting for incremental costs over a long time horizon. In the current analysis, specific investments and operational decisions associated with each policy scenario are simulated through 2020, while accounting for associated incremental system costs through 2040.

EPMM determines competitive energy prices by balancing supplies of and demands for electricity by year, season, and by time of day for each of the 33 electric markets (regions) while taking into account the potential for transmission of electricity from one region to another.

[10] For some NERC sub-regions where there were important internal transmission constraints, sub-regions were further divided.

Figure III-1. Regional Detail in EPMM
(Five Canadian regions not shown)

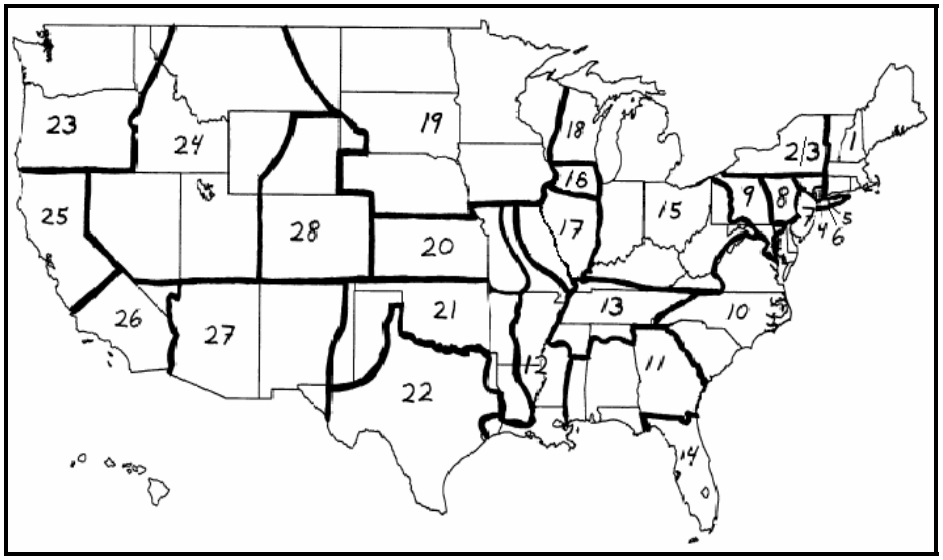

1. New England	2. NYISO, West
3. NYISO, Capital	4. NYISO, Hudson Valley
5. NYISO, New York City	6. NYISO, Long Island
7. PJM East	8. PJM Central
9. PJM West	10. VACAR
11. Southern	12. Entergy
13. TVA	14. FRCC
15. ECAR	16. Com Ed
17. South MAIN	18. WIUM
19. MAPP	20. SPP North
21. SPP South	22. ERCOT
23. Washington/Oregon	24. Idaho, Utah, Montana
25. Northern California	26. Southern California/Nevada
27. Arizona/New Mexico	28. RMPP

Electricity demands are represented with a set of load duration curves that reflect the peak demands, energy requirements, and hourly load variations specific to each region. For each region and year, there is a separate load duration curve for each of four seasons with each of these curves divided into five blocks, or load periods, having different average demands that reflect peak load, three levels of mid-level load, and a base load. The initial shapes of each region's load duration curves reflect historical hourly electricity demands of the region. Over the period of analysis, usually through 2020, the demand levels for each load period and each season change depending on projected demand growth. Also, the relative demands (the shape of the load duration curve) in each season change to the extent that peak demands and energy requirements grow at different rates leading to changes in load factors.

Electricity supplies include all existing utility and non-utility generating units, generating facilities under construction, and potential generic new additions as well as purchase power agreements. Supplies also include possible transmission from units in other regions, subject to explicit transmission limits among regions.[11] Generating units are dispatched in least-cost order to meet the demands reflected in the load duration curves in each region.[12] The unit costs that EPMM takes into account in setting the dispatch order include:

- Fuel costs, which are calculated given each unit's characteristics, including unit type, fuel type, fuel price, and heat rate.

- The unit's non-fuel variable operating cost, which includes costs of existing emissions control equipment.

- When an emissions cap is in effect, variable costs also include the emissions rate of the unit (given whatever control retrofit may have been adopted) multiplied by the current price of allowances.

- If an inflexible emissions limit is imposed on a unit (i.e., there is no emissions trading allowed), that unit must be able to meet its limit in order to remain on-line (even if it is not dispatched), and the variable cost of the associated emissions control action is also included in the dispatch cost.

- The cost of power imported from units in other regions includes losses during transmission.

In dispatching the units, EPMM also takes into account any limits on each unit's operation including forced outage rates, maintenance requirements, and equivalent availability factors.

The dispatch logic is combined with the level of demand in each load block to determine which units are dispatched. The dispatch cost of the last unit in the dispatch order is the energy price for that load period. This process provides projections of the energy prices that would emerge in a competitive power market because, under competition, output will be produced at lowest cost.

[11] When the difference in energy prices between interconnected markets exceeds the losses associated with transmitting power between the markets, the units will be re-dispatched in the two markets. Generation will increase in the region with the lower costs and decrease in the region with higher costs. This re-dispatch continues until (1) the difference in prices in the particular season and load period just equals losses from moving power between the markets or (2) the limit on power flows between the two regions is reached.

[12] Nondispatchable units are dispatched first to meet demands irrespective of their variable operating costs.

Unit dispatch decisions are just one of several actions that are taken in the model to meet demand at least cost. New capacity must also be built if demand grows to the point where regional capacity falls below required reserve margins. Also, environmental constraints must be met, and the model determines the least-cost way of doing this while accounting for how units will be dispatched and what new units will become part of the mix. The model uses linear programming logic to determine the simultaneous combination of all available system operation choices that minimizes the present value of the *incremental* costs over the period of the analysis across all of the interconnected markets.

In addition to projecting competitive regional energy and capacity prices, EPMM outputs include:

- The types, amounts, and timing of new capacity additions.
- Capacity factors of existing and new generating units.
- Prices of emissions allowances.
- Retrofits for complying with emissions constraints.
- Fuel use by type for existing and new generating facilities.
- Maintenance scheduling for existing and new units.
- Economic capacity and energy transactions among regions.

There are many inputs, or assumptions, underlying the projections produced by such a model. The following is a list of the most important input assumptions in EPMM. They are specified for each region. Specific assumptions for the key inputs in the list below are provided in Section IV:

- Existing utility and non-utility generating units, generating units currently under construction, and on-going modifications to existing facilities. Data required for each unit are:
  - Capacity
  - Unit type
  - Fuel type
  - Heat rate
  - Non-fuel O&M costs
  - Equivalent forced outage rate
  - Maintenance requirements
  - Emissions rates and limits, where applicable, for SO_2, NO_x, Hg, and CO_2
  - Existing emissions control equipment for PM, SO_2, and NO_x
  - Percentage removal rates of emissions for existing equipment configuration

  - Unit-specific retrofit control equipment options for SO_2, NO_x, and Hg.

- New generation capacity options (in addition to units under construction) that the model can add. In addition to the existing unit characteristics listed above, new generating options require assumptions on their capital and variable operating costs.

- Retrofit control technologies available to reduce SO_2, NO_x, and Hg. Assumptions describing each option are capital cost, fixed and variable operating costs, and emissions removal efficiency.

- Peak demand and energy requirements.

- Hourly variations in electricity demand.

- Capacity reserve margin requirements.

- Projections of regional fuel prices.

- Transmission-related information:
  - Limits on capacity and energy transactions among regions in a market
  - Losses for interregional power flows
  - Wheeling charges for interregional transactions.

- Finance-related information:
  - Capital structure and cost of money
  - Income tax rates
  - Property tax and insurance rates
  - Book life for new generating options
  - Tax life for new generating options
  - Treatment of deferred taxes
  - Construction period for new generating options.

COMPARISON OF EPMM TO THE IPM MODEL USED IN EPA ANALYSES

EPA uses the IPM model for its analysis of costs and emissions of proposed policies that impact the electricity sector. The IPM model is very similar methodologically to EPMM. Both are dynamic linear programming models of U.S. electricity markets. Both minimize a comparable measure of incremental system costs subject to a similar set of operational constraints. The primary difference between the two models is in the assumptions that are used in each model. Other minor differences exist in the choice of model disaggregation. Table III-1 compares the key assumptions of the two models. Section IV

provides the specific quantitative values used for some of the key assumptions that differ from those of IPM.

DESCRIPTION OF HOW MERCURY EMISSIONS ARE SPECIATED

The EPMM model produces projections of total Hg emissions, as that is the basic form of Hg policy prescriptions. However, projections of Hg deposition require information on whether the Hg is emitted in the ionic, elemental, or particulate form (Hg^{2+}, Hg^{0}, and Hg^{p}, respectively). In order to meet the needs of the fate and transport modeling step, CRA developed a post-processor module that would take the EPMM outputs on Hg emissions and break them into their individual species, using other output from EPMM. As this is a new component of CRA's modeling approach, and one that was developed specifically for this particular analysis, this section describes the method is some detail. Associated speciation assumptions are provided in the next section.

Speciation was estimated individually for each unit group in the model, and for each modeled year (because the control equipment in place changes over time as retrofits are installed). Hg^{p} is only a very small fraction of the Hg that is emitted, because this is the species that is most effectively captured in all types of units.[13] The amount of Hg^{p} also does not change very much as a result of new retrofit controls being considered. For this reason, the calculation divided all the emitted Hg into only Hg^{0} and Hg^{2+}. The small fraction emitted as Hg^{p} was assumed to remain equal to amounts estimated in the ICR data, and this constant was subtracted from the projected Hg^{2+} for each unit.

Emission controls for SO_2 and NO_x have significant effects on Hg speciation. For example, wet FGDs tend to remove Hg^{2+} because that species is soluble. The net result is a decrease in emissions, but also a shift of the remaining Hg emitted towards a greater fraction that is Hg^{0}. SCRs can convert Hg^{0} into Hg^{2+}, creating a direct shift of the fraction of total Hg emitted towards Hg^{2+}. When an SCR is installed on a unit that also has a wet FGD, overall Hg emissions fall, but the net effect on the share that is Hg^{2+} can vary. These "co-controls" can create a complex set of possible net changes to the speciation of the Hg emissions. In contrast, the primary control option designed specifically to address Hg emissions – activated carbon injection (ACI) – removes both ionic and elemental species in approximately the same proportion.

[13] Particulate matter (PM) controls, which are installed on almost every unit remove most of the Hg^{p} in the flue gas. This explains the very small amount of Hg^{p} from any type of generating unit.

Table III-1. Comparison of EPMM and IPM[14]

		EPMM	IPM *(citations to IPM documentation in italics)*
Model Detail and Structure	Number of Regions	33 (including 5 in Canada)	26 (does not include Canada - specifies a level of net imports) *pp. 3-2, 3-7*
	Number of Modeled Unit Groups	Approximately 1,100 (nearly 600 coal unit-groups)	Approximately 1,400 (650 coal unit-groups) *p. 4-9*
	Reporting Years	2004, 2008, 2010, 2012, 2015, 2018, 2020	2005, 2010, 2015, 2020, 2026 *p. 6-2*
	Model Terminal Effects	Terminates costs and benefits of new units over 20 years (2020-2040)	Terminates costs and benefits over 6 years (2026-2030) *p. 6-2*
	Fossil Unit Mothballing/ Retirements	Allows mothballing and economic retirements of fossil units. There are no fixed operating lives for fossil units.	Allows economic retirements for fossil units (mothballing not listed as option in documentation) *pp. 3-11, 6-2, 6-3*
	Nuclear Units	All nuclear units are assumed to receive life extensions, based on determination that these extensions are economic	All nuclear units are assumed to receive life extensions, based on determination that these extensions are economic *p. 3-11*
	Timing of Retrofits	Allows one retrofit decision per unit after any 2004 retrofit actions	Allows two retrofit decisions per unit over the time horizon *p. 6-2*
	New Unit Types	Conventional coal, IGCC, 2 types of CC and 2 types of GT; also range of renewables	Conventional coal, IGCC, CC, 2 types of GT, advanced nuclear; also range of renewables *pp. 4-9, 4-16*
	Repowering	Assumed to be uneconomic relative to building new capacity	Repowering allowed if economic (coal to CC or IGCC, oil/gas steam to CC) *p. 4-31*
Key Data and Assumptions	Mercury Control Costs	Variable O&M costs and effectiveness from EPRI; costs can improve over time	Cost and effectiveness based on update of NETL/EPA's ORD pilot study; ACI has higher cost per pound removed than EPMM *L1 p. L1-2*
	Mercury Control Options	ACI - % incremental removal based on needs of unit - from 0% to 90% (for bituminous/sub-bituminous); 0% to 75% (lignite)	ACI - either a 60% total removal or 90% total removal; 60% removal only in sensitivity runs *L1 p. L1-2*
	NO_x and SO_2 Controls	Cost and percentage removals are EPA's assumptions for IPM	NO_x costs and performance based on EPA's ORD and Bechtel Power Corporation; SO_2 costs and effectiveness based on EPA's ORD *pp. 5-4, 5-8*
	Coal Unit Availability	80%	85% *p. 3-8*
	Nuclear Capacity Factors	85% for all units	85% to 90% as a national average *p. 4-29*
	Fixed O&M	Fixed over life of unit	Variable depending on unit age *p. 4-10*
	Life Extension Costs	Not included	$5/kW-Yr for fossil units after 30 years (based on AEO 2003) *Table of Updates, p. 3*
	Electricity Demand Growth	Based on detailed forecasts from NERC, approximately 1.7% per year	Based on AEO 2003, with modifications for Climate Change Action Plan (CCAP), approximately 1.1% per year *B, p. B-*
	Coal and Gas Prices	Gas prices based on AEO 2004; coal prices based on FERC 423 but with AEO efficiency improvements over time	Gas prices based on ICF Consulting's North American Natural Gas System, with prices much lower than AEO 2004; coal prices based on AEO 2003 coal supply curves *Table of Updates, pp. 6-7*

The determinants of speciation are the type of coal burned, and control technology combination for each unit-group. Control technologies and type of coal burned may change in each modeled year for the same unit, so the speciation is updated for each modeled year. Multiple retrofits may be added during the same year and not installed on the entire modeled unit; therefore a unit may have emissions calculated from multiple control technology combinations.

To transfer the speciated emissions data into the fate and transport model, a spreadsheet was created that provided a mapping between the unit-groups in EPMM and the "stacks" that represent the point sources modeled in TEAM. The units in each model were matched based upon the plant ORISPL number.[15] TEAM's set of stacks is based on 1998/1999 unit data; EPMM's unit data are periodically updated to reflect new information. Where EPMM units could not be not matched via the ORISPL number, the EPMM unit was located geographically, then mapped to the geographically nearest plant in the TEAM model.

EPMM also projects new unit construction in each of the 28 regions in the model, but does not site such new capacity at specific locations within the region. Additionally, without substantial additional modeling, TEAM is constrained to have all utility emissions assigned to one of the existing stacks. Therefore, the emissions from projected new units were dispersed among all coal units in the same model region, based upon a weighted average of capacity of existing coal units. Overall, the emissions from new units are relatively small compared to older units as new units meet the NSPS for Hg (and have both FGD and SCR systems).

LIMITATIONS OF MODEL RESULTS

All models are an idealization of the real world and there are limitations in how one can interpret their results. These limitations apply to both EPMM and IPM alike:

- The models present an idealized response to policies that reflects perfect foresight of market outcomes up to 25 or 35 years into the future. Real world choices may differ from the model results because of expectations different from those in the model forecasts, or because of risk aversion.

- The models do not reflect or capture many real-world constraints, such as resource limitations, that may be associated with many utilities simultaneously attempting to retrofit a large portion of their capacity.

- The models probably overstate the ease of compliance in the near-term as neither one estimates or applies upper bounds on rates of retrofitting, and neither

accounts for the possible difficulties imposed by the immature state of Hg control technology.

Model results from both EPMM and IPM should therefore be interpreted with caution. At best, they should be viewed as estimates of how much control action would be desired to meet emissions targets in a "perfect" world, with no uncertainty and no resource limitations. Model projections of control measures should not be automatically accepted as feasible or realistic.

IV. ASSUMPTIONS FOR KEY MODEL INPUTS

UNIT DATA AND AGGREGATION

Generating units in EPMM are often aggregated together to form "unit-groups." Most large units are individually represented, and it is primarily the smaller units that are grouped together. As a result, there are over 500 coal unit-groups in the current version of EPMM, compared to about 1100 individual coal-fired units. The unit-groups consist of units within the same region that have similar characteristics and would thus be dispatched and retrofitted similarly. Characteristics that determine unit grouping include: regional location, unit capacity, prime mover, pollution control equipment, heat rate, fuel choice, sulfur content of current coal burned and operating costs.

There are 305 GW of coal-fired generating capacity among the existing units in the EPMM data base. Of this, 83 GW already have either wet or dry scrubbers. Also, there are 87 GW of SCR or SNCR among the existing units. When retrofits are reported for EPMM scenarios, those numbers are incremental to these existing control technology installations.

DEMAND

The fundamental driver of generation in each region is demand. Table IV-1 provides each region's annual total demand for each of the modeled years, and Table IV-2 provides each region's peak demand. These inputs are obtained from the NERC's Electricity Supply & Demand (ES&D) forecasts.

The demands in Tables IV-1 and IV-2 are configured into the load duration curves that determine when generating units are dispatched. There is a different load curve for each of four "seasons" and the load curve in each season is represented by five load blocks, each with a different average demand level. The five load blocks comprise peak load, three levels of mid-level load, and base load. There are different numbers of hours in each of these five load levels, and the number of hours varies by the season. The hours in each block were selected to provide a good approximation of each season's unique load duration curve shape. Table IV-3 shows how the five load periods were defined for each season.[16]

Table IV-1. Annual Energy Demand
(thousands of MWh)

Sub-Region	2004	2008	2010	2012	2015	2018	2020
NEPP	130,286	138,099	142,242	147,426	154,833	162,612	168,013
NYISO, West	54,112	55,881	56,791	57,694	59,153	60,721	61,803
NYISO, Capital	11,750	12,134	12,331	12,528	12,844	13,185	13,420
NYISO, Hudson Valley	21,909	22,625	22,994	23,359	23,950	24,585	25,023
NYISO, New York City	53,294	56,512	58,163	59,811	62,282	64,755	66,401
NYISO, Long Island	21,596	22,867	23,481	24,358	25,522	26,805	27,743
PJM Eastern	154,318	163,038	167,196	171,478	178,157	185,095	189,871
PJM Central	43,949	46,825	48,243	49,704	51,982	54,364	56,012
PJM Western	83,670	89,548	92,166	94,799	98,945	103,273	106,263
VACAR	309,733	338,054	351,316	365,014	386,636	409,539	425,556
SOU	244,670	268,672	281,790	295,641	317,630	341,254	357,972
Entergy	142,628	148,704	154,304	160,174	169,353	179,059	185,836
TVA	172,610	186,495	192,701	196,094	203,616	211,427	216,800
FRCC	220,249	245,426	256,880	268,265	286,778	306,568	320,515
ECAR	584,897	621,737	640,910	660,539	691,221	723,329	745,558
Com Ed	100,950	106,700	109,650	112,607	117,250	122,085	125,419
South MAIN	106,001	112,872	116,383	120,066	125,760	131,721	135,850
WIUM	69,355	73,851	76,148	78,558	82,283	86,183	88,885
MAPP	157,110	167,768	172,696	177,824	185,760	194,050	199,781
SPP North	65,741	72,347	75,739	79,333	85,013	91,098	95,396
SPP South	139,709	149,693	157,262	162,412	172,655	183,544	191,182
ERCOT	313,603	349,675	369,733	390,941	425,056	462,148	488,657
WA, OR	134,015	141,437	146,057	150,677	158,002	165,682	171,009
ID,UT,MT	97,847	103,265	106,638	110,012	115,359	120,967	124,856
N California	129,280	134,325	136,831	139,286	143,126	147,073	149,764
S California/Nevada	140,053	145,519	148,234	150,893	155,054	159,329	162,244
Arizona/New Mexico	123,034	138,004	144,834	151,832	163,104	175,214	183,782
RMPP	58,116	63,718	66,775	70,028	75,167	80,683	84,583

Table IV-2. Peak Energy Demand
(MW)

Sub-Region	2004	2008	2010	2012	2015	2018	2020
NEPP	25,066	26,442	27,210	28,137	29,478	30,884	31,858
NYISO, West	9,691	10,069	10,245	10,422	10,712	11,016	11,223
NYISO, Capital	2,104	2,186	2,225	2,263	2,326	2,392	2,437
NYISO, Hudson Valley	3,924	4,077	4,148	4,220	4,337	4,460	4,544
NYISO, New York City	11,196	11,702	11,922	12,142	12,472	12,802	13,022
NYISO, Long Island	4,926	5,236	5,400	5,603	5,913	6,251	6,465
PJM Eastern	32,463	34,558	35,597	36,626	38,263	39,973	41,156
PJM Central	6,935	7,311	7,493	7,678	7,960	8,254	8,455
PJM Western	15,136	16,372	16,972	17,630	18,644	19,717	20,466
VACAR	58,201	62,864	65,427	67,977	72,083	76,437	79,484
SOU	48,765	54,244	57,117	60,161	65,019	70,269	74,003
Entergy	26,172	27,696	28,786	29,889	31,647	33,508	34,810
TVA	28,257	30,941	31,835	32,712	34,107	35,560	36,564
FRCC	41,596	45,620	47,757	49,993	53,546	57,351	60,037
ECAR	101,436	109,609	112,738	116,622	122,175	127,993	132,024
Com Ed	22,750	24,700	25,700	26,720	28,343	30,064	31,269
South MAIN	19,669	20,936	21,669	22,482	23,715	25,016	25,923
WIUM	12,869	13,698	14,178	14,710	15,517	16,368	16,961
MAPP	28,355	30,834	31,842	32,862	34,470	36,157	37,328
SPP North	14,389	15,763	16,498	17,251	18,458	19,749	20,660
SPP South	27,585	29,735	31,156	32,100	33,997	36,006	37,411
ERCOT	63,028	70,314	74,638	79,228	86,648	94,763	100,591
WA, OR	23,660	24,759	25,555	26,396	27,693	29,055	30,000
ID,UT,MT	17,274	18,077	18,658	19,271	20,219	21,213	21,902
N California	24,883	26,492	27,330	28,182	29,520	30,922	31,894
S California/Nevada	26,957	28,699	29,607	30,531	31,981	33,499	34,552
Arizona/New Mexico	25,759	29,023	30,563	32,131	34,678	37,428	39,381
RMPP	9,836	10,840	11,410	11,956	12,869	13,850	14,546

Table IV-3. Number of Hours in Each Seasonal Load Period

Months/Load Period	1	2	3	4	5
Jun, Jul, Aug	50	139	476	676	867
Dec, Jan, Feb	29	409	925	655	142
May, Sept.	12	85	420	593	354
Mar, Apr, Oct, Nov	24	170	841	1,186	707

The electricity demand level associated with each of these blocks is tailored to reflect each region's own pattern of variability in load levels. For each model region, the average load observed in each block of hours is estimated as a percentage of the season's peak load for that region. These percentages indicate the load shapes within each region. Table IV-4 shows the initial load shapes for each of the U.S. model regions. These load shapes were based on recent historical demand patterns reported to the NERC.

The model adjusts the initial load shapes over time to reflect each region's forecasted growth in the peak loads and energy demands of Tables IV-1 and IV-2. The future load shapes mirror the initial load shapes if peak load and energy demand grow proportionally. If energy demand grows at a more rapid rate than peak load in a region, then the incremental demand is allocated to the four non-peak load blocks in such a way that the load curve is proportionately flattened for that region relative to its initial shape.

Table IV-4. Energy Demand in Each Load Period as Percent of Peak Hour Load

Region	Months	1	2	3	4	5
NEPP	Jun, Jul, Aug	96.7	89.5	79.2	67.7	50.6
NEPP	Dec, Jan, Feb	88.9	80.2	70	54.9	46
NEPP	May, Sept.	90.9	78.6	68.9	55.8	41.9
NEPP	Mar, Apr, Oct, Nov	82.4	76.3	69.6	58.3	44.4
NYISO, West	Jun, Jul, Aug	95.8	91.3	84.9	74.9	61.7
NYISO, West	Dec, Jan, Feb	97.3	90.3	80.7	67.6	59.4
NYISO, West	May, Sept.	90.8	85	78.5	65.7	54.7
NYISO, West	Mar, Apr, Oct, Nov	91.5	86.6	80.4	69.7	58.1
NYISO, Capital	Jun, Jul, Aug	95.9	89.4	78.2	65.8	49.3
NYISO, Capital	Dec, Jan, Feb	79.2	71.2	62.4	50.3	42.9
NYISO, Capital	May, Sept.	89.6	77.3	64.1	52.8	40.2
NYISO, Capital	Mar, Apr, Oct, Nov	74.6	68.9	62.7	53.5	41.9
NYISO, Hudson Valley	Jun, Jul, Aug	95.9	89.4	78.2	65.8	49.3
NYISO, Hudson Valley	Dec, Jan, Feb	79.2	71.2	62.4	50.3	42.9
NYISO, Hudson Valley	May, Sept.	89.6	77.3	64.1	52.8	40.2
NYISO, Hudson Valley	Mar, Apr, Oct, Nov	74.6	68.9	62.7	53.5	41.9
NYISO, NYC	Jun, Jul, Aug	95.2	87.2	75.1	61.9	45.7
NYISO, NYC	Dec, Jan, Feb	69.6	62.3	53	39.3	32.6
NYISO, NYC	May, Sept.	92.8	75.8	60.5	47.5	34
NYISO, NYC	Mar, Apr, Oct, Nov	68.9	63.4	56.6	45.4	33.1
NYISO, Long Island	Jun, Jul, Aug	94.2	85.2	72.6	60.2	42.8
NYISO, Long Island	Dec, Jan, Feb	73.1	63.3	53.2	40.5	33.2
NYISO, Long Island	May, Sept.	90.2	70.6	56.1	45	31.8
NYISO, Long Island	Mar, Apr, Oct, Nov	68	61.1	53.7	44.6	32.5
PJM Eastern	Jun, Jul, Aug	95.3	87.7	76.9	65.5	49.9
PJM Eastern	Dec, Jan, Feb	80.5	71.8	62.7	51.5	43.5
PJM Eastern	May, Sept.	91.3	74.8	62.3	51.2	39.6
PJM Eastern	Mar, Apr, Oct, Nov	74.1	67.9	61.3	52.3	41.6
PJM Central	Jun, Jul, Aug	89.3	82.7	74.3	64.7	49.4
PJM Central	Dec, Jan, Feb	95.4	85.3	74.4	61.6	50.8
PJM Central	May, Sept.	82.3	73	65.8	54.3	42.2
PJM Central	Mar, Apr, Oct, Nov	86.1	79.3	70.3	60	47
PJM Western	Jun, Jul, Aug	96	88.8	78.2	65.8	49.8
PJM Western	Dec, Jan, Feb	86.3	74.3	63.8	53	43.7
PJM Western	May, Sept.	91	75.4	61	50.5	38.7
PJM Western	Mar, Apr, Oct, Nov	76.7	68.7	60.3	51.9	40.8
VACAR	Jun, Jul, Aug	95.3	89.3	80.7	68.7	52.9
VACAR	Dec, Jan, Feb	87.5	74.2	63.4	53.8	44.4
VACAR	May, Sept.	89.6	79.2	65.8	54.3	42.7
VACAR	Mar, Apr, Oct, Nov	78	69.3	60.5	53.2	43.2
SOU	Jun, Jul, Aug	97.2	92.5	84.6	71.3	54
SOU	Dec, Jan, Feb	79.8	66.6	56.9	47.9	39.7
SOU	May, Sept.	91.9	84.1	71.3	56.6	43.7
SOU	Mar, Apr, Oct, Nov	75.6	66.1	58.2	50.6	40.9
Entergy	Jun, Jul, Aug	97.3	93.3	86.6	75.5	60.4
Entergy	Dec, Jan, Feb	79.3	67.4	59.2	51.8	45.4
Entergy	May, Sept.	92.9	85.4	74.6	61.4	50
Entergy	Mar, Apr, Oct, Nov	78	69	61	54.4	46.3
TVA	Jun, Jul, Aug	94.1	86.6	68.1	73.1	64.7
TVA	Dec, Jan, Feb	91.5	77.8	66.7	57.3	48.1
TVA	May, Sept.	89.5	82	69.4	57.8	46.7
TVA	Mar, Apr, Oct, Nov	81.4	72.6	63.9	56.8	47.2
FRCC	Jun, Jul, Aug	96.4	91.2	82.8	69.5	50.2
FRCC	Dec, Jan, Feb	81.7	63.1	52.5	40.7	31.7
FRCC	May, Sept.	92.7	86.7	76	58.9	42.6
FRCC	Mar, Apr, Oct, Nov	84.8	75.6	62.9	49.5	36.2

Region	Months	1	2	3	4	5
ECAR	Jun, Jul, Aug	96.2	89.5	80.8	70.4	56
ECAR	Dec, Jan, Feb	87.3	78.7	70.5	59.8	51.8
ECAR	May, Sept.	86.6	78.9	69.3	59.2	48.6
ECAR	Mar, Apr, Oct, Nov	79.8	75.4	69.5	60.9	50.9
Com Ed	Jun, Jul, Aug	94.6	85	72.6	60.3	46
Com Ed	Dec, Jan, Feb	72.1	65.2	57.5	46.8	40.8
Com Ed	May, Sept.	83.4	70.2	58.7	48	38
Com Ed	Mar, Apr, Oct, Nov	67.4	62.5	57.9	48.6	39.5
South MAIN	Jun, Jul, Aug	96.7	89.5	78.8	65.9	52.2
South MAIN	Dec, Jan, Feb	78.6	70	62.4	53.3	46.5
South MAIN	May, Sept.	83.8	72.9	61.1	52.5	43.7
South MAIN	Mar, Apr, Oct, Nov	73.1	67.3	62	54.2	45.7
WIUM	Jun, Jul, Aug	95.9	90	81.7	72	57.1
WIUM	Dec, Jan, Feb	86	79.1	70.5	57.7	49.1
WIUM	May, Sept.	88.6	81.1	73	61.4	49.1
WIUM	Mar, Apr, Oct, Nov	83.9	78.4	72.7	61.8	50.2
MAPP	Jun, Jul, Aug	95.7	88.7	79.3	68.6	53.6
MAPP	Dec, Jan, Feb	86.2	79.1	69.5	58.5	50.9
MAPP	May, Sept.	87.2	76.1	66.9	56.3	45.3
MAPP	Mar, Apr, Oct, Nov	80.5	75.6	69.2	59.4	48.8
SPP North	Jun, Jul, Aug	96.6	90.3	80	65.3	48.8
SPP North	Dec, Jan, Feb	68	60.7	53.6	44.9	39.1
SPP North	May, Sept.	89.2	78.1	61.1	49	38.4
SPP North	Mar, Apr, Oct, Nov	66.7	59.8	54.5	47.2	38.6
SPP South	Jun, Jul, Aug	96.8	91.8	83.4	70.3	54.7
SPP South	Dec, Jan, Feb	70.2	60.9	53.6	45.7	37.4
SPP South	May, Sept.	90.7	80.5	65.5	53.1	42.8
SPP South	Mar, Apr, Oct, Nov	68.9	61	55.2	49.3	41.5
ERCOT	Jun, Jul, Aug	96.8	92.3	84.8	72.5	56.4
ERCOT	Dec, Jan, Feb	75.8	61.9	52.9	45.1	38.2
ERCOT	May, Sept.	92.3	85	71.8	57.2	44.6
ERCOT	Mar, Apr, Oct, Nov	77.3	65.8	55.8	48.5	39.6
WA, OR	Jun, Jul, Aug	76.6	73.5	69.4	63.6	52.6
WA, OR	Dec, Jan, Feb	95.7	84.6	74.6	63.3	54.6
WA, OR	May, Sept.	73.6	70.6	66.3	58.8	48.6
WA, OR	Mar, Apr, Oct, Nov	87.6	79.4	71	62.4	52.2
ID,UT,MT	Jun, Jul, Aug	96.7	93	86.9	77.9	63.8
ID,UT,MT	Dec, Jan, Feb	94.4	85.2	75.6	65.4	56.6
ID,UT,MT	May, Sept.	88.8	83.8	76.2	66.3	55.1
ID,UT,MT	Mar, Apr, Oct, Nov	87.6	80.4	73.5	65.6	55.3
Northern California	Jun, Jul, Aug	94.2	86.6	76.6	64.6	48.5
Northern California	Dec, Jan, Feb	74	65.9	57.1	44.8	37.9
Northern California	May, Sept.	89.1	79.1	66.8	54.2	41.6
Northern California	Mar, Apr, Oct, Nov	73.6	67.3	61.4	51.5	39.8
S California and Nevada	Jun, Jul, Aug	94.4	85.8	75.3	62.5	46.5
S California and Nevada	Dec, Jan, Feb	71.3	63.7	54.7	42.6	37.1
S California and Nevada	May, Sept.	95.9	84	68.2	53.6	41.1
S California and Nevada	Mar, Apr, Oct, Nov	78.4	69.8	61.7	50.2	39.4
Arizona/New Mexico	Jun, Jul, Aug	96.6	91.8	84.5	72.6	54.7
Arizona/New Mexico	Dec, Jan, Feb	69.8	61.4	53.7	45.8	39.2
Arizona/New Mexico	May, Sept.	92.7	85	72.5	57.1	43.3
Arizona/New Mexico	Mar, Apr, Oct, Nov	78.5	65.8	56.4	49.2	39.3
RMPP	Jun, Jul, Aug	96.8	91.9	84.3	74.5	59.8
RMPP	Dec, Jan, Feb	90.3	82.4	74.1	61.5	53.1
RMPP	May, Sept.	89.9	83	74.2	64.1	51.9
RMPP	Mar, Apr, Oct, Nov	85.3	79.4	73.6	65.4	53.5

FUEL PRICES – NATURAL GAS

Natural gas prices are based on Henry Hub wellhead prices from the Reference Case in *AEO 2004*, but gas futures prices are applied for the period 2004-2007. These are provided in Table IV-5. Delivery costs are added to these basic gas price assumptions to obtain the regional delivered prices that are used to determine unit fuel costs in each region. Table IV-6 shows the delivered gas prices that are input to the model.

Table IV-5. Henry Hub Wellhead Gas Price Assumptions
(1999$/MMBtu)

Year	$/MMBtu
2004	$4.98
2008	$3.56
2010	$3.33
2012	$3.65
2015	$4.06
2018	$4.03
2020	$4.13

FUEL PRICES – COAL

Coal prices are based on delivered spot price data reported to FERC. Current assumptions are based on the 1999 price data. The reported delivered spot price data were divided into the price of each coal type delivered within its supply region and the incremental cost of that type of coal delivered to each of the other regions in the model. The price between a supply region and an electric market in the same general location is treated as comparable to an FOB price (although it should be noted that this price includes local delivery costs and is thus not formally an FOB price). The other destinations (not in the same general location) include a transportation adder. Table IV-7 shows the within-region prices for each coal type from each coal-producing region. Table IV-8 presents the transport costs to the different demand regions in the model. If there is no entry in the coal transport cost table, then it is not possible in EPMM for coals to be shipped between that origin-destination pair.

Table IV-6. Delivered Natural Gas Prices
(1999$/MMBtu)

Sub-Region	2004	2008	2010	2012	2015	2018	2020
NEPP	$5.35	$3.92	$3.68	$3.99	$4.37	$4.34	$4.42
NYISO, West	$5.35	$3.92	$3.68	$3.99	$4.37	$4.34	$4.42
NYISO, Capital	$5.35	$3.92	$3.68	$3.99	$4.37	$4.34	$4.42
NYISO, Hudson Valley	$5.35	$3.92	$3.68	$3.99	$4.37	$4.34	$4.42
NYISO, New York City	$5.44	$4.00	$3.76	$4.07	$4.45	$4.41	$4.49
NYISO, Long Island	$5.44	$4.00	$3.76	$4.07	$4.45	$4.41	$4.49
PJM Eastern	$5.35	$3.92	$3.68	$3.99	$4.37	$4.34	$4.42
PJM Central	$5.35	$3.92	$3.68	$3.99	$4.37	$4.34	$4.42
PJM Western	$5.35	$3.92	$3.68	$3.99	$4.37	$4.34	$4.42
VACAR	$5.26	$3.83	$3.59	$3.91	$4.30	$4.26	$4.35
SOU	$5.26	$3.83	$3.59	$3.91	$4.30	$4.26	$4.35
Entergy	$5.12	$3.70	$3.46	$3.78	$4.18	$4.15	$4.24
TVA	$5.12	$3.70	$3.46	$3.78	$4.18	$4.15	$4.24
FRCC	$5.26	$3.83	$3.59	$3.91	$4.30	$4.26	$4.35
ECAR	$5.17	$3.74	$3.51	$3.82	$4.22	$4.19	$4.28
Com Ed	$5.17	$3.74	$3.51	$3.82	$4.22	$4.19	$4.28
South MAIN	$5.03	$3.61	$3.38	$3.70	$4.10	$4.07	$4.17
WIUM	$5.17	$3.74	$3.51	$3.82	$4.22	$4.19	$4.28
MAPP	$5.03	$3.61	$3.38	$3.70	$4.10	$4.07	$4.17
SPP North	$5.03	$3.61	$3.38	$3.70	$4.10	$4.07	$4.17
SPP South	$5.12	$3.70	$3.46	$3.78	$4.18	$4.15	$4.24
ERCOT	$5.12	$3.70	$3.46	$3.78	$4.18	$4.15	$4.24
WA, OR	$4.89	$3.48	$3.25	$3.58	$3.98	$3.96	$4.06
ID,UT,MT	$5.12	$3.70	$3.46	$3.78	$4.18	$4.15	$4.24
N California	$5.21	$3.79	$3.55	$3.86	$4.26	$4.22	$4.31
S California/Nevada	$5.77	$4.31	$4.06	$4.36	$4.73	$4.68	$4.75
Arizona/New Mexico	$5.21	$3.79	$3.55	$3.86	$4.26	$4.22	$4.31
RMPP	$5.12	$3.70	$3.46	$3.78	$4.18	$4.15	$4.24

Table IV-7. Coal Prices Delivered to Model Region Containing Coal Source
(1999$/MMBtu)

***Supply Region*:**	**AL**	**IL**	**IN**	**KS**	**KY**	**LA**	**MD**	**MT**	**ND**	**NM**	**OH**	**PA**	**TN**	**TX**	**VA**	**WV**	**WY**
Coal Type																	
Bit, Low, Low	1.41		1.20		1.37										1.47	1.28	
Bit, Low, Med												1.35					
Bit, Med, Low	1.36	1.37	1.15		1.28								1.49		1.34	1.26	
Bit, Med, Med												1.27					
Bit, High, Low		1.17	1.01	1.04	1.24												
Bit, High, Med							1.17								1.34	1.12	
Bit, High, High	1.34										1.02	1.15					
Sub, Low, Low								1.23		1.16							1.01
Sub, Low, Med								1.25		1.12							1.31
Lignite						1.36			0.73					1.01			

COAL SWITCHING LIMITATIONS

Certain types of coal switching are limited. No units may switch into or out of lignite coals in the EPMM runs. Further, EPMM limits the degree to which units currently burning bituminous coal can switch to subbituminous coals. Specifically, the Btu input of subbituminous coal at a unit designed to burn bituminous coal could not exceed 50 percent.[17]

Finally, there is a limit on the amount of each type of coal that is available. The availability of each type of coal is allowed to grow over the period of analysis by 2 percent per year. This assumption was based on historically observed rates, combined with the judgments of coal industry experts. The maximum quantity of each coal available in each modeled year is provided in Table IV-9.

Table IV-8. Coal Transportation Costs (1999$/MMBtu)

Supply Region:	**AL**	**IL**	**IN**	**KS**	**KY**	**LA**	**MD**	**MT**	**ND**	**NM**	**OH**	**PA**	**TN**	**TX**	**VA**	**WV**	**WY**
Delivery Area																	
NEPP					0.65						0.56	0.50			0.24	0.63	
NYISO, West												0.27				0.21	
NYISO, Capital					0.68							0.27				0.21	
NYISO, Hudson Valley																0.53	
NYISO, Long Island					0.32						0.54						
PJM Eastern					0.32						0.54	0.11			0.24	0.24	
PJM Central					0.32						0.54	0.11			0.24	0.24	
PJM Western					0.21		0.00					0.11			0.24	0.24	
VACAR	0.00	0.36			0.29							0.23	0.34		0.05	0.17	
SOU															0.26	0.27	0.80
Entergy		0.00			0.04												0.70
TVA					0.43								0.00		0.06	0.00	
FRCC		0.05	0.00		0.00			0.00			0.00				0.40	0.31	
ECAR		0.48										0.00			0.00	0.00	0.47
Com Ed		0.13	0.26														0.54
South MAIN		0.60	0.37		0.56												0.41
WIUM		0.26	0.48		0.34			0.08				0.42				0.29	0.38
MAPP		0.85		0.00				0.10	0.00		0.38	0.52				0.49	0.25
SPP North																	0.14
SPP South														0.17			0.70
ERCOT				0.41		0.00											
WA, OR				0.41										0.00			0.48
ID,UT,MT				0.41				0.07									0.51
S California/Nevada				0.41													
Arizona/New Mexico				0.41													0.10
RMPP				0.41				0.07		0.00							0.65

Table IV-9. Maximum Coal Consumption by Coal Type
(Trillions of Btus)

Coal Type	Bituminous							Subbituminous		Lignite	Total
Sulfur Content	Low		Med		High			Low	Med		
Hg Content	Low	Med	Low	Med	Low	Med	High	Low			
2004	3,366	10	4,416	533	1,962	1,103	1,661	7,360	1,138	1,229	22,776
2008	3,644	10	4,780	577	2,123	1,194	1,798	7,966	1,232	1,330	24,653
2010	3,791	11	4,973	600	2,209	1,242	1,870	8,288	1,282	1,384	25,649
2012	3,944	11	5,174	624	2,298	1,292	1,946	8,623	1,333	1,439	26,686
2015	4,186	12	5,490	663	2,439	1,371	2,065	9,151	1,415	1,528	28,319
2018	4,442	13	5,826	703	2,588	1,455	2,191	9,711	1,502	1,621	30,052
2020	4,621	13	6,062	732	2,693	1,514	2,280	10,103	1,562	1,687	31,267

TRANSMISSION LIMITS

To ensure a realistic dispatch of units it is necessary to reflect constraints imposed by the transmission grid. Table IV-10 shows the maximum transmission flow among the 28 regions for the summer period.

Table IV-10. Maximum Transmission Flow for Summer Months
(MW)

From: / To:	NEPP	NYISO, West	NYISO, Capital	NYISO, Hudson Valley	NYISO, NYC	NYISO, Long Island	PJM Eastern	PJM Central	PJM Western	VACAR	SOU	Entergy	TVA	FRCC
NEPP		150	500	500		500								
NYISO, West	150		3,350	1,600			1,000		1,000					
NYISO, Capital	800	1,999		3,270										
NYISO, Hudson Valley	800	1,600	1,999		3,700	1,200	2,000							
NYISO, NYC				1,999		270	1,000							
NYISO, Long Island	500			1,200	420									
PJM Eastern		1,000		500	1,000			6,600						
PJM Central							6,600		4,700					
PJM Western		2,075						4,700		3,440				
VACAR									4,560		3,477		2,986	
SOU										623		2,749	2,776	3,600
Entergy											750		700	
TVA										2,986	3,224	3,177		
FRCC											2,600			
ECAR									2,773	2,522			679	
Com Ed														
South MAIN												2,825	3,972	
WIUM														
MAPP												2,020		
SPP North												1,379		
SPP South												1,379		
ERCOT														
WA, OR														
ID,UT,MT														
N California														
S California/ Nevada														
Arizona/New Mexico														
RMPP														

Table IV-10 (continued). Maximum Transmission Flow for Summer Months

From: / To:	ECAR	Com Ed	South MAIN	WIUM	MAPP	SPP North	SPP South	ERCOT	WA, OR	ID,UT,MT	N Calif	S Calif/ Nevada	Arizona/ New Mexico	RMPP
NEPP														
NYISO, West														
NYISO, Capital														
NYISO, Hudson Valley														
NYISO, NYC														
NYISO, Long Island														
PJM Eastern														
PJM Central														
PJM Western	4,077													
VACAR	3,528													
SOU														
Entergy			860		750	200	200							
TVA	1,621		2,028											
FRCC														
ECAR		4,000	2,000											
Com Ed	4,000		3,700	1,100										
South MAIN		2,300			300	1,178								
WIUM		2,000			750									
MAPP			1,862	950		2,077				200				310
SPP North			2,622		523		1,200							
SPP South						1,500		800					420	
ERCOT							800							
WA, OR										2,250	4,360	3,100		
ID,UT,MT					150				3,750		120	1,937	1,045	1,350
N California									3,675	100		3,000		
S California/ Nevada									3,100	1,417	2,400		9,578	
Arizona/New Mexico							420			1,115		10,118		650
RMPP					310					3,400			550	

RESERVE MARGINS

Capacity build is motivated by the need to serve growing loads. Table IV-11 provides the reserve margin requirements assumed for each region.

Table IV-11. Percentage Reserve Margin Requirement

Sub-Region	Percent Margin
NEPP	18
NYISO, West	18
NYISO, Capital	18
NYISO, Hudson Valley	18
NYISO, New York City	18
NYISO, Long Island	18
PJM Eastern	17
PJM Central	17
PJM Western	17
VACAR	16
SOU	16
Entergy	16
TVA	16
FRCC	20
ECAR	16
Com Ed	15
South MAIN	15
WIUM	15
MAPP	15
SPP North	13.6
SPP South	13.6
ERCOT	11
WA, OR	11
ID,UT,MT	11
N California	15
S California/Nevada	15
Arizona/New Mexico	13
RMPP	15

CONTROL TECHNOLOGIES

In modeling the scenarios described above, coal units were provided with retrofit options to meet SO_2, NO_x, and Hg restrictions. Wet FGDs are available as a retrofit to meet tighter SO_2 caps, SCRs are available for reducing NO_x emissions (SCRs are also available to steam oil/gas units);[18] and ACI were available to lower Hg emissions.[19] The costs and characteristics for each retrofit option are included in Table IV-12. The percentage removals for Hg are *incremental* to the Hg removals that occur due to co-benefits. (Total Hg removal may therefore exceed 90 percent.)

The cost and effectiveness of ACI control technology is by far the most uncertain. Assumptions used in EPMM were developed by EPRI control technology researchers, based on experience with a very limited number of pilot and test installations. In these model runs, ACIs were only available in combination with a COHPAC unit, unless the unit has a fabric filter (FF) already installed.[20] This assumption was made because off-line calculations indicated that the ACI+COHPAC combination would almost always have a lower cost per pound of Hg removed than the ACI alone. Thus, the ACI alone would almost never be selected even if it were available.[21] Data suggest that the amount of carbon injection required to remove particular percentages of Hg is higher for units burning lignite coal. Thus, the costs and characteristics of the ACI+COHPAC retrofit available to units burning lignite coal are different from those available to units burning bituminous and subbituminous coals.[22]

Table IV-12. Cost and Characteristics of Control Technologies
(Costs are in 1999$)

Retrofit	Reference Capital Cost* ($/kW)	Reference Fixed O&M Cost* ($/kW-yr)	Ref. Size (MW)	Scaling Ex-ponent	Variable Cost ($/MWh)	Incremental Percent Removed "R"
Wet FGD	$201.00	$8.00	500	0.60	$1.00	SO_2: 90%
SCR	$80.00	$0.53	243	0.35	$0.97	NO_x: 95%
ACI (on existing FF units only) *for bituminous & subbituminous*	$1.91	$0.77	250	0.35	$0.312 x (exp((1.1 x **R**)^1.7) -1)	Hg: 0% - 90%
ACI (on existing FF units only) *for lignite coal*	$1.91	$0.77	250	0.35	$0.395 x (exp((1.8 x **R**)^1.8) -1)	Hg: 0% - 75%
ACI+COHPAC *for bituminous & subbituminous*	$52.63	$0.96	250	0.35	$0.312 x (exp((1.1 x **R**)^1.7) -1)	Hg: 0% - 90%
ACI+COPAC *for lignite coal*	$52.63	$0.96	250	0.35	$0.395 x (exp((1.8 x **R**)^1.8) -1)	Hg: 0% - 75%

* Unit-Specific Cost = Reference Cost x (Reference Size/Unit MW)^(Scaling Exponent);
Maximum unit size for scaling is 500 MW for all technologies in table above.

EPMM has the capability to precisely adjust the percentage of Hg removal by an ACI or ACI+COHPAC retrofit to meet the needs of each unit. Rather than a fixed percentage

removal (*e.g.*, either 60% removal or 90% removal), the ACI+COHPAC can remove anywhere between 0% and 90% for bituminous and subbituminous coals, and anywhere between 0% and 75% for lignite coals. This is why the variable cost in Table IV-12 is an equation rather than a fixed number, increasing at an increasing rate as the percent removal, **R**, rises towards its maximum. EPMM recognizes the flexibility of ACI+COHPAC retrofits and allows each unit to meet precisely the percent reduction that would be required under a MACT-type of control.

MERCURY CO-BENEFITS AND MERCURY EMISSIONS SPECIATION

Table IV-13 shows the Hg co-benefits, or percent removal, assumed for each of the combinations of unit equipment before any ACI controls might be added. The values on the left of the slashes are the EPMM assumptions. These values were based primarily on EPRI's analysis of the 1999 ICR data, and were adjusted judgmentally to reflect more recent experience of EPRI and industry researchers. The values on the right of the slashes are the respective assumptions being used at present by EPA in the IPM model. The EPA values are presented here because they are one of the most significant issues contributing to the differences between EPA and EPMM findings.

Table IV-13. Comparison of EPMM and EPA Hg Co-Benefits Assumptions (Percent Removal of Hg Relative to Inlet Hg)

Existing PM Collector	Existing SO_2 Controls	SCR	Bituminous * (EPMM / EPA)	Subbituminous * (EPMM / EPA)	Lignite * (EPMM / EPA)
FF	Dry FGD	no	85 / 95	25 / 25	10 / 0
		yes	90 / 95	25 / 25	10 / 0
	Wet FGD	no	85 / 97	75 / 73	40 / 44
		yes	90 / 90	75 / 85	40 / 44
	None	no	75 / 89	65 / 73	10 / 0
		yes	75 / 89	65 / 73	10 / 0
CSESP	Dry FGD	no	50 / 36	15 / 35	10 / 0
		yes	85 / 36	15 / 35	10 / 0
	Wet FGD	no	60 / 66	35 / 16	35 / 44
		yes	85 / 90	35 / 66	35 / 44
	None	no	35 / 36	20 / 3	10 / 0
		yes	35 / 36	20 / 3	10 / 0
HSESP	Dry FGD	no	*n/a* / 40	*n/a* / 15	*n/a* / 0
		yes	*n/a* / 40	*n/a* / 15	*n/a* / 0
	Wet FGD	no	55 / 42	30 / 20	30 / 0
		yes	85 / 90	30 / 25	30 / 0
	None	no	20 / 10	0 / 6	0 / 0
		yes	20 / 10	0 / 10	0 / 0

*Percent removals for EPA are sourced from IPM Model Documentation v.2.1.6, Attachment K

Table IV-14 presents the assumptions used to speciate the Hg emissions between elemental Hg and ionic Hg (data in the table are the percent of Hg emissions that is elemental Hg; the remaining Hg emissions are ionic). The speciation is a function of the rank of coal and the existing equipment on the unit that emits the coal. The assumptions for units without SCRs are based on the EPRI correlations developed from the ICR data, assuming ICR-based average chlorine contents for each of the coal ranks. The assumptions for units with SCRs (which were not represented in the ICR data) were the judgments of EPRI Hg technology research staff, taking into account a structural understanding of how the SCR affects flue gas speciation and field experience of the past several years.

Table IV-14 – Percent of Emissions Emitted as Hg^0

Existing PM Collector	Existing SO_2 Controls	SCR?	Bituminous	Subbituminous	Lignite
Fabric Filter	Dry FGD	None	70%	90%	95%
Fabric Filter	Dry FGD	SCR	30%	90%	95%
Fabric Filter	Wet FGD	None	45%	85%	85%
Fabric Filter	Wet FGD	SCR	40%	85%	85%
Fabric Filter	None	None	5%	30%	30%
Fabric Filter	None	SCR	5%	30%	30%
Cold-Side ESP	Dry FGD	None	90%	95%	95%
Cold-Side ESP	Dry FGD	SCR	60%	95%	95%
Cold-Side ESP	Wet FGD	None	85%	90%	90%
Cold-Side ESP	Wet FGD	SCR	60%	90%	90%
Cold-Side ESP	None	None	35%	60%	55%
Cold-Side ESP	None	SCR	10%	60%	55%
Hot-Side ESP	Dry FGD	None	40%	80%	80%
Hot-Side ESP	Dry FGD	SCR	40%	80%	80%
Hot-Side ESP	Wet FGD	None	80%	98%	95%
Hot-Side ESP	Wet FGD	SCR	60%	98%	95%
Hot-Side ESP	None	None	40%	70%	70%
Hot-Side ESP	None	SCR	10%	70%	70%
None	Dry FGD	None	90%	95%	95%
None	Dry FGD	SCR	50%	95%	95%
None	Wet FGD	None	90%	95%	95%
None	Wet FGD	SCR	50%	95%	95%
None	None	SCR	90%	95%	95%
None	None	None	91%	95%	95%

V. DETAILS OF SCENARIO SPECIFICATIONS

BASE CASE

The Base Case includes existing SO_2 (Title IV) and NO_x (SIP Call) regulations, as well as state regulations. Regulations for the following states are included: North Carolina, Connecticut, Massachusetts, New Hampshire, New York, Missouri, Illinois, Maine, and Texas. All of these regulations relate to SO_2 and/or NO_x. Connecticut also includes an emission limit for Hg. In addition to Title IV, the Western Regional Air Partnership (WRAP) has SO_2 caps for nine states beginning in 2018.[23] Table V-1 shows the emissions caps for the non-state programs that are applied in the Base Case.

Table V-1. Base Case Emissions Caps
(Short Tons)

	SO_2		NO_x
Year	**US**	**WRAP**	**SIP Call**
2004	9,480,000		517,199
2008	9,480,000		517,199
2010	8,950,000		517,199
2012	8,950,000		517,199
2015	8,950,000		517,199
2018	8,950,000	271,000	517,199
2020	8,950,000	271,000	517,199

CAIR ONLY

The CAIR Only case layers that proposed rule's SO_2 and NO_x regulations on top of the existing regulations in the Base Case, beginning in 2010. (However, given the way the SO_2 cap is proposed, banking of SO_2 prior to 2010 can be used to meet the CAIR SO_2 cap that is first implemented in 2010.) The simulation of the CAIR caps was performed for a geographic area slightly different from that specified in the proposed rule. The NO_x rules were applied to the states included in the East Region of the Clear Skies Act (CSA). This required some modification of the NO_x caps that were modeled. Specifically, tonnage for western Missouri, which is not included in the East Region of the CSA, was netted from the capped amounts of 1.6 million tons and 1.3 millions tons in 2010 and 2015, respectively. Tonnage was added for Florida, Maine, New Hampshire, Rhode Island,

Vermont, and the western portion of Texas, as these areas are part of the East Region of CSA, but not part of the CAIR region. The tons added (subtracted) were based on an emission rate of 0.150 lbs/MMBtu in 2010 and 0.125 lbs/MMBtu in 2015.[24] This resulted in slightly higher NO_x caps of approximately 1.7 million tons in 2010 and 1.4 million tons in 2015.

SO_2 was modeled with a single national cap. However, emissions for the District of Columbia and the 28 states included in the CAIR were applied using the ratios in the rule.[25] To compute a single national cap that allows trading at a national level, existing Title IV Phase II allowances were used for each state. States included in the CAIR had their allowances divided by two for the period 2010 through 2014 and divided by three for 2015 and later years. This resulted in a national cap of approximately 5.1 million tons in 2010 and 3.8 million tons in 2015.[26] Table V-2 below shows the modeled national and regional caps applied in the CAIR Only scenario.

Table V-2. CAIR Only Emissions Caps
(Short Tons)

	SO_2		NO_x	
Year	**US**	**WRAP**	**SIP Call**	**CAIR**
2004	9,480,000		517,199	
2008	9,480,000		517,199	
2010	5,086,400		517,199	1,675,968
2012	5,086,400		517,199	1,675,968
2015	3,798,600		517,199	1,363,307
2018	3,798,600	271,000	517,199	1,363,307
2020	3,798,600	271,000	517,199	1,363,307

CAIR + Hg CAP

The CAIR + Hg Cap case begins with the CAIR Only caps and adds a cap on Hg emissions as well. The cap on Hg emissions begins in 2010 with a cap of 34 tons, which is then reduced to 15 tons in 2015. Table V-3 shows the modeled national and regional caps applied in the CAIR + Hg Cap case.

Table V-3. CAIR + Hg Cap Emissions Caps
(Short Tons)

Year	SO_2		NO_x		Hg
	US	WRAP	SIP Call	CAIR	
2004	9,480,000		517,199		
2008	9,480,000		517,199		
2010	5,086,400		517,199	1,675,968	34.0
2012	5,086,400		517,199	1,675,968	34.0
2015	3,798,600		517,199	1,363,307	34.0
2018	3,798,600	271,000	517,199	1,363,307	15.0
2020	3,798,600	271,000	517,199	1,363,307	15.0

The Hg Cap & Trade policy proposal also includes a feature where units may borrow against their future Hg allocations at a maximum permit price of $2,187.50 per ounce ($35,000 per pound in 2004 dollars). This feature, often called a "safety valve," was added to provide stability in Hg allowance prices. Although it may dampen Hg allowance price volatility, its specific formulation in the proposed rule makes it unlikely to actually cap the equilibrium market price of Hg allowances.[27] Another reason this feature is unlikely to cap the market price of Hg allowances is because the proposed supplemental rule authorizes each state to decide whether or not to allow this "borrowing" at a maximum price. Current politics suggest that many states would not avail themselves of this feature.

Nevertheless, this feature was considered in the EPMM Hg Cap & Trade simulations. However, EPMM projected that equilibrium allowance prices are unlikely to exceed the maximum price of $35,000/lb. This policy scenario was run under a range of assumptions about the rate of technological improvement in the currently immature Hg control technology based on activate carbon injection. Costs of the technology were assumed to decrease by annual rates of 0% (i.e., no technological improvement at all), 1.5%, 2.5%, and 4.0% (the last of these rates was applied only to the variable operating cost component.) EPMM projects that Hg allowance prices would not exceed the safety valve price except in the case where there is no technological improvement at all over the next 16 years, and even then the exceedance would not occur until after 2018. In all the other years and in all the other cases, EPMM finds no equilibrium demand to use the safety valve feature.

The alternative assumptions about rates of technological improvement had no substantial effect on projected Hg emissions over time, or on markets and compliance methods for other emissions. The specific numerical results presented in this paper are from the zero technological change case.

CAIR + Hg MACT

The CAIR + Hg MACT case also begins with the CAIR Only caps and then adds an emissions rate limit for Hg beginning in 2008. The relevant rate limit is based on the rank of coal burned by a unit. The rate limit for bituminous coal is 2.0 pounds per trillion Btu; the rate limit for subbituminous coal is 5.8 pounds per trillion Btu; and the rate limit for lignite coal is 9.2 pounds per trillion Btu. For units that blend coals, the modeling requires that the respective rate limit for each coal must be met. For example, if a unit consumes bituminous and subbituminous coals in equal share, the model requires that the emissions rate limit on the bituminous portion is 2.0 pounds per trillion Btu and 5.6 pounds per trillion Btu on the subbituminous portion. Each unit must meet these constraints, and no trading is allowed.

VI. RESULTS OF SCENARIOS

Several important caveats are warranted regarding the results of the scenarios. In particular, the model runs presented here have not assigned any limitations or constraints on the numbers or aggregate capacity of retrofits that may be installed in any year. No lead times have been imposed for retrofits either, so that the model is free to start installing new control technologies such as FGD even in the 2004 model year. In reality, only FGDs that are already in the advanced planning phases (of which there are very few) could possibly be in place before 2007. To the extent that some scenarios project relatively large numbers of FGDs prior to 2008, model results must be viewed as unrealistic. Similarly, if the aggregate quantity of retrofits of any type of technology becomes large in a short period of time, model results must be interpreted with great caution. Finally, the modeling places no limit on when that the mercury control technology based on activated carbon injection (ACI) will be commercially available on a widespread basis. Model scenarios that indicate a need for large quantities of retrofits of this technology within the next few years should be viewed as potentially unrealistic.

Figure VI-1 shows the projected trends in total national emissions of Hg under each of the policies simulated with EPMM. Figure VI-2 shows the projected trends for Hg^{2+}, and Figure VI-3 shows the projected trends for Hg^{0}. (The sum of Hg emissions in Figures VI-2 and VI-3 equal those in Figure VI-1.)

Figure VI-1 reveals that co-benefits from FGD and SCRs projected under the CAIR Only scenario are projected to induce a reduction relative to the Reference Case of about 7 tons by 2010, bringing projected total Hg emissions to 40 tons in 2010. These are called "co-benefits" because they occur without any specific policy constraints on Hg emissions or emissions rates. EPMM's projection of 40 tons as the "co-benefits" level contrasts to the EPA estimate of 34 tons by 2010 due to the CAIR alone.

Because EPMM's projected co-benefits level of Hg emissions is higher than 34 tons, the Hg Cap & Trade scenario requires an additional 6 tons of Hg reduction by 2010. This is almost as large of an extra reduction as the co-benefits-based reduction. The result is that emissions are projected to fall just to the Phase I cap level at first. However, over the course of the Hg Cap & Trade's Phase I (2010-2017), Hg emissions do continue to decline gradually, to about 30 tons per year in the 2015-2017 period. A bank of Hg allowances is thus projected to accumulate to a level of about 18 tons at the beginning of Phase II in 2018. This bank is projected to be entirely used up by 2020, and projected Hg emissions reach the Phase II cap of 15 tons by 2020.

The Hg MACT, in contrast, reduces emissions sooner, but only reduces them to about 32 tons. After the initial introduction of the MACT constraints in 2008, there is only a small amount of further reduction in Hg through 2020. The model indicates that the

Hg Cap & Trade proposal will produce lower Hg emissions than the Hg MACT proposal after about 2012.

Figure VI-1. Projected Trends in National Hg Emissions

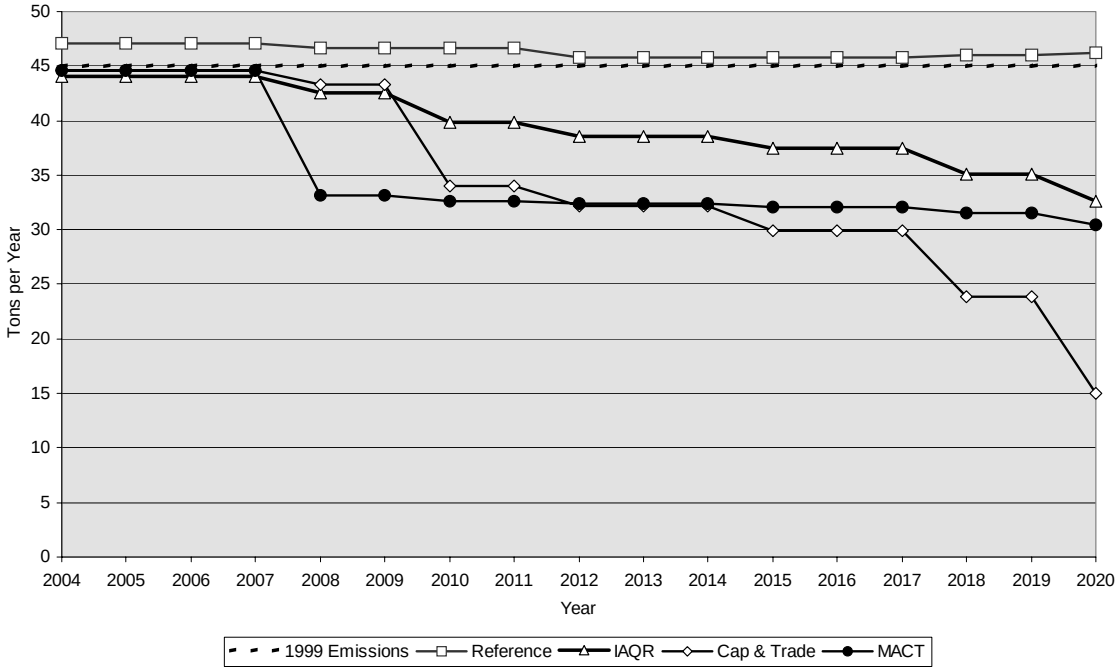

Figure VI-2. Projected Trends in National Hg^{2+} Emissions

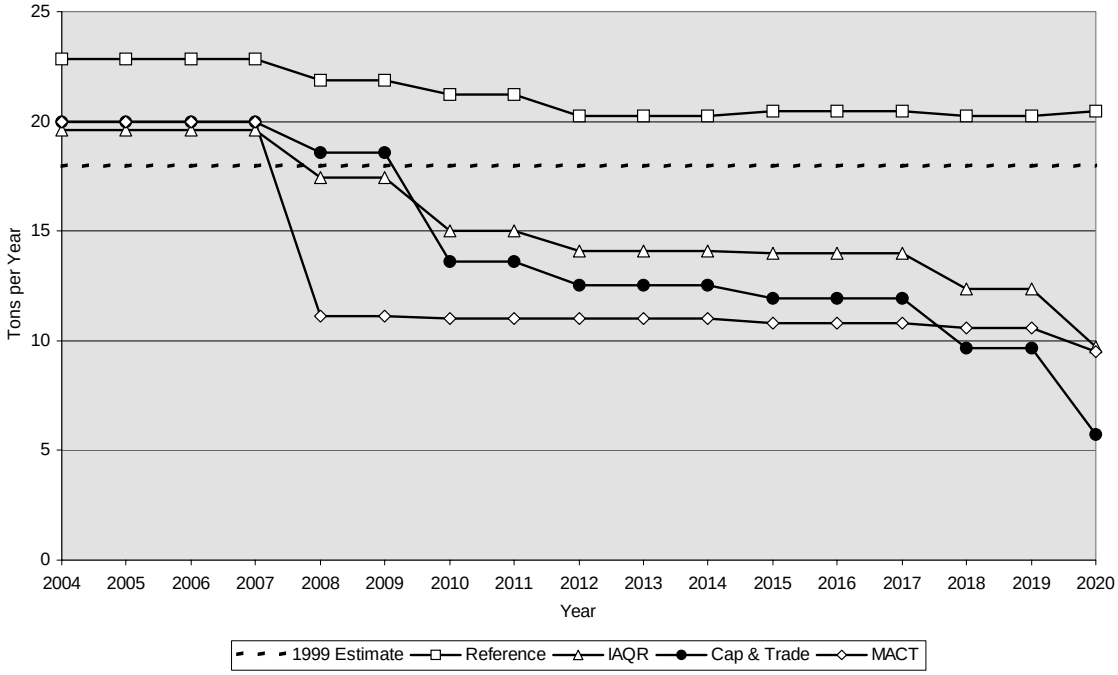

Figure VI-3. Projected Trends in National Hg^0 Emissions

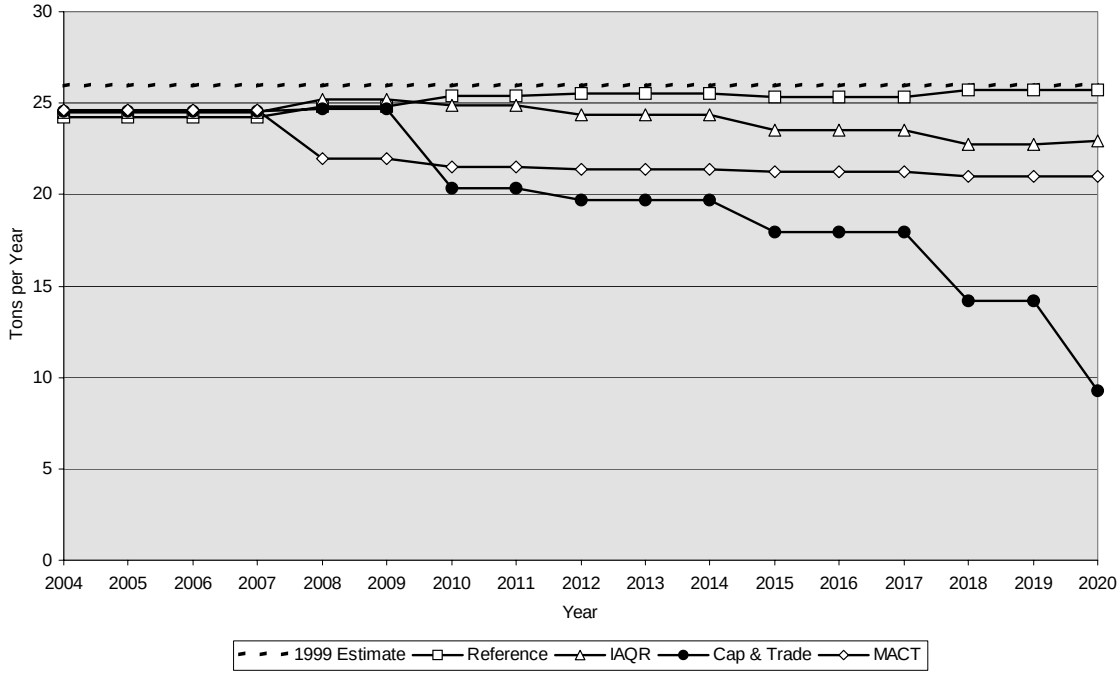

Table VI-1 shows the costs of each scenario relative to the Base Case. The Hg Cap & Trade case costs $2 billion more than the CAIR Only (on a net present value basis in 1999 dollars), while the Hg MACT case costs $10 billion more than the CAIR Only case. Thus the Hg Cap & Trade policy is projected to cost one-fifth what the Hg MACT policy would cost, despite the fact that the proposed Hg Cap & Trade policy would ultimately produce much lower Hg emissions than the proposed MACT policy. At an aggregate level, the main benefit of the Hg MACT appears to be that emissions would be lower for a few years before the Hg Cap & Trade would produce greater reductions.

Table VI-1. Annual and Present Value of Scenario Costs Incremental to Base Case (billions of dollars, $1999)

Year	CAIR	MACT	Cap & Trade
2004	$0.8	$0.7	$0.7
2008	1.2	4.4	0.8
2010	2.1	4.4	2.5
2012	2.5	4.3	3.2
2015	3.3	5.0	4.0
2018	4.5	5.3	5.3
2020	7.0	6.8	8.1
Present Value	**$17.7**	**$27.8**	**$19.7**
Incremental Present Value Cost of Adding Hg Provisions on Top of CAIR:		***$10.1***	***$2.0***

One purpose of this emissions analysis was to produce speciated emissions projections on a spatially-disaggregated scale, for input to the TEAM deposition modeling effort by AER, Inc. Although inputs to TEAM were disaggregated to individual stacks, Figure VI-4 provides a summary by state of the results. Figure VI-4 shows the 2020 emissions in each state under the MACT versus under the Hg Cap & Trade. The square dots reflect Hg^{2+} emissions of each state, and the solid chevron dots reflect Hg^{0} emissions of each state. (Thus, there are 48 dots of each type, for the 48 states represented in the model.) Dots occur above the diagonal line bisecting the graph when the state's 2020 emissions are higher under the MACT scenario than under the Hg Cap & Trade scenario. The deposition results themselves must be inspected to understand what these emissions projections imply, but Figure VI-4 indicates that the Hg Cap & Trade is likely to provide lower values of deposition relative to the Hg MACT over most areas of the U.S.

The rest of this section summarizes the patterns of retrofits and state-level emissions totals that underlie the trends shown above, and the deposition patterns that result for the more detailed unit-specific emissions are presented in the main body of EPRI's comments.

Figure VI-4. State-by-State Hg Species under Hg Cap & Trade vs. Hg MACT

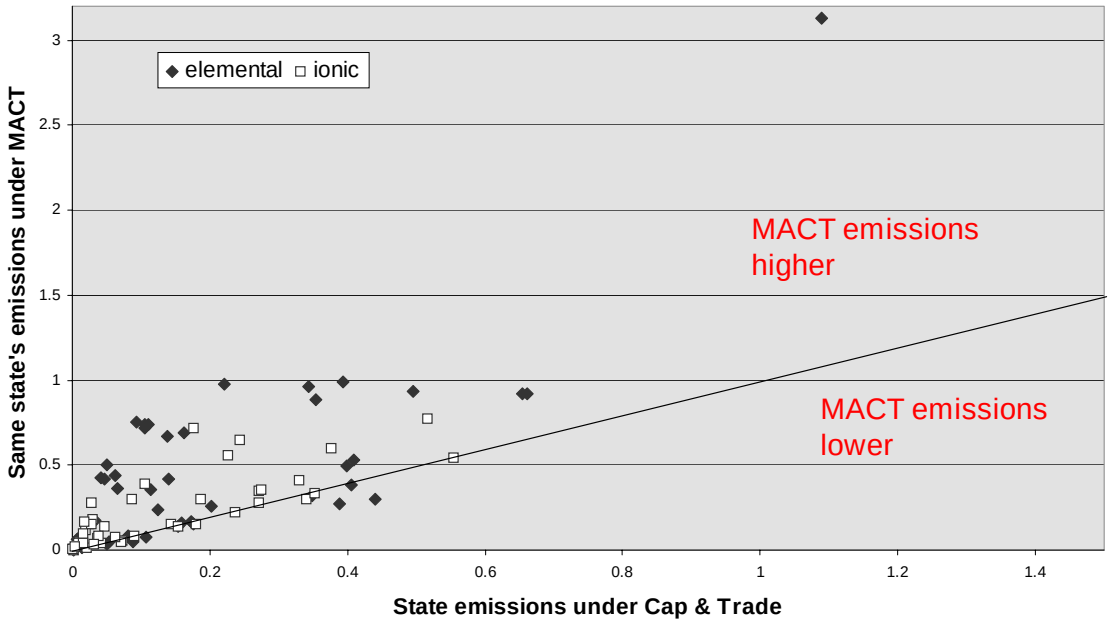

BASE CASE

As Table VI-2 shows, in the Base Case, 13 GW install wet FGDs by 2020 and 29 GW install SCRs by 2020. As a result of existing state regulations, 1 GW install ACI, either with an existing fabric filter (FF) or with a retrofitted COHPAC, by 2020. The FGDs are installed across several years reflecting the need for greater controls as demand grows and the SO_2 bank is drawn down. The SCR installations are focused in 2004 to meet the NO_x SIP Call.[28] Table VI-3 shows the Base Case emissions of SO_2, NO_x, and Hg by model region.

Table VI-2. Base Case Retrofits
(Megawatts)

Year	Wet FGD	Coal SCR	ACI+FF or +COHPAC
2004	563	18,508	979
2008	2,671	2,606	72
2010	1,913	252	0
2012	3,613	385	0
2015	0	0	0
2018	4,492	394	0
2020	95	6,575	0
Total	13,346	28,720	1,050

Table VI-3. Base Case Coal Plant Emissions

(SO_2 in thousands of short tons, NO_x and Hg in short tons)

	2004			2010			2020		
Region	**SO_2**	**NO_x**	**Hg**	**SO_2**	**NO_x**	**Hg**	**SO_2**	**NO_x**	**Hg**
NEPP	82	12,708	0.27	33	12,088	0.20	34	12,736	0.20
NYISO, West	82	28,315	0.33	97	27,187	0.40	86	26,923	0.35
NYISO, Capital	-	-	-	-	-	-	-	-	-
NYISO, Hudson Valley	26	6,815	0.09	26	6,815	0.09	26	6,815	0.09
NYISO, New York City	-	-	-	-	-	-	-	-	-
NYISO, Long Island	-	-	-	-	-	-	-	-	-
PJM Eastern	258	28,217	1.00	196	30,959	0.88	155	34,850	0.80
PJM Central	471	32,602	1.29	360	34,801	1.15	283	37,980	1.01
PJM Western	821	68,421	2.81	716	68,739	2.67	570	72,234	2.42
VACAR	1,274	166,752	3.74	802	138,649	2.68	756	154,066	2.53
SOU	1,157	207,544	3.95	1,150	209,845	3.95	1,004	221,496	3.59
Entergy	200	74,458	1.27	201	75,763	1.28	201	75,763	1.28
TVA	428	95,900	1.62	420	96,267	1.53	399	102,172	1.59
FRCC	184	69,531	0.98	187	83,246	0.94	178	100,125	1.04
ECAR	2,805	554,807	11.08	2,559	577,281	11.84	2,481	527,900	11.68
Com Ed	115	50,287	0.73	133	57,570	0.85	169	60,935	1.08
South MAIN	405	99,361	2.11	404	103,045	2.14	441	106,584	2.25
WIUM	178	79,639	1.09	178	79,711	1.09	184	82,085	1.12
MAPP	471	251,551	3.95	498	259,567	4.08	484	267,747	4.11
SPP North	316	110,457	1.35	199	110,608	1.41	223	118,887	1.51
SPP South	251	89,773	2.01	251	89,773	2.01	251	89,773	2.01
ERCOT	374	61,069	3.39	409	69,550	3.45	452	104,695	3.72
WA, OR	19	25,367	0.28	19	25,367	0.28	13	28,132	0.33
ID,UT,MT, parts of NV,WY	82	91,779	0.87	83	93,395	0.88	71	104,983	0.92
Northern California	-	-	-	-	-	-	-	-	-
Southern California and Nevada	-	-	-	-	-	-	-	-	-
Arizona and New Mexico	198	133,000	1.63	198	133,000	1.63	111	137,696	1.42
RMPP	161	116,351	1.23	161	116,351	1.23	113	115,075	1.19
Total	10,357	2,454,701	47.08	9,278	2,499,578	46.65	8,685	2,589,650	46.23

CAIR ONLY

Table VI-4 shows that in the CAIR Only case, when run with the standard EPMM assumptions, 118 GW install wet FGDs by 2020, and 64 GW install SCRs by 2020.[29] Once again, there is the 1 GW of ACI+COHPAC added by 2020 due to existing state regulations. The FGDs are installed in early years to build up the bank before the tighter CAIR SO_2 cap, and then the bank is drawn down to comply with the tighter CAIR SO_2 caps. Significant amounts of retrofits are also put on in the latter years to address limit emissions in the face of increasing demand, a tighter Phase II cap and a depleted SO_2 bank. SCRs are put on more evenly over the study period, first to meet the NO_x SIP Call, then to meet Phase I of the CAIR NO_x caps and finally to meet the tighter Phase II CAIR NO_x caps.

Table VI-4. CAIR Only – Retrofits
(Megawatts)

Year	Wet FGD	Coal SCR	ACI+FF or +COHPAC
2004	6,185	18,508	1,050
2008	14,444	2,921	0
2010	18,502	6,980	0
2012	9,843	10,103	0
2015	770	13,477	0
2018	21,997	7,190	0
2020	46,193	4,465	0
Total	117,934	63,644	1,050

Table VI-5 shows the emissions for 2004, 2010, and 2020 for the CAIR Only Case. As a result of the CAIR, SO_2 and NO_x emissions fall throughout the study period. The co-benefits of the FGD and SCR retrofits cause Hg emissions to fall throughout the modeled time period. Although the "co-benefits level" usually refers to emissions under the CAIR Only in 2010, they continue to reduce Hg emissions after that. Hg emissions fall from Base Case levels of about 47 tons to 40 tons in 2010, and by another 7 tons to 33 tons in 2020.

Table VI-5. CAIR Only – Coal Plant Emissions

(SO_2 in thousands of short tons, NO_x and Hg in short tons)

	2004			2010			2020		
Region	**SO_2**	**NO_x**	**Hg**	**SO_2**	**NO_x**	**Hg**	**SO_2**	**NO_x**	**Hg**
NEPP	82	12,888	0.27	31	11,745	0.19	33	12,582	0.20
NYISO, West	85	28,014	0.34	80	25,269	0.32	76	24,975	0.30
NYISO, Capital	-	-	-	-	-	-	-	-	-
NYISO, Hudson Valley	26	6,815	0.09	26	6,815	0.09	26	6,815	0.09
NYISO, New York City	-	-	-	-	-	-	-	-	-
NYISO, Long Island	-	-	-	-	-	-	-	-	-
PJM Eastern	117	28,217	0.54	108	30,549	0.56	88	29,215	0.51
PJM Central	75	32,594	0.45	60	25,885	0.46	67	26,989	0.49
PJM Western	228	67,918	1.31	174	60,682	1.36	117	47,585	1.02
VACAR	1,169	165,755	3.64	643	138,497	2.35	359	140,876	1.64
SOU	1,181	207,406	3.95	610	195,935	2.56	202	151,246	1.62
Entergy	200	74,458	1.27	201	75,763	1.28	103	76,600	1.15
TVA	428	95,900	1.62	366	94,162	1.39	276	69,901	1.21
FRCC	170	69,531	0.95	181	83,241	0.94	90	86,677	0.74
ECAR	2,413	553,878	10.88	1,742	513,229	10.18	977	359,803	6.74
Com Ed	116	50,982	0.74	113	42,864	0.72	116	33,571	0.84
South MAIN	413	100,511	2.13	357	88,771	1.96	150	67,468	1.27
WIUM	173	77,631	1.07	163	73,555	1.02	105	55,745	0.90
MAPP	462	250,913	3.99	435	241,635	3.82	243	221,152	3.53
SPP North	193	109,699	1.39	157	109,052	1.40	121	115,905	1.38
SPP South	251	89,773	2.01	251	89,773	2.01	150	90,471	1.84
ERCOT	374	61,069	3.39	269	65,182	3.28	204	100,154	3.36
WA, OR	23	25,367	0.33	21	25,367	0.30	6	27,447	0.28
ID,UT,MT, parts of NV,WY	82	91,779	0.87	80	93,152	0.90	71	107,290	0.95
Northern California	-	-	-	-	-	-	-	-	-
Southern California and Nevada	-	-	-	-	-	-	-	-	-
Arizona and New Mexico	198	133,000	1.63	181	132,915	1.57	112	137,864	1.42
RMPP	161	116,351	1.23	159	116,277	1.24	113	115,932	1.19
Total	8,617	2,450,449	44.10	6,407	2,340,312	39.89	3,803	2,106,262	32.66

CAIR + Hg CAP & TRADE

Table VI-6 shows that in the CAIR + Hg Cap & Trade Case, 109 GW install wet FGDs by 2020, 61 GW install SCRs by 2020, and 107 GW install ACI+COHPAC by 2020. FGD installations are driven by the tightening SO_2 caps under CAIR and the co-benefits for Hg reduction that can be achieved from FGD/SCR combinations. SCR installations are driven by the tightening NO_x caps under the CAIR and also the co-benefits that can be achieved from FGD/SCR combination. Beginning in 2010, ACI+COHPAC are installed to meet the Hg cap. There is also an increase in the number of FGDs and SCRs that are installed by 2010 compared to the CAIR Only case. These are installations that occur *earlier* than in the CAIR Only and they occur earlier due to the value of their Hg co-benefits created by the addition of the Hg cap in this scenario.[30]

Table VI-6. CAIR + Hg Cap & Trade - Retrofits
(Megawatts)

Year	Wet FGD	Coal SCR	ACI+FF or +COHPAC
2004	1,315	18,508	1,050
2008	8,159	3,005	1
2010	35,421	11,341	14,675
2012	11,289	11,065	3,085
2015	3,361	1,994	12,270
2018	15,975	7,704	25,202
2020	33,662	7,031	50,562
Total	109,181	60,648	106,844

The Hg Cap & Trade case was run with a variety of assumptions about the rate of technological improvement in the Hg control technology. The cases considered included no technological improvement at all (0% rate of change), a 1.5% per year reduction in capital and O&M costs, a 2.5% per year reduction in capital and O&M costs, a 2.5% per year reduction in variable O&M costs only, and a 4.0% per year reduction in variable O&M costs only. The most apparent effect of technological change assumption was to reduce the marginal cost of control (i.e., the allowance prices). In all cases except for 0% technological improvement in 2020, the projected allowance prices remained below the "safety valve" price of $35,000/lb (2004$). Table VI-7 presents the Hg allowance price projections for each of the cases, in 1999 dollars.[31]

Table VI-7. Projected Hg Allowance Prices Under Alternative Assumptions of Rates of Improvement in Hg Control Technology
($/lb Hg, in 1999$)

	Annual Rate of Technological Improvement on Activated Carbon Injection Control Methods				
	0%	1.5%	2.5%	2.5%	4.0%
Year		Capital and O&M	Capital and O&M	Variable O&M only	Variable O&M only
2010	$22,108	$21,850	$22,345	$20,854	$20,090
2012	$21,654	$19,623	$17,904	$18,727	$17,420
2015	$25,826	$23,404	$21,353	$22,335	$20,775
2018	$30,824	$27,933	$25,485	$26,657	$24,796
2020	$37,285	$28,495	$23,611	$32,536	$30,951

In all of the technological change cases, Hg emissions meet the Phase I cap of 34 tons in 2010 and the Phase II cap of 15 tons in 2020. There were only minimal differences in the pattern of retrofits, emissions, or banking over time due to the alternative assumptions about rates of technological change. Table VI-8 shows the emissions for 2004, 2010, and 2020 for the CAIR + Hg Cap & Trade case for the 0% technological improvement case, which was the case that was used to develop inputs for the TEAM deposition model.

Table VI-8. CAIR + Hg Cap & Trade - Coal Plant Emissions
(SO_2 in thousands of short tons, NO_x and Hg in short tons)

	2004			2010			2020		
Region	**SO_2**	**NO_x**	**Hg**	**SO_2**	**NO_x**	**Hg**	**SO_2**	**NO_x**	**Hg**
NEPP	82	12,889	0.27	30	11,580	0.19	33	12,470	0.20
NYISO, West	85	28,145	0.34	80	26,181	0.32	74	25,025	0.19
NYISO, Capital	-	-	-	-	-	-	-	-	-
NYISO, Hudson Valley	26	6,815	0.09	26	6,815	0.09	19	6,823	0.07
NYISO, New York City	-	-	-	-	-	-	-	-	-
NYISO, Long Island	-	-	-	-	-	-	-	-	-
PJM Eastern	117	28,217	0.54	109	25,880	0.47	78	24,788	0.38
PJM Central	133	32,431	0.43	69	22,308	0.36	65	22,832	0.38
PJM Western	289	68,027	1.39	193	44,305	1.03	104	37,973	0.79
VACAR	1,170	165,987	3.65	636	137,201	2.30	353	125,167	1.39
SOU	1,224	207,406	4.05	543	184,666	2.35	178	131,931	1.40
Entergy	200	74,458	1.27	185	69,190	1.07	198	75,791	0.13
TVA	428	95,900	1.62	319	94,203	1.34	190	75,442	0.68
FRCC	184	69,531	0.98	181	71,439	0.78	79	80,630	0.63
ECAR	2,505	554,208	11.12	1,604	522,226	8.31	837	373,163	4.16
Com Ed	116	51,047	0.74	107	43,904	0.68	134	54,370	0.25
South MAIN	425	100,553	2.16	325	87,008	1.78	174	61,930	0.46
WIUM	173	77,683	1.07	163	72,588	1.00	105	61,738	0.24
MAPP	462	250,808	3.99	416	239,276	2.92	297	238,862	0.86
SPP North	194	109,777	1.39	154	108,962	1.35	122	115,823	0.30
SPP South	251	89,773	2.01	251	89,773	1.40	251	89,773	0.37
ERCOT	374	61,069	3.39	255	65,035	2.77	249	98,566	1.11
WA, OR	23	25,367	0.33	19	24,535	0.27	6	27,229	0.05
ID,UT,MT, parts of NV,WY	82	91,779	0.87	80	93,371	0.60	69	105,148	0.31
Northern California	-	-	-	-	-	-	-	-	-
Southern California and Nevada	-	-	-	-	-	-	-	-	-
Arizona and New Mexico	198	133,000	1.63	168	132,915	1.43	97	135,827	0.44
RMPP	161	116,351	1.23	159	116,277	1.19	128	115,218	0.19
Total	8,900	2,451,218	44.58	6,071	2,289,635	34.00	3,837	2,096,517	15.00

CAIR + Hg MACT

As shown in Table VI-9, in the CAIR + Hg MACT Case, 98 GW install wet FGDs by 2020, 66 GW install SCRs by 2020, and 67 GW install ACI+COHPAC by 2020.[32] Most of the ACI+COHPAC installations appear in the 2008 model year when the MACT takes effect.[33]

This scenario indicates that the Hg MACT proposal would require a remarkable amount retrofitting within a very short time frame. Most of the 64 GW of ACI+FF in 2008 occurs on different units that those retrofitting the 67 GW of FGD. This means that compliance with the MACT would entail about 120 GW, or 40 percent of all coal-fired capacity, making some major form of retrofit in the period of time just prior to 2008 (only 3 years from now). These are quantities necessary to comply, but may reflect infeasible rates of retrofit and use of a still immature technology that may not be available on this scale by 2007. EPMM runs did not constrain rates of retrofitting or dates of full commercial availability for the ACI-based technology.

Table VI-9. CAIR + Hg MACT – Retrofits
(Megawatts)

Year	Wet FGD	Coal SCR	ACI+FF or +COHPAC
2004	1,309	18,508	1,072
2008	67,430	25,957	64,039
2010	1,488	2,207	1,623
2012	2,661	3,061	74
2015	2,090	3,336	21
2018	4,212	2,422	0
2020	18,211	10,139	0
Total	97,400	65,630	66,829

Table VI-10 shows the emissions for 2004, 2010, and 2020 for the CAIR + Hg MACT case. As a result of the CAIR, SO_2 and NO_x emissions fall throughout the study period. Hg emissions decline significantly in 2008 when the Hg MACT takes effect. Further Hg reductions after 2008 are the result of co-benefits from FGD and SCR installations to meet stricter SO_2 and NO_x caps.

Table VI-10. CAIR + Hg MACT - Coal Plant Emissions

(SO_2 in thousands of short tons, NO_x and Hg in short tons)

	2004			2010			2020		
Region	**SO_2**	**NO_x**	**Hg**	**SO_2**	**NO_x**	**Hg**	**SO_2**	**NO_x**	**Hg**
NEPP	82	12,888	0.27	33	10,723	0.13	33	10,723	0.13
NYISO, West	85	28,145	0.34	80	24,940	0.18	74	24,086	0.16
NYISO, Capital	-	-	-	-	-	-	-	-	-
NYISO, Hudson Valley	26	6,815	0.09	26	6,815	0.05	26	6,815	0.05
NYISO, New York City	-	-	-	-	-	-	-	-	-
NYISO, Long Island	-	-	-	-	-	-	-	-	-
PJM Eastern	117	28,217	0.54	68	19,657	0.25	85	25,115	0.37
PJM Central	133	32,431	0.43	69	24,075	0.30	63	20,268	0.34
PJM Western	289	68,027	1.39	124	38,761	0.69	128	39,053	0.75
VACAR	1,170	165,987	3.65	390	136,503	1.25	399	134,211	1.31
SOU	1,227	207,406	4.06	413	174,916	1.83	260	142,714	1.24
Entergy	200	74,458	1.27	201	75,763	1.28	161	61,685	1.23
TVA	428	95,900	1.62	326	96,397	0.85	276	90,451	0.78
FRCC	184	69,531	0.98	166	54,139	0.54	151	72,760	0.59
ECAR	2,502	554,199	11.12	1,218	477,642	7.71	1,032	416,731	6.75
Com Ed	116	51,047	0.74	121	51,530	0.77	131	33,518	0.85
South MAIN	425	100,553	2.16	285	81,040	1.67	176	70,521	1.31
WIUM	173	77,683	1.07	167	75,169	1.03	107	48,153	0.91
MAPP	462	250,808	3.99	439	254,002	3.87	277	224,224	3.60
SPP North	194	109,777	1.39	153	109,127	1.39	131	115,687	1.38
SPP South	251	89,773	2.01	251	89,773	1.79	237	89,793	1.76
ERCOT	374	61,069	3.39	257	64,714	3.03	265	88,257	3.20
WA, OR	23	25,367	0.33	23	25,367	0.33	6	27,331	0.28
ID,UT,MT, parts of NV,WY	82	91,779	0.87	69	93,242	0.85	69	104,850	0.92
Northern California	-	-	-	-	-	-	-	-	-
Southern California and Nevada	-	-	-	-	-	-	-	-	-
Arizona and New Mexico	198	133,000	1.63	177	132,823	1.54	112	137,866	1.42
RMPP	161	116,351	1.23	160	116,277	1.22	113	115,937	1.18
Total	8,900	2,451,209	44.59	5,215	2,233,393	32.55	4,310	2,100,750	30.51

VII. DIFFERENCES FROM EPA IN MERCURY BANKING

Although EPA has not formally released its own modeling results for the two Hg proposals, it is widely reported that EPA's projected national Hg emissions are not reduced to the level of the 15 ton Phase II cap even by 2026 (which is the last modeled year in the simulation). The reason is that the EPA model projects that a large bank would be built up during Phase I and it would still be being drawn down at the time of the last modeled period in the EPA model.

As was described in Section VI of this paper, EPMM simulations of the Hg Cap & Trade policy proposal have a different outcome: Hg emissions reach 15 tons by 2020. There is some banking in EPMM simulations, but not to the same degree as in IPM simulations. For example, EPMM estimates that emissions at the start of Phase II (in 2018) would be 23.9 tons, but they fall to 15 tons within two years because the bank is only projected to contain 17.7 tons by the end of Phase I.

There appear to be several reasons for the substantial differences in banking behavior between EPMM simulations and EPA's purported results. These causes fall into three categories, each of which will be substantiated in this section:

1. EPA's assumes larger co-benefits than the industry believes to be correct.

    (a) *Directly*, via the model inputs on the Hg removal for each existing technology and coal configuration (known as the "co-benefits" assumptions, and which were presented in Table IV-10.)

    (b) *Indirectly*, because a variety of EPA's modeling assumptions lead to a relatively greater reliance on FGD over coal switching for projected SO_2 compliance.

2. EPA's cost and effectiveness assumptions for removal of Hg using activated carbon injection are more pessimistic than those that industry has assembled.

The net effect of these three differences motivates substantially greater banking during Phase I in EPA's model than in EPMM. In brief, EPA's model would generate lower marginal costs ($/lb Hg removed) to exactly meet a Phase I cap of 34 tons, yet it would generate higher marginal costs to exactly meet a Phase II cap of 15 tons. This means that, in the absence of banking, allowance prices simulated by EPA's model would increase at a more rapid rate than they would increase in EPMM simulations. Both models are designed to seek the same concept of a least-cost solution, however, and if banking is allowed, the least-cost response would be to decrease emissions below the cap in the early phase(s) in such a way that the marginal cost is higher at the start, and lower at the end, up to the point where marginal costs would rise at the real market interest rate over the entire time horizon of the optimization.[34] If the EPA model faces a higher rate of increase in marginal costs prior to banking, then it would tend to generate a larger amount of banking in the early years, and a later date when the last cap is physically achieved.

EPA's DIRECT CO-BENEFITS ARE LARGER THAN INDUSTRY CO-BENEFITS

Table IV-10 presented EPMM and EPA co-benefits side-by-side. Those are the actual model inputs. However, to understand how they affect projected Hg emissions when FGDs or SCRs are added requires further computation.[35] For example, the effect of adding a wet FGD to a cold-side ESP unit burning subbituminous coal would be a 47 percent incremental Hg reduction in EPA's simulations, while it would be a 38 percent incremental reduction in EPMM. These may seem like similar numbers, but they imply that each such FGD retrofit would reduce current unit Hg emissions 24 percent more under the EPA assumptions than under the EPMM assumptions. This particular configuration of unit also accounts for about 44 percent of existing coal units, so it is likely to have a major effect on aggregate Hg reductions due to co-benefits. Other examples of the differences in incremental Hg removal created by adding an FGD, SCR, or both are provided below for types of units that represent 78 percent of the coal fleet:

- Incremental Hg removal by adding FGD+SCR to a CESP unit (~59 percent of coal capacity in 1999)
  - EPA: 84% (bituminous) 65% (subbituminous) 44% (lignite)
  - EPMM: 77% (bituminous) 19% (subbituminous) 28% (lignite)

- Incremental Hg removal by adding an FGD to a CESP unit (~59 percent of coal capacity in 1999)
  - EPA: 47% (bituminous) 13% (subbituminous) 44% (lignite)
  - EPMM: 38% (bituminous) 19% (subbituminous) 28% (lignite)

- Incremental Hg removal by adding an SCR to a CESP+wFGD unit (~18 percent of coal capacity in 1999)
  - EPA: 71% (bituminous) 61% (subbituminous) 0% (lignite)
  - EPMM: 63% (bituminous) 0% (subbituminous) 0% (lignite)

EPA'S ASSUMPTIONS APPEAR TO RESULT IN A GREATER RELIANCE ON FGD RETROFITS OVER COAL SWITCHING

There are more FGD retrofits in EPA's CAIR scenario than in the EPMM CAIR scenario. For example, in 2010, EPA's CAIR scenario entails 164 GW of scrubbed units,[36] whereas there are only 122 GW of scrubbed units in the EPMM projection for the same policy.[37] (The heightened importance of FGD over coal-switching is apparent in the Base Case as well. EPA projects 115 GW of FGDs by 2010 to meet the existing Title IV cap, while EPMM projects only 88 GW of FGDs by the same time.) These extra FGDs are not a result of EPA's higher Hg co-benefits assumptions because the CAIR has no Hg constraint, and thus will not motivate any incremental retrofits due to their ability to reduce Hg. However, they do increase the quantity of co-benefits projected under the CAIR Only scenario.

EPMM sensitivity cases on the CAIR Only scenario have indicated that the propensity to use FGD over coal-switching adds substantially to the projected co-benefits. In a sensitivity case for the CAIR Only scenario that led to 64 GW of FGD retrofits by 2010 (compared to 39 GW

under our base assumptions), 2010 Hg emissions dropped from 39.9 tons under the base assumptions to 36.3 tons.[38]

It is not clear why the EPA model finds FGDs more cost-effective than coal-switching compared to EPMM, but it is clear that such a difference exists. Some reasons might be differences in delivered coal prices, in the costs and other barriers to use of lower sulfur coals (either bituminous or subbituminous), differences in capitalization factors applied to capital investments, etc. A more in-depth data comparison is needed to understand which, if any, of these may be the cause. Nevertheless, the higher direct co-benefits that EPA associates with FGD installations (described in the previous section) will reinforce this greater propensity to rely on FGDs when a mercury constraint is added to the scenario.

EVIDENCE OF HIGHER CO-BENEFITS IN SIMULATION RESULTS

The combined effect of the direct and indirect causes of larger co-benefits in EPA's model can be observed in Figure VII-1, which contrasts EPMM's estimate of the co-benefits from just the CAIR to those estimated by EPA. One can see that EPA's co-benefits assumptions imply that Hg emissions would drop to about 34 tons by 2010, and EPMM's assumptions imply that Hg emissions would drop to only about 40 tons by 2010 if only the CAIR provisions (which cap only SO_2 and NO_x) were to be implemented.

Figure VII-1. Comparison of Overall Hg Co-Benefits Estimated in EPMM and IPM (Hg Trends in CAIR-Only Scenario)

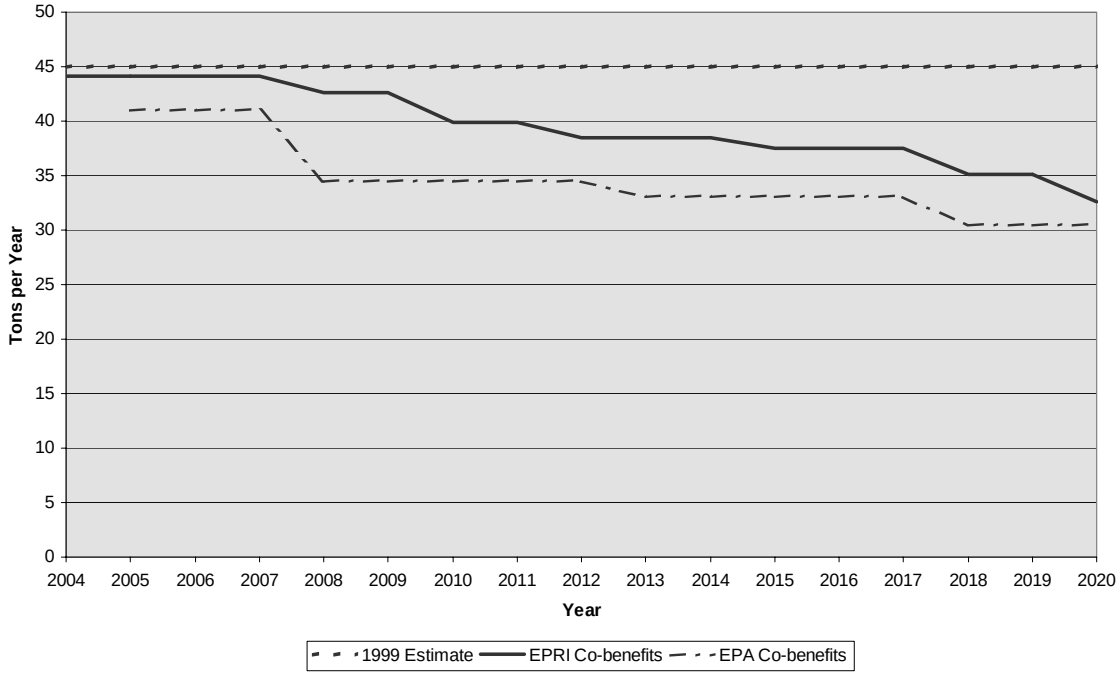

An important implication of these results is that the marginal cost of achieving a 34-ton cap is effectively $0/ton in the EPA scenarios. In contrast, the EPMM simulations imply that the

extra reduction from 40 tons down to the 34-ton cap would cost over $20,000/lb (1999$) at the margin.

EPA'S COST AND EFFECTIVENESS ASSUMPTIONS FOR REMOVAL OF HG WITH ACI ARE MORE PESSIMISTIC THAN EPMM'S

Table IV-8 presented the EPMM assumptions on the cost and removal efficiencies for activated carbon injection (ACI) technology. The comparable assumptions made by EPA are available in Attachment L1 of the IPM documentation report posted on EPA's website.[39] When either set of assumptions is combined with the respective co-benefits, one can estimate the $/lb removed implied by these inputs for each type of unit. CRA has done this for the mix technology configurations and coal types being burned in coal units in 1999, using average estimates of the coal Hg contents, heat rates, and capacity factors of all these units.
Figure VII-2 plots the resulting approximate $/lb removed against the total potential tons that could be removed at each cost level. These approximations of the marginal cost curves in the respective models indicate that the EPA marginal cost curve for ACI is higher and steeper for all but the first few of the lowest-cost ACI retrofit options (i.e., those in the far left of the graphs).

Figure VII-2. Comparison of $/lb Hg Removal Costs in EPA and EPMM Data

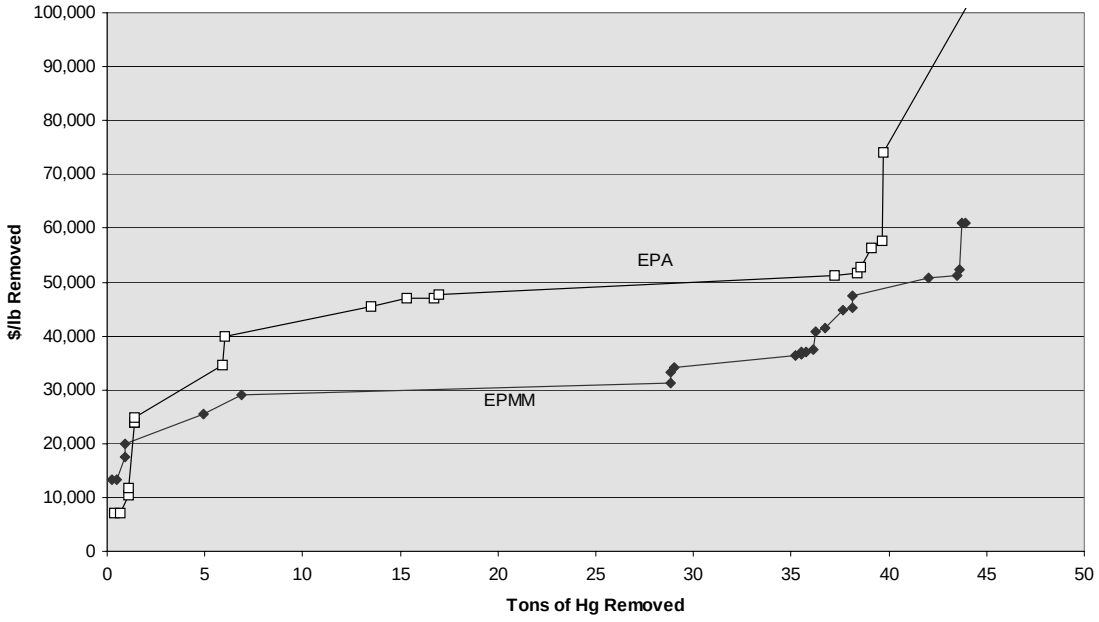

The curves in Figure VII-2 were estimated using the mix of technologies that were in place as of 1999's ICR data collection. This included about 80 GW of scrubbed units, and none with SCRs. Both curves will rotate upwards (becoming higher and steeper) as more capacity is retrofit with FGD or SCR+FGD, as is projected under both the EPMM and EPA CAIR scenarios. Thus, the actual marginal costs associated with ACI-based controls will be higher than these curves indicate once one has layered on the co-benefits from CAIR-motivated retrofits. Given that the incremental Hg removal from most FGD and FGD+SCR installations is higher in EPA's assumptions than in the EPMM assumptions, the EPA curve would rise

more than the EPMM curve if it were to be recalculated taking into account the effect of controls projected under the proposed CAIR scenario.

The EPA curve of Figure VII-2 will rise even more than the EPMM for a second reason, which is the relatively greater reliance on FGDs for SO_2 compliance. To the extent that more FGDs are installed in an EPA scenario, this will drive a yet wider wedge between the EPA and EPMM ACI-related marginal cost curves.

This comparison of the implications of the ACI technology assumptions further illuminates the reason the EPA model banks more Hg than EPMM during Phase I. It indicates that once co-benefits have been exhausted, and the electricity generating system must turn to ACI for further Hg reductions, the costs of those remaining reductions will be higher in the EPA model than in EPMM. It also indicates that EPA's model will see a much higher marginal cost to reduce annual Hg emissions to 15 tons than EPMM.

SYNOPSIS ON DIFFERENCES IN MODELS' MERCURY BANKING RESULTS

Thus, for any Phase II Hg cap that eventually exceeds the level of co-benefits, the EPA model will have a greater propensity to bank in a Phase I set at 34 tons than will be found in the EPMM model using its current assumptions. When the initial cap is set literally at co-benefits, one has created a very substantial ability to bank large amounts, because controls that generate bankable allowances are at the lowest part of the marginal cost curve. A much smaller incentive to bank is created under EPMM model assumptions because even achieving the 34-ton cap of 2010 is projected to cost $20,000 to $22,000/lb (1999$), while achieving 15 tons would only cost about $24,000 to $37,000/lb (see Table VI-7).

APPENDIX B.3

METHODOLOGY FOR ESTIMATING HOW REDUCTION IN MERCURY DEPOSITION WOULD AFFECT EXPOSURES VIA FISH CONSUMPTION

Introduction

EPA is evaluating alternatives for controlling emissions of mercury from utilities. The alternatives include a proposed rule requiring utilities to install controls known as "maximum achievable control technologies" (MACT) under section 112 of the Clean Air Act. An alternative proposed rule would establish "standards of performance" limiting mercury emissions from new and existing utilities. This proposal, under section 111 of the Clean Air Act, would create a market based "cap-and-trade" program that, if implemented, would reduce nationwide utility emissions of mercury in two distinct phases. In the first phase, due by 2010, emissions will be reduced by taking advantage of "co-benefit" controls- that is mercury reductions achieved by reducing SO_x, and NO_x emissions. In addition to these two programs that specifically target mercury emissions, the EPA's proposed Interstate Air Quality Rule (CAIR) would also affect the future adoption of power plant control systems, and thereby affect mercury emissions.

The goal of this analysis is to quantitatively evaluate the potential impact of air mercury emission reductions under the proposed EPA alternatives (MACT, Cap-and-Trade, and CAIR) on exposures from fish consumption, using data on both a regional and state-by-state basis. By relating reductions in air depositions rates to reductions in fish tissue concentrations, this evaluation is one component of an overall emission reduction benefit analysis.

Technical Approach

As is described in the following sections, the distribution of the upper tail of the methylmercury exposure distribution is estimated for the base year of 1999 on a state-by-state basis. The state level adjustment includes regional variations in fish consumption, state differences in the mix of marine and freshwater fish consumption based on recreational fishing data. Finally, state data on the methylmercury concentrations of fish are used to estimate state-by-state exposures built up from the state-specific estimates of freshwater and marine fish consumption, using state average fish tissue concentrations.

This analysis describes the exposure Base Case, against which future changes in average state mercury deposition rates are used to estimate changes in exposure. To link changes in deposition to exposure, freshwater fish methylmercury concentrations are assumed to scale in direct proportion to average state deposition, based on 2000-2001 fish data and deposition estimates. Changes in the marine fish contribution to exposure are also estimated, based on the assumption that the reductions in power

plant mercury emissions are reduced, relative to total annual mercury emissions from all sources globally, will produce a proportional reduction in the methylmercury concentrations of marine fish.

Air Deposition

Estimates of air deposition of mercury were generated (AER 2004) using a regional air deposition model for the baseline scenario (1999), and projected scenarios in the year 2020 under MACT, CAIR, and cap-and-trade. Although this air dispersion analysis was conducted using a 20-km grid, the results were aggregated to provide state average deposition rates. State average deposition rates were used because some of the other data needed to estimate the effect of emission reductions on exposure were only available on a state or regional basis.

Exposure via Fish Consumption

A baseline exposure scenario is analyzed using 1999 emission data and the associated modeled deposition rates, data on freshwater fish tissue collected by EPA starting in 1999, (National Fish Tissue Study – Year One (1999-2000) and Year Two (2001)) and the 1999-2002 NHANES data on blood concentrations of mercury in US women aged 16 to 49. The exposures of greatest interest and concern are those to women who consume above-average quantities of fish.

The best available information concerning the most highly exposed US women comes from the NHANES blood mercury and methylmercury measurements. Food diary studies are often used to estimate consumption rates, but such studies are not as well suited for estimating the upper tail of the exposure distribution as is the direct measurements of mercury in blood and hair.

The NHANES blood concentrations were converted to an equivalent intake rate of methylmercury, using the relationship that a steady-state intake rate of 10 µg/day would produce a blood concentration of 8 ppb (this value is used in a 2004 by Tran et al, citing two earlier studies). This means that the distribution of blood concentrations measured in the NHANES study can be converted into an equivalent distribution of methylmercury intake rates. This relationship is next converted into an equivalent fish consumption distribution, based on a calculated average fish methylmercury concentration of 0.12 mg/kg methylmercury. While this is a comparatively low concentration, it is representative of the concentration of canned tuna, the most widely consumed fish. Many marine fish have higher methylmercury concentrations, but other marine seafood is lower in methylmercury, for example, shrimp. This average marine fish tissue concentration of 0.12 mg/kg was calculated based on measured blood methylmercury concentrations. If it is assumed that the average concentration of marine seafood is 0.12 mg/kg, the NHANES blood concentrations are consistent with a mean consumption rate of 14 gm/day and a 95^{th} percentile consumption of 68.75 gm/day These values are comparable to the mean fish consumption rate of 14.3 g/day cited in EPA's Exposure Factor's Handbook, and 61.63 gm/day 95^{th} percentile consumption estimate reported in EPA's 2002 Fish Consumption Report. Both EPA estimates are based on the USDA's data from the Continuing Survey of

Food Intake by Individuals (CSFII). The distribution of the top 20th percentile fish consumption derived from the NHANES data is indicated in the following graph.

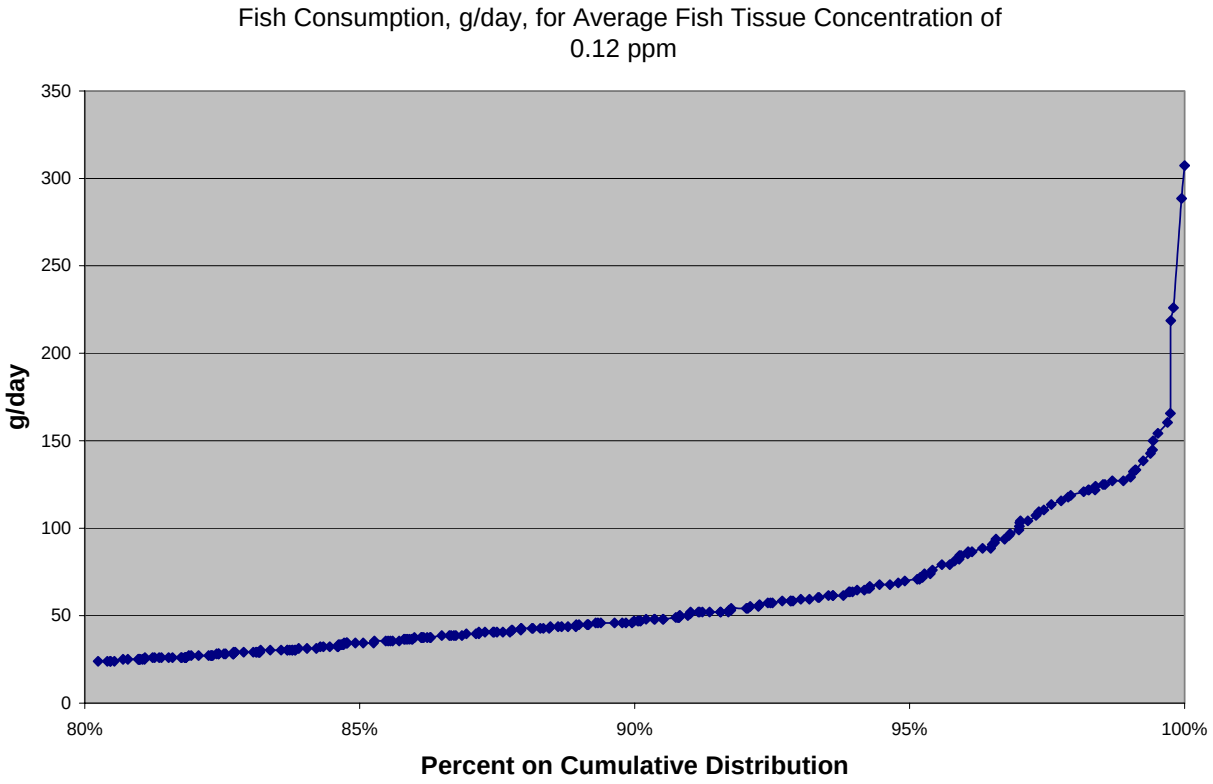

This curve represents the 1999 reference case, expressed as the estimated fish consumption rates of women with the highest 20% blood methylmercury levels in the NHANES study. As this curve indicates, the woman with the highest blood mercury levels is estimated to consume slightly over 300 grams of fish per day.

Regional Adjustments to Fish Consumption Rates

EPA's 1997 Exposure Factors Handbook cites USDA CSFII data from 1994-96 regarding how fish consumption rates vary by region of the country. These estimates are provided in the following table, both in terms of the mean consumption rate in grams per day, and as a normalized index based on the mean value of 14.3 g/day. The normalized index was used to adjust the distribution curve shown above upward or downward, on a state-by-state basis. Although the mercury deposition analysis was done on a grid scale smaller than a state, the state was used as the geographic unit of analysis because data on the methylmercury concentrations of wild freshwater fish and on the rates of recreational fishing were available on a state basis.

Table B.3-1: Fish Consumption by U.S. Census Region

Census Bureau Region	g/day	normalized
New England (CT,ME, MA, NH, RI, VT)	16.3	1.14
Mid-Atlantic (NJ, NY, PA)	16.2	1.13
East-North Central (IL, IN, MI, OH, WI)	12.9	0.90
West-North Central (IA, KS, MN, MO, NE, ND, SD)	12.0	0.84
South Atlantic (DE, DC, FL, GA, MD, NC, SC, VA, WV)	15.2	1.06
East South Central (AL, KY, MS, TN)	13.0	0.91
West South Central (AR, LA, OK, TX)	14.4	1.01
Mountain (AZ, CO, ID, NM, MT, NV, UT, WY)	12.1	0.85
Pacific (AK, CA, HI, OR, WA)	14.2	0.99

Marine versus Freshwater Fish

Ideally, one would like to know the relative contributions to the blood concentrations measured in the NHANES study from consumption of marine versus wild freshwater fish. The NHANES study did include a survey of fish consumption, but the data collected does not provide a useful description of the freshwater and marine contributions.

The NHANES participants for whom blood mercury measurements were taken reported consumption of 3541 fish meals, of which 384 were of freshwater fish species. However, of the 384 freshwater fish meals, 302 were of catfish and trout, fish that are the top two US farm-raised fish. The distinction between farmed and wild fish is important in assessing mercury exposure because farmed fish are typically very low in mercury. There were only 82 fish meals out of 3541 of fish that are of freshwater fish that are not farmed. The portion of the catfish and trout that were wild is not known. In addition, slightly over 500 fish meals were reported as “other” and “unknown” fish; the fraction of these fish that are wild freshwater fish is also not known. The wild freshwater fraction of the catfish, trout, and other and unknown fish consumed is not known, yet the number of meals in these four categories is much larger than the number of meals that are clearly of wild freshwater fish.

The situation with other food consumption data sources such as the CSFII is not much better. The 1994-1996 CSFII data for fish consumption by women aged 15-44 indicate that roughly 38% of fish consumed are estuarine and freshwater fish, however, this total is dominated by shrimp, consumption which is estimated to be 2.4 g/day out of the 5.6 g/day total for estuarine and freshwater consumption. Shrimp is increasingly farm-raised and low in mercury even if not farm-raised, so exposures to methylmercury from consumption of non-farmed shrimp are not likely to be significant. If only freshwater fish are considered, that is, if estuarine seafood and shellfish are excluded, the daily consumption rate is estimated to be about 1.16 g/day, of which more than 0.8 g/day comes from catfish and trout. The CSFII data does not distinguish between farm-raised and wild freshwater fish, but as noted, catfish and trout are the primary farm-raised fish in the US. In addition, the relative mix of

freshwater and marine fish among the women in the top of the blood methylmercury distribution is not known.

Faced with the limited data regarding the consumption of wild freshwater fish, a simple assumption is used that the split between marine and wild freshwater fish consumption if 90%/10%. The total estimated estuarine and freshwater fish consumption from the CSFII data is higher than 10%, but much of this is due to shrimp and farm-raised catfish and trout. The 1994-1996 CSFII data in particular suggest that a 10% estimate for wild freshwater fish is high. However, absent better data, a 10% estimate is used here.

State-level Adjustments to Freshwater Fish Consumption

Data concerning the rates of wild freshwater fish consumption by state are not available. However, as an alternative to simply ignoring state-to-state differences, it was possible to adjust the estimated consumption rates of freshwater fish based on recreational fishing data available from the Census Bureau at http://www.census.gov/prod/www/abs/fishing.html. These data are provided in the first two columns of the table below. These data for recreational fishing specific to freshwater fish are for 2001. There were normalized using state population data for 2000.

The third column in this table simply restates the per capita fishing days on a normalized basis. A normalized value of 2 means that the residents of such a state spend twice as much time fishing as do average US residents.

The assumed 90%/10% mix of marine and freshwater fish consumption described above was modified based on the normalized recreational fishing data. The 10% freshwater fish fraction was scaled by the normalized recreational fishing value. For a state with a normalized recreational fishing ratio of 2, the mix of freshwater fish would be increased to 20%, so that the marine fraction would be reduced to 80%.

Table B.3-2: Recreational Fishing Rates for Freshwater Fish, 2001

	Per Capita Fishing Days	Normalized	Freshwater Fraction	Marine Fraction
Alabama	2.02	1.40	14.03%	85.97%
Alaska	2.48	1.72	17.20%	82.80%
Arizona	0.75	0.52	5.20%	94.80%
Arkansas	4.30	2.99	29.88%	70.12%
California	0.55	0.39	3.85%	96.15%
Colorado	1.51	1.05	10.46%	89.54%
Connecticut	0.93	0.65	6.48%	93.52%
Delaware	0.51	0.35	3.51%	96.49%
Florida	1.20	0.84	8.35%	91.65%
Georgia	1.53	1.07	10.65%	89.35%
Hawaii	0.16	0.11	1.11%	98.89%
Idaho	2.27	1.58	15.79%	84.21%
Illinois	1.12	0.78	7.76%	92.24%
Indiana	2.05	1.42	14.25%	85.75%
Iowa	2.41	1.67	16.73%	83.27%
Kansas	2.05	1.42	14.22%	85.78%
Kentucky	2.76	1.91	19.15%	80.85%
Louisiana	1.78	1.23	12.34%	87.66%
Maine	2.24	1.56	15.57%	84.43%
Maryland	0.61	0.42	4.24%	95.76%
Massachusetts	0.68	0.48	4.75%	95.25%
Michigan	1.18	0.82	8.19%	91.81%
Minnesota	5.26	3.65	36.55%	63.45%
Mississippi	2.64	1.83	18.31%	81.69%
Missouri	2.02	1.40	14.04%	85.96%
Montana	3.90	2.71	27.06%	72.94%
Nebraska	1.70	1.18	11.83%	88.17%
Nevada	0.71	0.49	4.94%	95.06%
New Hampshire	1.93	1.34	13.37%	86.63%
New Jersey	0.61	0.42	4.24%	95.76%
New Mexico	1.15	0.80	7.98%	92.02%
New York	0.60	0.42	4.16%	95.84%
North Carolina	1.42	0.98	9.83%	90.17%
North Dakota	3.07	2.13	21.29%	78.71%
Ohio	1.27	0.88	8.82%	91.18%
Oklahoma	3.59	2.49	24.94%	75.06%
Oregon	2.15	1.49	14.91%	85.09%
Pennsylvania	1.31	0.91	9.06%	90.94%
Rhode Island	0.52	0.36	3.62%	96.38%
South Carolina	2.08	1.44	14.45%	85.55%
South Dakota	2.96	2.06	20.59%	79.41%
Tennessee	2.36	1.64	16.37%	83.63%
Texas	1.19	0.83	8.27%	91.73%
Utah	2.11	1.46	14.62%	85.38%
Vermont	2.77	1.92	19.21%	80.79%
Virginia	1.46	1.01	10.14%	89.86%

	Per Capita Fishing Days	Normalized	Freshwater Fraction	Marine Fraction
Washington	1.61	1.12	11.15%	88.85%
West Virginia	2.15	1.49	14.90%	85.10%
Wisconsin	2.93	2.04	20.37%	79.63%
Wyoming	3.61	2.51	25.06%	74.94%

Data on Methylmercury Concentrations in Freshwater Fish

Many states have extensive sampling results for mercury or methylmercury in freshwater fish. Such data are often the basis for state fish advisories. However, these data are typically biased because the state agencies sample more frequently where there is a concern that fish have high levels of contaminants, for example, in water bodies near known point sources.

Given the known bias of the existing fish tissue data towards problem locations, EPA has initiated a fish sampling effort focused on provided representative data on pollutants of concern in fish from US lakes. By design, this sampling study only includes lake fish. River fish are not included. In this study, typically five fish of a given species and from a specific lake were combined into a single sample.

Details on this 4-year sampling effort can be found at http://www.epa.gov/waterscience/fishstudy/. Data from the first two years of this program are available (see Table B.3-3 below). The number of data points is limited. The Year 1 data for mercury include 288 composite samples from 1406 fish collected in 40 states. The Year 2 results, just released, provide an additional 233 composite samples from 1190 fish. When the data from the two years are combined, there are six states for which no data were collected: Alaska, Delaware, Hawaii, Maryland, Missouri, and Rhode Island. While data are available regarding the mercury concentrations of fish in these states, these data are not collected in a study design that is comparable to that of the EPA National Fish Tissue Study. Comparisons of the relative geographic effect of mercury emission reductions would not be valid. For this reason, these states were not included in the analysis.

Despite the limited extent of the first two year results for the EPA National Fish Tissue Study, the representativeness of the sampling effort makes these the data of choice for an exposure assessment. Ideally, one would like to have data representative of fish as consumed, but no such data set exists. Even an unbiased data collection effort such as what EPA is conducting is likely to overestimate methylmercury exposure from freshwater fish consumption, because fish advisories may limit consumption of fish from water bodies with above average methylmercury concentrations. The effect of fish advisories, to the extent that they are followed, will be to redirect consumption of freshwater fish to areas without advisories. Such areas will provide fish that are relatively low in methylmercury in comparison to all fish, and especially in comparison to fish from locations where state sampling efforts have been focused.

Table B.3-3: EPA National Fish Tissue Study Year 1 and 2 Average Composite Data for Methylmercury in Fish, mg/kg

Alabama	0.168	Nevada	0.261
Arizona	0.127	New Hampshire	0.294
Arkansas	0.214	New Jersey	0.485
California	0.266	New Mexico	0.260
Colorado	0.120	New York	0.266
Connecticut	0.418	North Carolina	0.271
Florida	0.258	North Dakota	0.256
Georgia	0.265	Ohio	0.257
Idaho	0.251	Oklahoma	0.238
Illinois	0.175	Oregon	0.055
Indiana	0.246	Pennsylvania	0.111
Iowa	0.118	South Carolina	0.137
Kansas	0.140	South Dakota	0.111
Kentucky	0.119	Tennessee	0.194
Louisiana	0.315	Texas	0.204
Maine	0.453	Utah	0.304
Massachusetts	0.368	Vermont	0.553
Michigan	0.186	Virginia	0.195
Minnesota	0.178	Washington	0.110
Mississippi	0.287	West Virginia	0.203
Montana	0.284	Wisconsin	0.295
Nebraska	0.073	Wyoming	0.095

To illustrate how much of a bias may be present in fish data, the average methylmercury concentration of the composite samples in the EPA National Fish Tissue Study is 0.22 mg/kg. In comparison, the average concentration in over 16,000 samples reported in EPA's Mercury Maps data set is 0.41 mg/kg, almost twice as high. The Mercury Maps data were collected from water bodies with fish advisories.

Given the limited number of fish samples in the National Fish Tissue Study, the estimates for several states come from only one or two composite fish samples, and may, therefore, not be representative of the fish of that state. For example, the fish sampled in the state with the lowest average concentration, Oregon, were all Kokanee salmon, and salmon typically are very low in mercury.

The average fish tissue was calculated for each state for which mercury data is available in the National Fish Tissue Study. The average was actually calculated in two ways, first, as the average of the reported composite sample results, and second, where the composite samples were weighted based on the number of fish in the composite to give the average for each fish. These results were compared with the calculated 1999 state mercury deposition rates, and the correlations examined. In both cases, a positive association was present between deposition and fish concentration, but the fit was poor. For the case in which the average of the composite samples was used, the R^2 was 0.075. For the average based on each fish, the R^2 was 0.055. Given the higher R^2 for the composite average, these values were used to represent the fish concentration in each state.

Effect of Emission Reductions

The analysis considers the effect of emission reductions on wild freshwater fish and marine fish. Farm-raised fish were excluded because they are raised and fed in a way that typically results in very low methylmercury concentrations; for example, the major farm-raised fish in the US is catfish, raised on feed typically based on soybeans, wheat, and corn. For this reason, farm-raised fish are not considered to be a significant source of methylmercury exposure, and are not included in the calculations of how emission reductions would affect exposure.

Marine fish make up the largest source of fish consumption in the US. However, methylmercury concentrations in marine fish are not likely to be sensitive to changes in US emissions. For example, the most frequently consumed fish, canned tuna, are caught mainly within ± 20 degrees of the equator. In the calculations of exposure reductions, the methylmercury concentrations of marine fish were assumed to decline in proportion to the reduction in global emissions when power plant controls were implemented in the United States. Global mercury emissions were assumed to be 6000 metric tons per year through the year 2020, less the reductions in US power plant emissions associated with the three scenarios. The reductions in emissions under these scenarios are small in comparison to the 6000 metric tons per year, on the order of 15 to 30 tons per year. For this reason, the effect of emissions reductions on exposure from consumption of marine fish is considered, but is relatively low.

For freshwater fish, AER produced estimates of the average deposition in each state in 1999, and in 2020 for the CAIR, MACT, and Cap & Trade scenarios. This analysis simply and conservatively assumes that the fish tissue concentrations in each state will change from their 1999 levels in proportion to changes in deposition.

Results and Discussion

The results of this exposure calculation are indicated in the following table. The results are shown for the states for which fish tissue mercury data were available in the first year results from the National Fish Tissue Study. These reductions are calculated based on the assumption that eating habits of any individual do not change over the period of the comparisons (1999 through 2020), so that changes in exposure are due strictly to reductions in the methylmercury concentrations of fish. This means that the estimated exposure reductions, expressed as a percentage, are applicable to all members of the population including both males and females. The actual estimates of exposure reduction in units of µg/day apply to women of childbearing age, because the underlying exposure distribution used was that for women in the NHANES study. The final row of this table indicates the national changes in average exposure, based on the average reduction in each states with appropriate population weighting. As this last row indicates, the largest reductions occur when the 2020 Cap & Trade scenario is compared with the 1999 Base Case. In addition to providing a greater reduction on average, there are no states in which the MACT or CAIR scenarios produce larger reductions than the Cap & Trade scenario. The reductions for 2020 Cap & Trade relative to 2020 CAIR or 2020 MACT are smaller than those relative to 1999, but are

still positive for each state. The 2020 CAIR versus MACT comparison produced mixed results.

The relative contributions to the reductions from freshwater and marine fish for the Cap & Trade scenario are indicated in Table B.3-5. On a population weighted basis, 60% of the overall reduction in exposure to methylmercury comes from reductions in the concentrations in freshwater fish. As this table indicates, the contributions to exposure reductions from freshwater fish are much greater in the eastern states than in the western states. This is due mainly to the greater changes in deposition estimated to occur in the eastern states. Although the relative change in the methylmercury concentration of marine fish is small, about 0.4% for the Cap & Trade case and less for CAIR and MACT, this is partially offset by the fact that much more marine fish is consumed than wild freshwater fish.

Table B.3-4: Exposure Changes Relative to 1999 for the Three 2020 Scenarios

	Percent Reduction in MeHg Exposure from 1999 level			Difference in Percent Reductions for 2020 Scenarios		
	2020 Cap & Trade	2020 CAIR	2020 MACT	Cap & Trade minus MACT	Cap & Trade minus CAIR	MACT minus CAIR
Alabama	1.94%	1.47%	1.61%	0.33%	0.47%	0.14%
Arizona	0.44%	0.16%	0.19%	0.24%	0.27%	0.03%
Arkansas	2.61%	1.25%	0.91%	1.70%	1.36%	-0.34%
California	0.40%	0.15%	0.18%	0.22%	0.25%	0.03%
Colorado	0.59%	0.23%	0.26%	0.33%	0.36%	0.03%
Connecticut	1.20%	0.73%	0.87%	0.33%	0.48%	0.15%
Florida	0.75%	0.42%	0.42%	0.32%	0.32%	0.00%
Georgia	1.54%	1.06%	1.16%	0.38%	0.47%	0.10%
Idaho	0.40%	0.14%	0.17%	0.23%	0.25%	0.03%
Illinois	1.47%	0.74%	0.70%	0.77%	0.73%	-0.05%
Indiana	2.84%	1.80%	1.71%	1.12%	1.04%	-0.08%
Iowa	1.32%	0.38%	0.36%	0.96%	0.94%	-0.02%
Kansas	0.85%	0.22%	0.17%	0.68%	0.63%	-0.05%
Kentucky	3.18%	2.10%	2.21%	0.97%	1.08%	0.11%
Louisiana	1.20%	0.48%	0.43%	0.77%	0.71%	-0.05%
Maine	1.44%	0.90%	0.88%	0.56%	0.54%	-0.02%
Massachusetts	0.95%	0.59%	0.71%	0.24%	0.36%	0.12%
Michigan	1.56%	0.75%	0.70%	0.86%	0.81%	-0.05%
Minnesota	2.32%	0.33%	0.28%	2.03%	1.99%	-0.04%
Mississippi	1.89%	1.09%	1.13%	0.75%	0.80%	0.04%
Montana	0.47%	0.10%	0.12%	0.35%	0.37%	0.02%
Nebraska	0.66%	0.20%	0.18%	0.48%	0.46%	-0.03%
Nevada	0.42%	0.16%	0.19%	0.23%	0.26%	0.03%
New Hampshire	2.03%	1.47%	1.54%	0.49%	0.56%	0.07%
New Jersey	1.35%	0.82%	1.07%	0.28%	0.54%	0.26%
New Mexico	0.53%	0.17%	0.19%	0.34%	0.36%	0.02%
New York	1.19%	0.71%	0.82%	0.37%	0.48%	0.11%
North Carolina	2.20%	1.45%	1.82%	0.38%	0.75%	0.37%
North Dakota	2.62%	1.32%	1.29%	1.33%	1.30%	-0.03%
Ohio	3.29%	2.48%	2.38%	0.91%	0.81%	-0.09%
Oklahoma	2.02%	0.81%	0.36%	1.66%	1.21%	-0.45%
Oregon	0.42%	0.16%	0.19%	0.23%	0.26%	0.03%
Pennsylvania	2.57%	2.12%	2.21%	0.37%	0.45%	0.09%
South Carolina	1.46%	0.95%	1.15%	0.31%	0.51%	0.20%
South Dakota	1.00%	0.36%	0.33%	0.66%	0.64%	-0.02%
Tennessee	2.57%	1.28%	1.79%	0.77%	1.29%	0.52%
Texas	0.86%	0.43%	0.40%	0.46%	0.43%	-0.03%
Utah	0.54%	0.20%	0.24%	0.30%	0.34%	0.04%
Vermont	2.93%	1.96%	1.85%	1.08%	0.97%	-0.11%
Virginia	2.39%	1.79%	1.98%	0.41%	0.60%	0.19%
Washington	0.49%	0.21%	0.24%	0.24%	0.27%	0.03%
West Virginia	6.53%	5.48%	5.38%	1.15%	1.05%	-0.10%
Wisconsin	2.88%	0.67%	0.59%	2.28%	2.20%	-0.08%
Wyoming	0.67%	0.18%	0.21%	0.46%	0.49%	0.03%
U.S. Average	1.46%	0.85%	0.90%	0.57%	0.61%	0.04%

Table B.3-5: The Fraction of 2020 Cap & Trade Exposure Reductions Relative to 1999 Due to Freshwater Fish

Alabama	81.99%	Nevada	8.41%
Arizona	7.32%	New Hampshire	84.68%
Arkansas	90.68%	New Jersey	73.17%
California	2.24%	New Mexico	32.43%
Colorado	35.08%	New York	67.19%
Connecticut	71.32%	North Carolina	84.38%
Florida	51.93%	North Dakota	89.64%
Georgia	77.94%	Ohio	89.21%
Idaho	22.61%	Oklahoma	87.22%
Illinois	74.03%	Oregon	5.71%
Indiana	88.74%	Pennsylvania	84.76%
Iowa	72.90%	South Carolina	75.43%
Kansas	57.64%	South Dakota	65.42%
Kentucky	89.11%	Tennessee	87.32%
Louisiana	73.83%	Texas	56.78%
Maine	82.50%	Utah	44.19%
Massachusetts	60.79%	Vermont	93.02%
Michigan	75.94%	Virginia	84.87%
Minnesota	90.02%	Washington	21.04%
Mississippi	85.23%	West Virginia	94.94%
Montana	51.56%	Wisconsin	90.86%
Nebraska	40.01%	Wyoming	49.36%

An Example – Details on How the Calculations Were Made

To illustrate how the methodology described above is implemented, the process by which the calculations for each state were made is illustrated using Pennsylvania as an example. The changes in exposure at the 95th upper percentile are used to show the calculations.

Using the NHANES data prior to making any state-specific adjustments, the 95th percentile blood methylmercury concentration of women ages 16-49 in the NHANES study is 6.7 ppb. This blood concentration corresponds to a methylmercury intake rate of 8.4 µg per day, based on the ratio of methylmercury in blood to methylmercury in intake described earlier. An intake rate of 8.4 µg/day from fish with an average concentration of methylmercury of 0.12 mg/kg, corresponds to consumption of 70 grams of fish per day (70 grams/day x 0. 12 mg/kg). So before state adjustments are made, the starting intake rate for the 95th percentile Pennsylvania woman is 70 g/day.

The first adjustment is to account for the regional differences in consumption between different parts of the country. As indicated in Table B.3-1, people in the Mid-Atlantic census region (which includes Pennsylvania) are estimated to eat 1.13 times as much fish as the average American. On this basis, the total fish consumption is adjusted from 70 g/day to 79.1 g/day. The next adjustment is to account for state-level

differences in recreational fishing. Based on Table B.3-2, people in Pennsylvania participated in recreational fishing at 91% of the national average rate. On this basis, the mix of marine to freshwater fish consumed by this hypothetical person is changed from 90%/10% marine/freshwater to 90.9%/9.1% marine/freshwater.

The 1999 Base Case exposure to this 95th percentile PA resident is now calculated by adding the marine fish contribution (90.9% of 79.1 g/day times a methylmercury concentration of 0.12 mg/kg), 8.63 µg/day, to the freshwater fish contribution, which is estimated as 9.1% of 79.1 g/day, or 7.2 g/day. From Table B.3-3, the average fish tissue concentration in Pennsylvania is 0.111 mg/kg, so the intake rate of methylmercury from freshwater fish corresponds to 0.8 µg/day (7.2 g/day times 0.111 mg/kg). Combined, the total methylmercury intake rate (the sum of the marine and freshwater contributions) is 9.43 µg/day.

The effect of alternative control scenarios can be assessed against this Base Case. The results of the air dispersion and deposition analysis conducted by AER, averaged over the grid cells covering Pennsylvania, are indicated in Table B.3-6. These rates are used to calculate the effect of reduced emissions on the concentration of methylmercury in wild freshwater fish. As Table B.3-6 indicates, the estimated deposition rate in 2020 under the Cap and Trade scenario is 26% lower than in 1999.

Table B.3-6: Deposition Rates, µg/m^2-year

	1999 basecase	2020 C&T	2020 CAIR	2020 MACT
Pennsylvania	27.293	20.212	20.883	20.698

In this analysis, it is assumed that fish tissue concentration will scale in direct proportion to changes in deposition. Therefore, the freshwater fish exposure to methylmercury is calculated to drop from 0.8 µg/day to 0.59 µg/day for the 95th percentile Pennsylvania consumer. For the marine fish exposure, the reduction in US power plant mercury emissions in 2020 under the Cap and Trade scenario, relative to 1999 emissions, is 25.7 Mg/year. Based on an estimated global mercury emission rate of 6,000 Mg/year, the marine fish contribution would be reduced by slightly less than one half a percent, i.e., (6000-25.7)/6000 = 99.6%. This leads to a reduction in the calculated contribution from marine fish from 8.63 to 8.59 µg/day. The total change in exposure, from 9.43 µg/day to 9.18 µg/day corresponds to about a 2.6% reduction.

The absolute amount of reduction in exposure to methylmercury will be higher for those who eat relatively more fish than for those who eat less fish. However, the percentage decrease in exposure is the same across the exposure distribution.

Limitations and Uncertainties

In a 2003 analysis of how alternate mercury control scenarios would affect exposure, the national average reduction was calculated. In this analysis the method has been extended to a state level analysis, were adjustments were made to account for data

on differences in the state average concentrations of methylmercury in wild freshwater fish, in fish consumption rates, in recreational fishing activities, and in the calculated deposition rates on a state basis.

Even with the consideration of such state-specific data, important limitations should be recognized:

- In the National Fish Tissue Study's first year results, the number and type of fish sampled is small, averaging about seven composite samples in the 40 states for which data have been collected. This situation should improve as data from the full four year study become available.
- The study sampled only lake fish; river fish were not sampled.
- The extent to which fish advisories reduce consumption from water bodies with fish with above-average methylmercury concentration, and with concentrations below those used in this study, is not known.
- The actual consumption rates of wild freshwater fish are poorly known; the 10% estimate used in this analysis appears to be a high estimate based on the 1994-1996 CSFII data.
- The variability in the mix of freshwater and marine fish consumption among consumers within a state was not included due to the lack of data. A fixed ratio was used for each state based on the recreational fishing data for that state. The average figure would understate the methylmercury exposure reduction experienced by women who eat relatively more freshwater fish.
- The assumption that the concentration of methylmercury in freshwater fish scales directly and instantaneously with changes in state mercury deposition overstates the probable effect of deposition changes and ignores the time required for aquatic ecosystems to adjust.
- No changes in global mercury emissions, other than from US power plants are accounted for during the 1999 to 2020 period.
- No changes in the quantity or type of fish consumed are projected to occur between 1999 and 2020.

REFERENCES, SECTION B.3

Santerre, C.R., P.B. Bush, D.H. Xu, G.W. Lewis, J.T. Davis, R.M. Grodner, R. Ingram, C.I. Wei, and J. Hinshaw, "Metal Residues in Farm-Raised Channel Catfish, Rainbow Trout and Red Swamp Crayfish from the Southern U.S.," *Food Science*, February, 2001. See also
http://news.uns.purdue.edu/UNS/html4ever/010131.Santerre.metals.html

Tran, N.L., Barraj, L., Smith, K., Javier, A., and Burke, T., "Combining Food Frequency and Survey Data to Quantify Long-Term dietary Exposure; A Methyl Mercury Case Study," *Risk Analysis*, Vol. 24, No. 1, 2004.

U.S. Centers for Disease Control and Prevention, National Center for Health Statistics, National Health and Nutrition Survey (NHANES). The data are available at http://www.cdc.gov/nchs/about/major/nhanes/NHANES99_00.htm. An early report on the first year data, "Blood and hair mercury levels in young children and women of

childbearing age—United States, 1999," was published in *Morbidity and Mortality Weekly Report*, Vol. 50, No. 8, March 2, 2001.

U.S. Department of Agriculture, Economic Research Service, March 6, 2002, *Aquaculture Outlook,* LDP-AQS-15.

U.S. EPA, 2001, Integrated Risk Information System's Methylmercury Assessment (CASRN 22967-92-6).

U.S. EPA, 1999, *Mercury Study Report to Congress, Volume IV: An Assessment of Exposure to Mercury in the United States*. EPA-452/R-97-006, December.

U.S. EPA, 1997, *Exposure Factors Handbook, Volume II, Food Ingestion Factors*, EPA/600/P-95/002Fb, August.

U.S. EPA, 2002, *Estimated Per Capita Fish Consumption in the United States,* EPA-821- C- 02-003, August, available at http://www.epa.gov/waterscience/fish/consumption_report.pdf

SECTION C. SUPPORTING TECHNICAL DOCUMENTS

The following list of publications and reports is being submitted electronically separately to the EPA docket in support of the EPRI comments to EPA on the utility mercury rulemaking. In addition, printed copies are available from EPRI upon request

Journal Articles, Research Briefings, and Meeting Papers

Allen, B,. Clewell, C., Hack, E. & Yager, Y., (2004): Use of Markov Chain Monte Carlo Analysis with a Physiologically Based Pharmacokinetic Model of Methylmercury to Estimate Exposures in U.S. Women of Child-Bearing Age, Accepted by *Risk Analysis*

Edgerton, E, June 8, 2004, Comments on Mercury Speciation in Coal-Fired Power Plant Plumes.

Hintlemann, H., Harris, R., Heyes, A., Hurley, J., Kelly, C., Krabbenhoft, D., Lindberg, S.,Rudd, J., Scott, K. & St. Louis, V. (2002). Reactivity and Mobility of New and Old Mercury Deposition in a Boreal Forest Ecosystem during the First Year of the METAALICUS Study, *Environ. Sci. Technol.,* 36: 5034-5040

Lohman, K., Seigneur, C. & Jansen, J., Modeling Mercury Transformation in Power Plant Plumes, *7th International Conference on Mercury as a Global Pollutant.*

Mink, P. and Goodman, M., (In Press): Evaluation of uncontrolled confounding in studies of environmental exposure and neurobehavioral testing in children, Epidemiology

Seigneur, C., Vijayaraghavan, K., Lohman, K., Karamchandani, P, Scott, C., (2004): Global Source Attribution for Mercury Deposition in the United States, *Environ. Sci. Technol.,* 38, 555-569.

Seigneur, C., Lohman, K., Vijayaraghavan, K., Jansen, J. & Levin, L., Comparison of Grid-based and Plume Modeling to Estimate the Local Impacts of Large Mercury Point Sources, *7th International Conference on Mercury as a Global Pollutant.*

Vijayaraghavan, K., Lohman, K., Chen, S., Karamchandani, P, Seigneur, C., Smith, A., Jansen, J. & Levin, L., Sensitivity of Mercury Atmospheric Deposition to Anthropogenic Emissions in the United States, *7th International Conference on Mercury as a Global Pollutant.*

Vijayaraghavan, K., C. Seigneur, K. Lohman, P. Karamchandani, L. Levin, J. Jansen, 2003. Simulation of mercury deposition over the eastern United States with a fine spatial resolution. Air Quality-IV: Mercury, Trace Elements, and Particulate Matter, September 22-24, 2003, Arlington, Virginia

EPRI Reports

A Framework for Assessing the Cost-Effectiveness of Electric Power Sector Mercury Control Policies, EPRI, Palo Alto, CA: 2003. 1005224.

Atmospheric Mercury Research Update, EPRI, Palo Alto, CA: 2004. 1005500.

Characterizing Coal-Fired Power Plant Mercury Emissions Variability at Low Concentrations, EPRI, Palo Alto, CA: 2003. 1009150.

Characterizing Variation in Mercury Emissions from Coal-Fired Power Plants, EPRI, Palo Alto, CA: 2003. 1005401.

Effect of Selective Catalytic Reduction on Mercury, EPRI, Palo Alto, CA: 2003. 1005558.

Factors Affecting the Predicted Response of Fish Mercury Concentrations to Changes in Mercury Loading, EPRI, Palo Alto, CA: 2003. 1005521

Power Plant Evaluation of the Effect of Selective Catalytic Reduction in Mercury, EPRI, Palo Alto, CA, U.S. Department of Energy, Pittsburgh, PA, and U.S. Environmental Protection Agency, Research Triangle Park, NC: 2002. 1005400.

Prenatal Methylmercury Exposure and Developmental Effects, A Systematic Review of the Literature, EPRI, Palo Alto, CA (not yet published)